H.A. Hurlow   Geology of Kamas-Coalville Region   UGS WRB29

THE GEOLOGY OF THE KAMAS-COALVILLE REGION, SUMMIT COUNTY, UTAH, AND ITS RELATION TO GROUND-WATER CONDITIONS

by

Hugh A. Hurlow
Utah Geological Survey

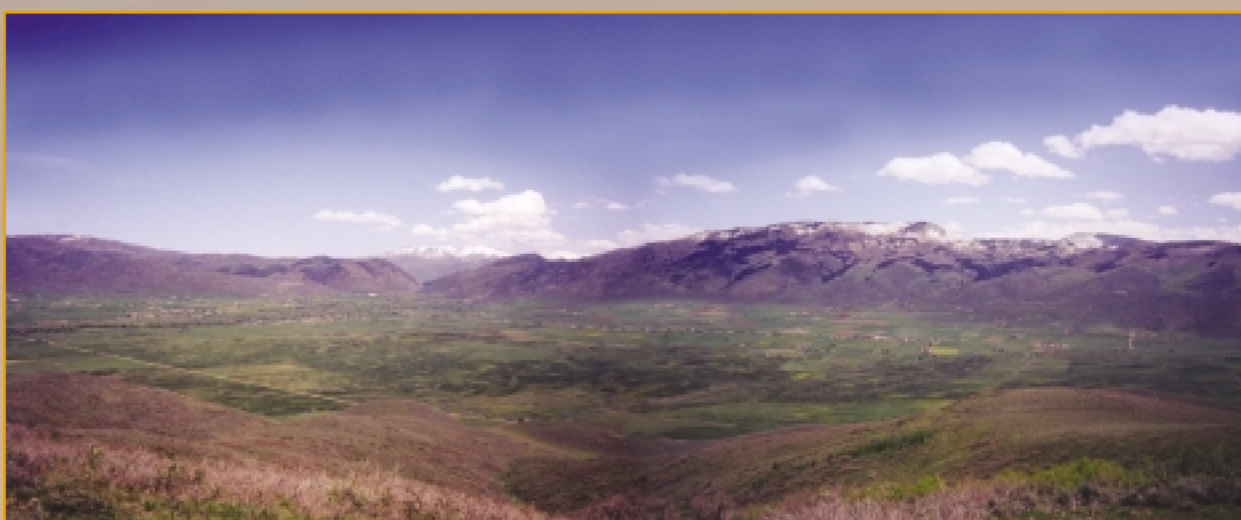

View to the northeast of northern Kamas Valley, from the West Hills.

WATER RESOURCE BULLETIN 29
Utah Geological Survey
a division of
Utah Department of Natural Resources
2002

UTAH GEOLOGICAL SURVEY

THE GEOLOGY OF THE KAMAS-COALVILLE REGION, SUMMIT COUNTY, UTAH, AND ITS RELATION TO GROUND-WATER CONDITIONS

by

Hugh A. Hurlow
Utah Geological Survey

ISBN 1-55791-656-X

WATER RESOURCE BULLETIN 29
UTAH GEOLOGICAL SURVEY
a division of
Utah Department of Natural Resources
2002

UTAH GEOLOGICAL SURVEY

UTAH GEOLOGICAL SURVEY

The **UTAH GEOLOGICAL SURVEY** is organized into five geologic programs with Administration and Editorial providing necessary support to the programs. The **ENERGY & MINERAL RESOURCES PROGRAM** undertakes studies to identify coal, geothermal, uranium, hydrocarbon, and industrial and metallic resources; initiates detailed studies of these resources including mining district and field studies; develops computerized resource data bases, to answer state, federal, and industry requests for information; and encourages the prudent development of Utah's geologic resources. The **GEOLOGIC HAZARDS PROGRAM** responds to requests from local and state governmental entities for engineering-geologic investigations; and identifies, documents, and interprets Utah's geologic hazards. The **GEOLOGIC MAPPING PROGRAM** maps the bedrock and surficial geology of the state at a regional scale by county and at a more detailed scale by quadrangle. The **GEOLOGIC INFORMATION & OUTREACH PROGRAM** answers inquiries from the public and provides information about Utah's geology in a non-technical format. The **ENVIRONMENTAL SCIENCES PROGRAM** maintains and publishes records of Utah's fossil resources, provides paleontological and archeological recovery services to state and local governments, conducts studies of environmental change to aid resource management, and evaluates the quantity and quality of Utah's ground-water resources.

The UGS Library is open to the public and contains many reference works on Utah geology and many unpublished documents on aspects of Utah geology by UGS staff and others. The UGS has several computer databases with information on mineral and energy resources, geologic hazards, stratigraphic sections, and bibliographic references. Most files may be viewed by using the UGS Library. The UGS also manages the Utah Core Research Center which contains core, cuttings, and soil samples from mineral and petroleum drill holes and engineering geology investigations. Samples may be viewed at the Utah Core Research Center or requested as a loan for outside study.

The UGS publishes the results of its investigations in the form of maps, reports, and compilations of data that are accessible to the public. For information on UGS publications, contact the Natural Resources Map/Bookstore, 1594 W. North Temple, Salt Lake City, Utah 84116, (801) 537-3320 or 1-888-UTAH MAP. E-mail: nrugs.geostore@state.ut.us and visit our web site at mapstore.utah.gov.

UGS Editorial Staff

J. Stringfellow	Editor
Vicky Clarke, Sharon Hamre	Graphic Artists
Patricia H. Speranza, James W. Parker, Lori Douglas	Cartographers

12/01

TABLE OF CONTENTS

TABLES

ILLUSTRATIONS

APPENDICES

PLATES

THE GEOLOGY OF THE KAMAS-COALVILLE REGION, SUMMIT COUNTY, UTAH, AND ITS RELATION TO GROUND-WATER CONDITIONS

by
Hugh A. Hurlow

ABSTRACT

The Kamas-Coalville region is in the Middle Rocky Mountains physiographic province, about 30 miles (48 km) east of the Wasatch Front urban area. Rapid population growth and increased water use are the impetus for a collaborative study of water resources in the Kamas-Coalville region, which includes geologic (this study) and hydrologic components. This study describes the geologic framework of the Kamas-Coalville region, emphasizing geologic features that most strongly influence ground-water occurrence, flow, and development. The main topics include: (1) the stratigraphy and structural geology of bedrock, (2) the nature and geometry of unconsolidated deposits in Kamas Valley, (3) the hydrostratigraphy of the study area, and (4) the structure of bedrock units below Kamas Valley.

Kamas Valley is a depositional basin bounded on its east and west margins by normal faults. New gravity data, while not definitive, suggest that this basin is asymmetric, thickening to the east, and that the combined thickness of Tertiary Keetley Volcanics plus younger sediments locally exceeds 3,500 feet (1,067 m) adjacent to the East Kamas Valley fault zone, which forms the eastern structural boundary of the basin.

Quaternary deposits in the northern half of Kamas Valley are chiefly alluvium, glacial outwash, and alluvial-fan deposits. Alluvial fans emanate from the western Uinta Mountains, grading into alluvium in the central and western parts of the basin. Alluvial fans are absent in the southern half of the valley, which is dominated by Pleistocene outwash.

The hydraulic conductivity of unconsolidated deposits in Kamas Valley likely varies with age and depositional environment. Deposits formed during and immediately after glacial episodes have relatively high clay content, possibly resulting in lower hydraulic conductivities compared to similar deposits formed during interglacial periods. Alluvial-fan deposits are more homogeneous and likely have lower average hydraulic conductivities, due to poorer sorting, than alluvium. Based on these relations, the average hydraulic conductivity in unconsolidated deposits in Kamas Valley likely decreases with depth due to increased clay content and compaction, and increases from east to west as the relative proportion of alluvium to alluvial-fan deposits increases.

The hydrogeologic properties of bedrock units in the study area depend strongly on lithology and fracture characteristics, attributes that vary significantly among the different stratigraphic units. The stratigraphic column can be divided into stratigraphic ground-water compartments (SGWCs) and low-permeability units. SGWCs are composed of formations, groups of formations, or individual members within formations. Heterogeneous SGWCs consist of complexly layered rock sequences whose individual beds have variable thickness, lateral extent, and hydraulic conductivity. SGWCs and clustered sandstone beds in heterogeneous SGWCs should be the primary targets for future water wells.

Regionally continuous fault zones may partition the Kamas-Coalville region into large-scale structural ground-water compartments. Compartment boundaries are internally complex and likely restrict transverse flow of ground water due to severing of SGWCs and the presence of fine-grained, impermeable fault rock along the fault plane.

INTRODUCTION

This report describes the geologic framework of the Kamas-Coalville region in Summit County, Utah (figure 1), emphasizing the characteristics of bedrock and unconsolidated deposits that most strongly influence the occurrence and movement of ground water. The Kamas-Coalville region is about 30 miles (48 km) east-northeast of Salt Lake City, and consists of relatively small intermontane valleys, including Kamas Valley and valleys associated with the Weber and Provo Rivers (figure 1), and adjacent mountains of moderate relief. Intermontane valleys, where most development and ground-water withdrawal occur, are underlain by unconsolidated sediments of limited extent and thickness. The hydrogeologic properties of bedrock and the interaction between ground water in bedrock and valley fill are, therefore, important to understanding the hydrogeology of such areas.

The Kamas-Coalville region is experiencing rapid residential and industrial development and related increases in use and development of ground water. According to data from the Utah Division of Water Rights, use of ground water by municipal and industrial entities increased by 107% between 1980 and 1997, including a 400% increase in withdrawal of water from wells and a 76% increase in use of spring water (Utah Division of Water Rights, 1982, and unpublished data). Most new municipal wells are completed in bedrock. In response to this growth, the Division of Water Rights initiated a multidisciplinary, cooperative study to better understand the hydrogeology of the Kamas-Coalville region, with emphasis on Kamas Valley and the Coalville-Chalk Creek area (figure 1). This study provides information on the physical character, stratigraphy, and subsurface structure of bedrock and unconsolidated aquifers in the study area. A companion study by the Water Resources Division of

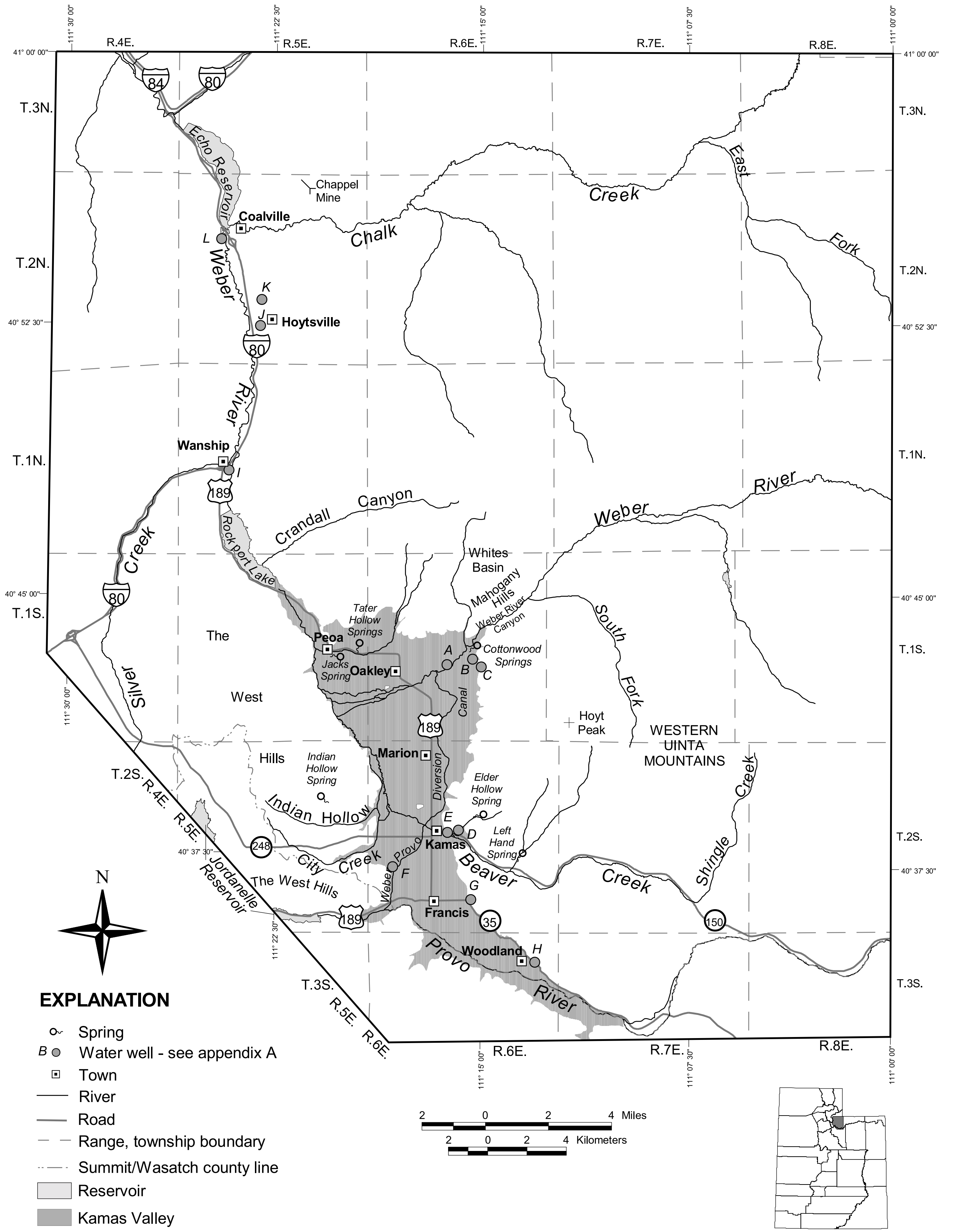

Figure 1. Selected geographic and hydrologic features of the Kamas-Coalville region.

the U.S. Geological Survey quantifies the water budget and describes the ground-water dynamics of Kamas Valley and the hydrogeologic properties of its aquifers.

The principal products of this study include:

1. a digital (GIS-format) geologic map (plates 1 and 2), derived from Bryant (1990),
2. new geologic cross sections (plate 3) based on Bryant's (1990) map and cross sections, new mapping, field structural data, reinterpretation of Bryant's (1990) work, and other published sources,
3. an isopach map (plate 4) showing the thickness of unconsolidated deposits and structure-contour maps (plate 5) showing subsurface elevations of established and potential aquifers in the Kamas Valley area, and
4. data on orientation and density of fractures in the principal bedrock aquifers (appendix C; plate 6).

Use of technical geologic terms is an unavoidable component of any geologic report. To assist non-geologists, many geologic terms used in the text are defined in the glossary located after the references.

Geologic ages are reported as the abbreviations ka for thousands of years before present and Ma for millions of years before present. For example, the phrase "the Pleistocene epoch lasted from 1.8 Ma to 10 ka" means that the Pleistocene epoch began 1.8 million years before present and ended 10,000 years before present. Figure 2 shows the geologic time scale.

This report discusses hydrogeologic implications of the stratigraphy and structure of all geologic units in the Kamas-Coalville region, despite the fact that ground-water development is relatively limited and is concentrated in just a few population centers. To account for this lack of hydrogeologic data, the term stratigraphic ground-water compartment (SGWC) is adopted, following Ashland and others (2001), to supplement the established term aquifer. Use of the term stratigraphic ground-water compartment allows application of lithology-based hydrostratigraphy to large areas for which little or no hydrologic data exists, and avoids the implications conveyed by the term aquifer that these units currently produce water to wells and that their hydrogeologic properties are at least somewhat known.

A stratigraphic ground-water compartment is a consolidated geologic formation, member, or group of formations or members that are bounded by low-permeability units, and which likely have sufficient hy-

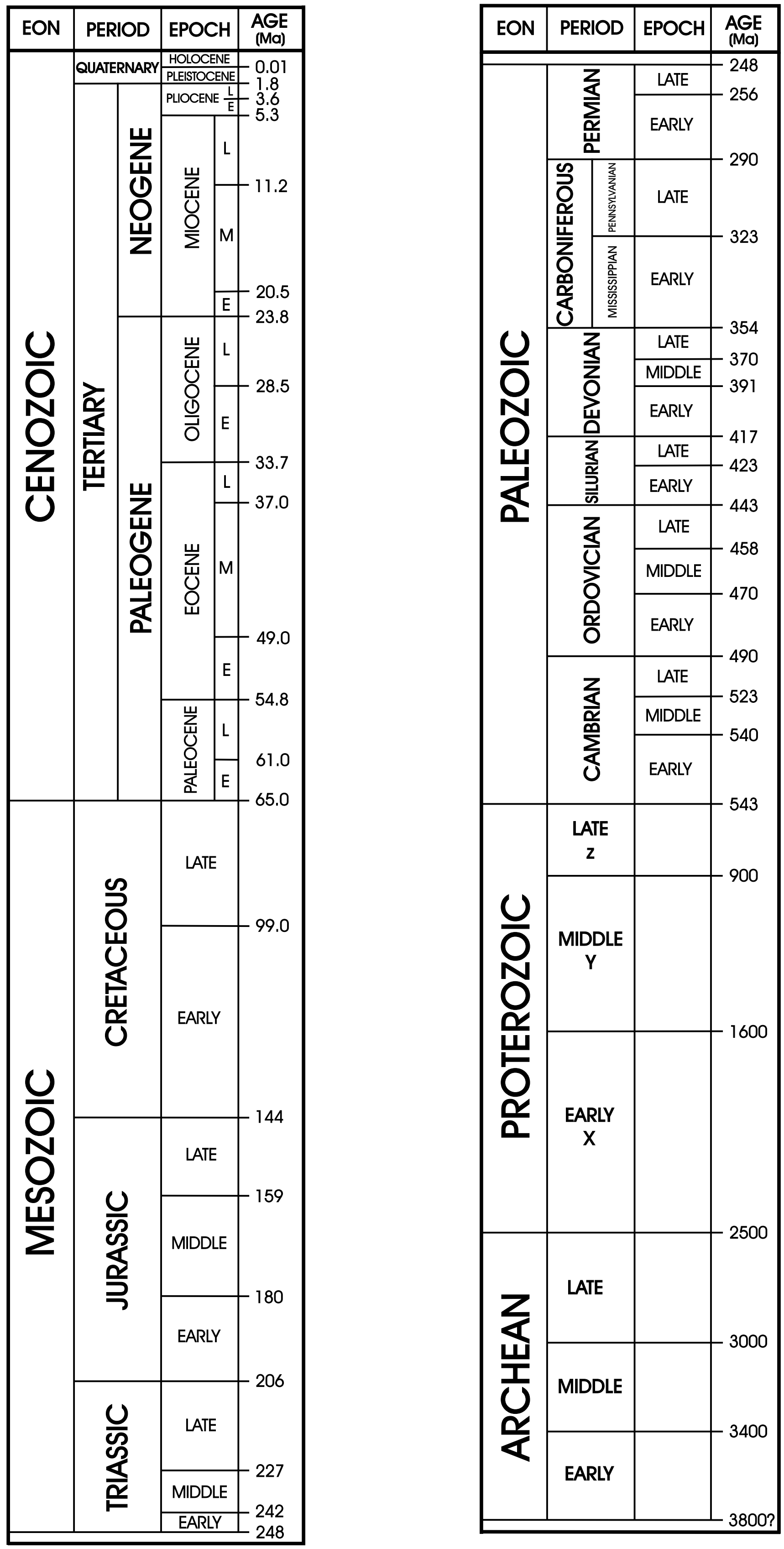

Figure 2. *Geologic time scale, after Palmer and Geissman (1999).*

draulic conductivity to serve as aquifers. A low-permeability unit retards or prevents ground-water flow into or out of a SGWC over time scales relevant for flow to wells (days to tens of years). Some SGWCs are bounded above by unconsolidated deposits and/or the land surface. The hydraulic conductivity of a SGWC is qualitatively determined from lithology and hydrogeologic data from nearby areas. Some geologic units or groups of units in the study area are characterized by interbedding at scales of feet to tens of feet of rock types with varying hydrogeologic properties, such as the Cretaceous Kelvin and Frontier Formations which consist of interbedded mudstone, sandstone, and conglomerate. Such units are impractical to subdivide and are referred to as heterogeneous SGWCs to emphasize this internal variability.

A structural ground-water compartment is a SGWC or group of SGWCs that is bounded by a relatively impermeable fault zone, and/or is segmented into discontinuous masses due to faulting, erosion, or some combination thereof (figure 3) (Al-Raisi and others, 1996; Ashland and others, 2001). The continuity and degree of connection of ground-water flow within and between structural compartments depends on the internal stratigraphy and structure of the compartment and on the physical properties of its bounding faults, as well as the sources and locations of recharge and outflow (Caine and others, 1996; Ashland and others, 2001).

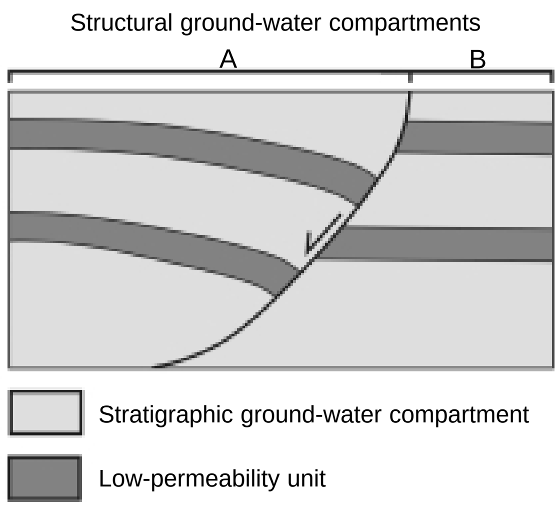

Figure 3. *Schematic illustration of structural ground-water compartments. A normal fault offsets a package of stratigraphic ground-water compartments (SGWCs), dividing the rock mass into two structural ground-water compartments, labeled A and B. Hydrologic communication between the structural ground-water compartments depends on the permeability of fault-zone material, and on location along the fault. If the fault contains low-permeability gouge and/or cement it may impede or prevent ground-water flow across its plane. A densely jointed damage zone adjacent to the fault plane may enhance ground-water flow parallel to the fault plane. If some ground water flows across the fault, this flow may be retarded where low-permeability units abut SGWCs. See text for discussion.*

GEOLOGIC SETTING

Geologic Evolution

The study area is in the Middle Rocky Mountains physiographic province, and includes several important tectonic features (figure 4). An east-west-trending tectonic boundary juxtaposing Archean continental crust to the north and Proterozoic continental crust to the south is present in the subsurface just north of the Uinta Mountains (Bryant and Nichols, 1988). Up to 23,000 feet (7,000 m) of sediment accumulated south of this boundary during Middle to Late Proterozoic time, whereas 0 to 328 feet (0-100 m) of sediment was deposited north of the boundary during the same time period (Bryant and Nichols, 1988). This boundary strongly influenced the subsequent depositional and tectonic evolution of northeastern Utah (Crittenden, 1976; Bruhn and others, 1986; Bryant and Nichols, 1988).

The Cordilleran hinge line, which trends north-south and marks a dramatic westward thickening of Late Proterozoic through Paleozoic sediments, underlies the study area (figure 4; Hintze, 1988). The Cordilleran hinge line resulted from Late Proterozoic rifting of the North American continent, forming a westward-deepening ocean basin that accumulated up to 30,000 feet (9,140 m) of marine sediment (Stewart, 1980). During Late Pennsylvanian through Permian time more localized subsidence, related to plate tectonic processes in the Gulf of Mexico region (Kluth, 1986), created the Oquirrh basin west of the Cordilleran hinge line (figure 4). Slowly subsiding, dominantly marine conditions were reestablished during Triassic through Late Jurassic time, punctuated by deposition of eolian sandstones of the Nugget Sandstone during Jurassic time.

The Uinta-Cottonwood arch (figure 4) is an east-west-trending topographic and structural high that experienced episodic uplift during Paleozoic through Cenozoic time, and extends along the length of the Uinta Mountains westward into the Wasatch Range (Crittenden, 1976; Bruhn and others, 1986; Bryant and Nichols, 1988). Kamas Valley and the West Hills are in a relative structural low along the Uinta-Cottonwood arch (Bryant and Nichols, 1988; Bradley and Bruhn, 1988).

The study area includes the Idaho-Wyoming-Utah segment of the Cordilleran thrust belt in its northern half and the Rocky Mountain foreland tectonic province in its eastern part (figure 4). The Cordilleran thrust belt consists of chiefly east-directed thrust faults and related folds, formed during Cretaceous to early Tertiary time (about 121 to 50 Ma; Armstrong, 1968; Lamerson, 1982; Allmendinger, 1992; Royse, 1993). Most thrust faults dipped west while active, moving hanging-wall rocks eastward. The four major thrust systems in southwest Wyoming and northeast Utah are, from oldest to youngest and west to east, the Willard, Crawford, Absaroka, and Hogsback thrust systems (figure 4; Royse and others, 1975).

A north-south-trending, west-deepening foreland basin formed adjacent to and east of the Cordilleran thrust belt during Cretaceous to Early Eocene time. The Cordilleran foreland basin in northern Utah accumulated 8,200 to 23,000 feet (2,500-7,000 m) of fluvial and marine sediment derived from erosion of rocks uplifted by thrusts and folds in the Wasatch Range (Royse and others, 1975; Lamerson, 1982; Royse, 1993; Steidtmann, 1993; DeCelles, 1994). Foreland basin sediments derived from the early stages of thrusting were deformed by younger, more easterly thrusts and folds (Royse and others, 1975; Lamerson, 1982; Royse, 1993; DeCelles, 1994), and the area of active subsidence likewise migrated eastward.

Numerous oil and gas fields are in the hanging wall of the Absaroka thrust system in southwest Wyoming and

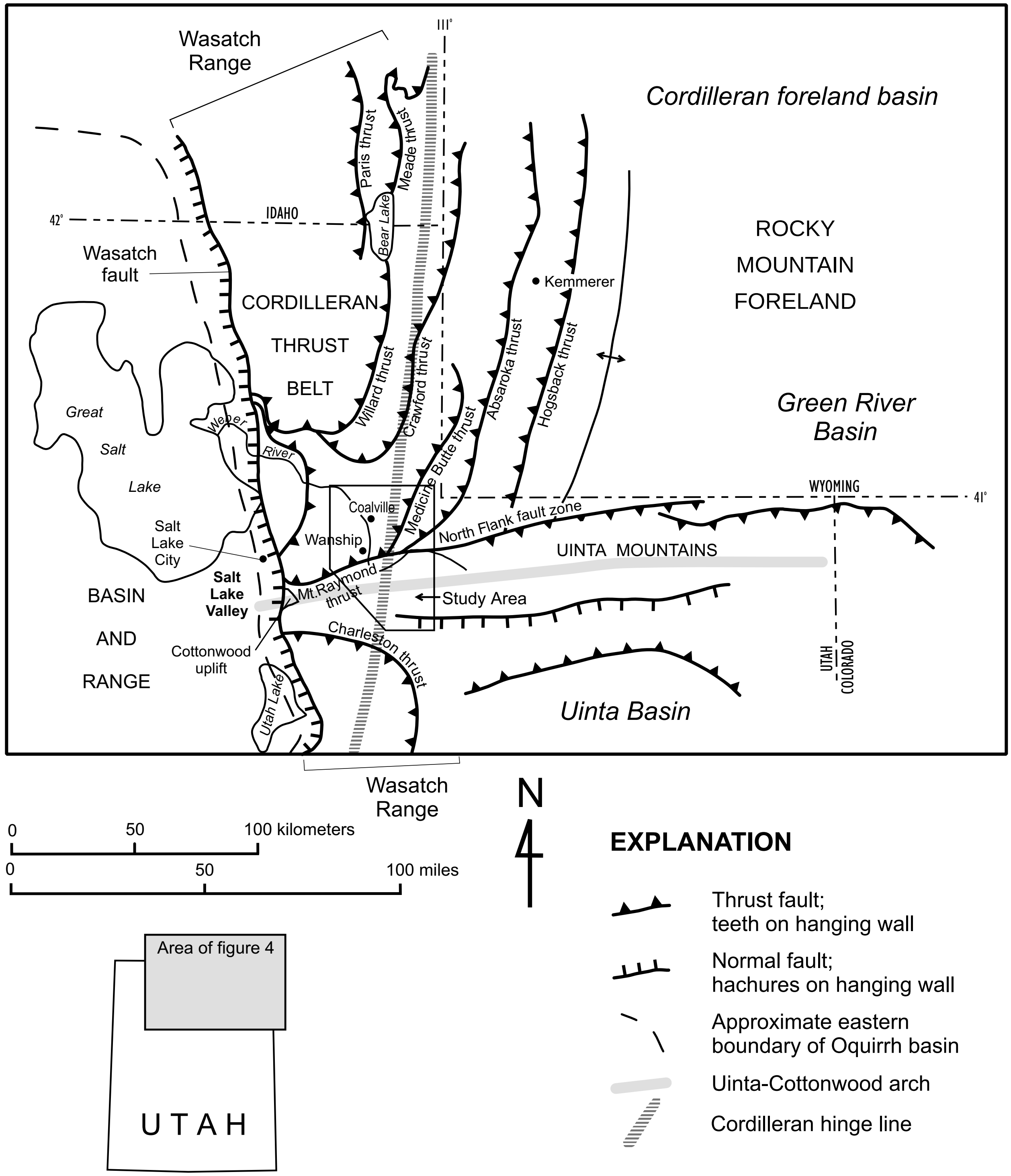

Figure 4. *Tectonic setting of Kamas-Coalville region. Modified from Bryant and Nichols (1988).*

northeast Utah, including the Pineview and Lodgepole fields in the study area (plate 1; Lamerson, 1982; Chidsey, 1999). The organic-rich Cretaceous Aspen Shale and Mississippian limestone units in the footwall of the Absaroka thrust system are the primary source rocks, and the main reservoir rocks are folded Jurassic Nugget Sandstone and Twin Creek Limestone (Lamerson, 1982; Chidsey, 1999).

The Rocky Mountain foreland region from Montana to southern New Mexico experienced reverse faulting and related folding from latest Cretaceous to Late Eocene time (about 70 to 37 Ma; Lowell, 1983; Peterson, 1986). The structural style of the Rocky Mountain foreland differed markedly from that of the Cordilleran thrust belt (figure 5). The Cordilleran thrust belt cuts only post-Precambrian rocks and exhibits ramp-flat geometry (figure 5). In contrast, reverse faults of the Rocky Mountain foreland are approximately planar, cut down into Precambrian igneous and metamorphic rocks, and are more widely spaced (Smithson and others, 1979; Peterson, 1986). Initial normal faulting in the Rocky Mountain foreland overlapped with the end of fault-

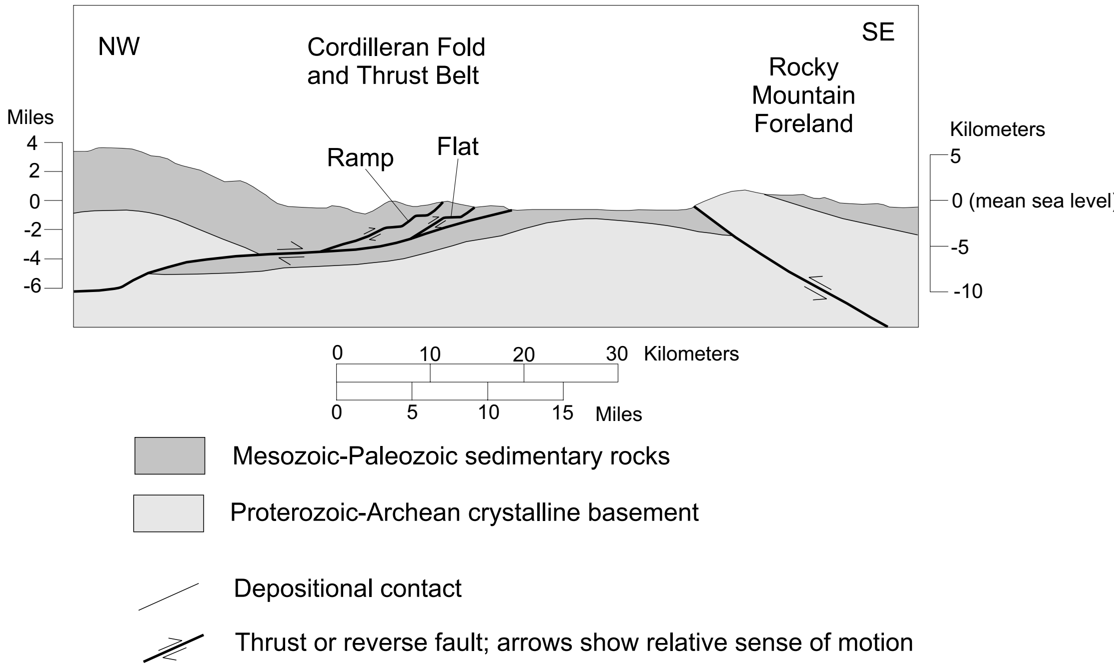

Figure 5. *Schematic cross section of the Mesozoic-early Cenozoic compressional orogen of northeastern Utah, illustrating basic geometries of thrust faults in the Cordilleran fold and thrust belt and Rocky Mountain foreland. Horizontal and vertical scales are approximate. Modified from Allmendinger (1992).*

ing in the Cordilleran thrust belt spatially and temporally, creating structurally complex zones of interaction (Schmidt and Perry, 1988). The Uinta Mountains were uplifted in the Rocky Mountain foreland by north- and south-directed reverse faults (Hansen, 1986; Bruhn and others, 1986).

Subsidence of the earth's surface adjacent to the Rocky Mountain foreland uplifts created major depositional basins (Lowell, 1983; Dickinson and others, 1988). Uplift of the Uinta Mountains created the Green River Basin to the north, which accumulated about 9,000 feet (2,740 m) of fluvial and lacustrine sediments, and the Uinta Basin to the south, which accumulated about 15,600 feet (4,755 m) of fluvial and lacustrine sediments (figure 4; Bruhn and others, 1986; Dickinson and others, 1988).

Volcanism occurred within and near the study area during Eocene to Oligocene time. Normal faulting accompanied and outlasted the volcanism, and continued into Quaternary time (Sullivan and others, 1988; Constenius, 1996). The Wasatch Range west of the study area is bounded by the Wasatch normal fault, which marks the eastern boundary of the Basin and Range tectonic province of late Tertiary to Quaternary age (figure 4). Quaternary to late Tertiary normal faulting in the study area represented an eastward continuation of Basin and Range normal faulting.

Stratigraphy

The geologic evolution outlined above was reconstructed in part from the stratigraphy of the study area and adjacent regions. Stratigraphy also strongly influences occurrence and flow of ground water, as discussed in later sections of this report. This section briefly describes the stratigraphy of the Kamas-Coalville region; figure 6, plate 2, and appendix D provide more detail.

Proterozoic Rocks

The oldest rocks exposed in the study area are the Middle Proterozoic Uinta Mountain Group, consisting of about 12,100 feet (3,700 m) of quartzite and shale which accumulated south of the Archean-Proterozoic crustal boundary described above. The Red Pine shale is dominantly shale with sparse interlayered quartzite, and the Hades Pass and Mount Watson units are dominantly quartzite with interlayered shale.

Paleozoic Rocks

The Tintic Quartzite overlies the Uinta Mountain Group along an unconformity observed throughout North America (Hintze, 1988). The Tintic Quartzite has variable thickness and is absent over much of the study area due to deposition on paleotopography, combined with erosion during Silurian through Middle Devonian(?) time along the Uinta arch (Bryant and Nichols, 1988).

Upper Devonian through Pennsylvanian rocks are chiefly marine limestone. The Madison Limestone and Humbug Formation exhibit significant thickness variations (figure 6; plate 2), due to an erosional unconformity between the two formations (Bryant and Nichols, 1988).

The Pennsylvanian Morgan Formation consists of interlayered limestone, sandstone, and siltstone. The Pennsylvanian Weber Sandstone is primarily quartzarenite that varies substantially in thickness, probably due to localized subsidence related to the development of the Oquirrh basin. The maximum thickness of 2,600 feet (792 m) cited for the Weber Sandstone in figure 6 exceeds the range given by Bryant (1990), but was derived from his map relations. The Permian Park City Formation consists of interlayered cherty limestone and sandstone, with a phosphatic shale layer in the middle of the formation.

EON	PERIOD	GEOLOGIC UNIT	MAP SYMBOL (plate 1)	THICKNESS IN FEET (m)
CENOZOIC	Q	Alluvial, glacial, landslide, & colluvial deposits	Q	0-500 (0-152)
CENOZOIC	Tertiary	Keetley Volcanics and related intrusive rocks	Tkf, Tkb, Tkt, Tlp, Tki	0-1,640 (0-500)
CENOZOIC	Tertiary	older conglomerate	Toc	0-984 (0-300)
CENOZOIC	Tertiary	Bulldog Hollow Mbr. of Fowkes Fm.	Tfb	0-500 (0-152)
CENOZOIC	Tertiary	Wasatch Formation	Tw, Twc	3,930 (1,200)
MESOZOIC	Cretaceous	Hams Fork Member of Evanston Formation	Keh	<2,620 (<800)
MESOZOIC	Cretaceous	Adaville & Hilliard Formations	Kah	4,495? (1,370?)
MESOZOIC	Cretaceous	Echo Canyon Conglomerate	Ke	2,620 (800)
MESOZOIC	Cretaceous	Henefer Formation	Khe	2,620 (800)
MESOZOIC	Cretaceous	Frontier Formation: upper member	Kfu	2,620-3,600 (800-1,100)
MESOZOIC	Cretaceous	Frontier Formation: Oyster Ridge Sandstone	Kfo	200-330 (60-100)
MESOZOIC	Cretaceous	Frontier Formation: lower member	Kfl	4,495 (1,370)
MESOZOIC	Cretaceous	Aspen Shale, Sage Junction Fm.	Ka, Ksj	<525 (<160)
MESOZOIC	Cretaceous	Kelvin Fm: upper member; Cokeville & Thomas Fork Fms.	Kk, Kc, Ktf	1,640-4,265 (500-1,300)
MESOZOIC	Cretaceous	Kelvin Fm: Parleys Member; Cokeville & Thomas Fork Fms.	Kkp	164 (50)
MESOZOIC	Jurassic	Morrison Formation	Jm, Jms	260 (80)
MESOZOIC	Jurassic	Stump Formation	Js, Jms	200 (60)
MESOZOIC	Jurassic	Preuss Sandstone	Jp	984 (300)
MESOZOIC	Jurassic	Twin Creek Limestone: Giraffe Creek Member	Jtgc	82 (25)
MESOZOIC	Jurassic	Twin Creek Limestone: Leeds Creek Member	Jtl	776 (236)
MESOZOIC	Jurassic	Twin Creek Limestone: Watton Canyon Mbr	Jtw	220 (67)
MESOZOIC	Jurassic	Twin Creek Limestone: Boundary Ridge Mbr	Jtb	107 (33)
MESOZOIC	Jurassic	Twin Creek Limestone: Rich & Sliderock Mbrs	Jtrs	172 (52)
MESOZOIC	Jurassic	Twin Creek Limestone: Gypsum Spring Mbr	Jtg	22 (7)
MESOZOIC	Jurassic	Nugget Sandstone	Jn	919-1,250 (280-381)
MESOZOIC	Triassic	Ankareh Formation: upper member	TRau	361 (110)
MESOZOIC	Triassic	Ankareh Formation: Gartra Member	TRag	66-98 (20-30)
MESOZOIC	Triassic	Ankareh Formation: Mahogany Member	TRam	738 (225)
MESOZOIC	Triassic	Thaynes Limestone	TRt	650-1,175 (148-358)
MESOZOIC	Triassic	Woodside Formation	TRw	700 (213)
PALEOZOIC	Permian	Park City Formation	Ppc	775-950 (236-290)
PALEOZOIC	Penn	Weber Sandstone	IPw	1730-2,600 (527-792)
PALEOZOIC	Penn	Morgan Formation	IPm	200-500 (61-52)
PALEOZOIC	Penn	Round Valley Limestone	IPr	170-700 (52-213)
PALEOZOIC	Miss	Doughnut Formation	Mdo	175-650 (53-198)
PALEOZOIC	Miss	Humbug Formation	Mh	420-1,500 (128-457)
PALEOZOIC	Miss / Dev	Madison Limestone & Upper Devonian rocks	MDmu	325-1,250 (99-381)
PALEOZOIC	Cam	Tintic Quartzite	Ꞓt	0-328 (0-100)
PROTEROZOIC	Middle Proterozoic	Uinta Mtn Group: Red Pine Shale	Yur	2,953 (900)
PROTEROZOIC	Middle Proterozoic	Uinta Mtn Group: Hades Pass unit	Yuh	5,906 (1,800)
PROTEROZOIC	Middle Proterozoic	Uinta Mtn Group: Mount Watson unit	Yuw	3,281 (1,000)

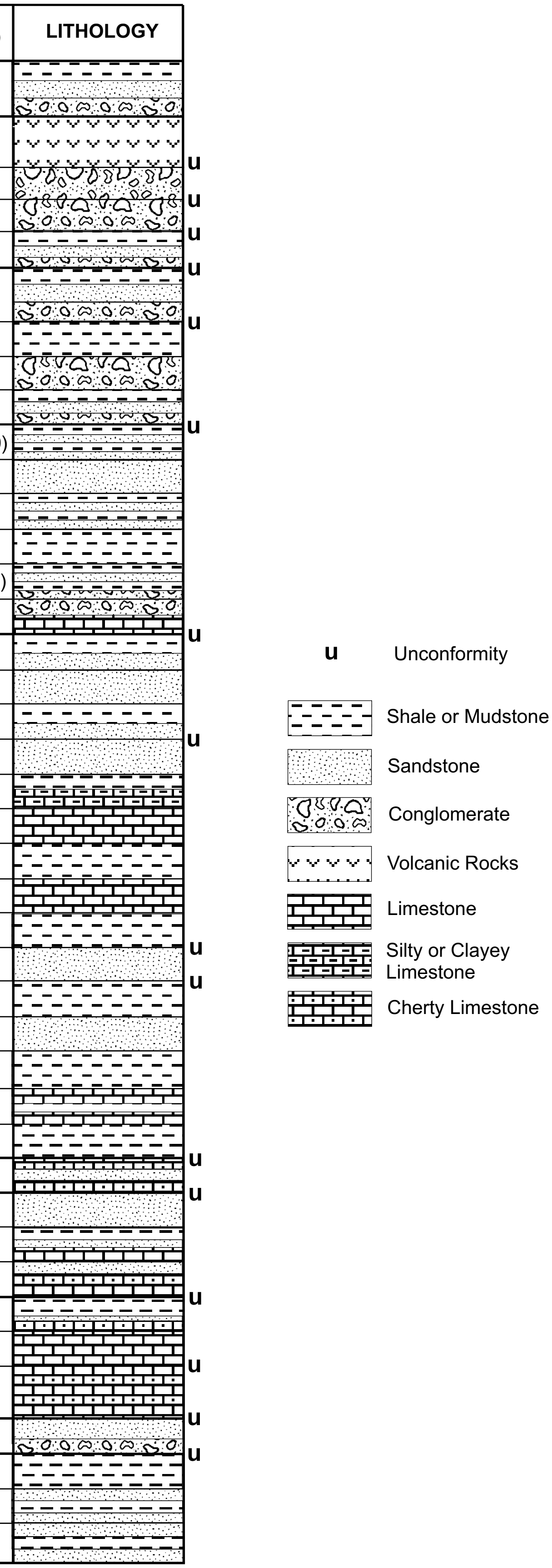

Figure 6. *Stratigraphic column for Kamas-Coalville region, after Imlay (1967) and Bryant (1990). Abbreviations of geologic ages: Q is Quaternary, Penn is Pennsylvanian, Miss is Mississippian, Dev is Devonian, and Cam is Cambrian. The Rich-Sliderock member of the Jurassic Twin Creek Limestone combines the formally designated Rich and Sliderock Members of Imlay (1967). Refer to figure 2 for dates of period boundaries. Map units Tlam and Tlae are not shown because they are volumetrically very minor.*

Mesozoic Rocks

The Triassic section in the study area is largely reddish mudstone, siltstone, and sandstone; exceptions include interbedded limestone and sandstone of the Thaynes Formation and sandstone and conglomerate of the Gartra Member of the Ankareh Formation. The Jurassic Nugget Sandstone was deposited in an eolian environment that extended over much of the western United States. The Nugget dunes were submerged by ocean waters, in which the Jurassic Twin Creek Limestone was deposited.

The Twin Creek Limestone can be divided into seven lithologically defined members (figure 6; Imlay, 1967). The Gypsum Springs, Boundary Ridge, and Leeds Creek Members are clay-rich, calcareous mudstones and siltstones; the Sliderock and Rich Members (combined in this study) consist of clayey micrite and packstone (Imlay, 1967); the Watton Canyon Member is hard, clayey micrite; and the Giraffe Creek Member is a sandy calcarenite to calcareous sandstone.

The rest of the Jurassic section consists of interbedded shale, sandstone, and mudstone of the Preuss Sandstone, Stump Formation, and Morrison Formation. The Preuss Sandstone contains a lower layer of salt, which localizes fault zones and may flow laterally and vertically beneath the surface (Lamerson, 1982).

Cretaceous through early Tertiary formations in the study area are dominantly fluvial and marine sandstone, mudstone, and conglomerate that were deposited in response to uplift of the Wasatch and Uinta Mountains, driven by thrust faulting and folding in the Cordilleran thrust belt and Rocky Mountain foreland (Lamerson, 1982; Bruhn and others, 1986; DeCelles, 1994).

Tertiary Rocks

The early Tertiary Wasatch Formation consists of a lower, conglomerate-dominated part overlain by fluvial sandstone, conglomerate, and mudstone with interbedded lacustrine deposits. Conglomerate of possibly Eocene age locally overlies the Wasatch and older rocks north of Kamas Valley (Bryant, 1990).

The Oligocene to Late Eocene Keetley Volcanics consist of andesitic to dacitic volcanic breccia, flows, tuff, and shallow intrusive rocks erupted from a source area in the West Hills southwest of the study area (Woodfill, 1972; Leveinen, 1994). Although Woodfill (1972) defined an internal stratigraphy for the Keetley, complex interlayering of different rock types and lateral discontinuity of the layers are common within each unit. The Keetley Volcanics underlie much of Kamas Valley, as revealed by logs from oil-test and water wells.

Quaternary Sediments

Quaternary sediments in the study area include alluvial, alluvial-fan, mass-movement (landslide), and glacial deposits. Glacial till and outwash, and alluvial, alluvial-fan, and landslide deposits accumulated during Pleistocene time. Holocene deposits are primarily alluvium (Sullivan and others, 1988; Bryant, 1990). Quaternary deposits and stratigraphy are described in greater detail in the section "Geology of Unconsolidated Deposits."

HYDROLOGIC SETTING

Introduction

This section briefly describes the principal surface- and ground-water systems of the study area, based primarily on the work of Baker (1970). Public water systems rely on both surface and underground sources (Utah Division of Water Rights, 1995, and unpublished water-use data). Most water for culinary use comes from underground sources, primarily springs, but reliance on wells is increasing dramatically (Utah Division of Water Rights, 1995, and unpublished water-use data).

Climate and Precipitation

The climate in the study area is cool, with relatively short summers and long, but not severe, winters (Baker, 1970). The amount of precipitation and the severity and length of winter increase with elevation. The annual normal precipitation is 16.0 to 19.9 inches (40.6-50.6 cm) in Kamas Valley and 25.0 to 29.9 inches (63.5-76.0 cm) in the western Uinta Mountains; average annual snowfall is 100.0 to 149.9 inches (254.0-380.8 cm) in the western Uinta Mountains and 40.0 to 69.9 inches (101.6-177.6 cm) in Kamas Valley (Ashcroft and others, 1992). Precipitation and snowfall totals in the West Hills are similar to, but slightly higher than, those in Kamas Valley.

Surface Water

Weber River and Tributaries

The study area includes much of the headwaters and upper drainage basin of the Weber River (Baker, 1970). The Weber River flows west from its headwaters located in the northwestern Uinta Mountains through the northern part of Kamas Valley. Major tributaries in or below Kamas Valley include: Beaver Creek, which emanates from the southwestern Uinta Mountains; Silver Creek, which originates southeast of the study area in the Wasatch Range and joins the Weber River within the study area near Wanship; and Chalk Creek, which flows south from the northwestern Uinta Mountains then west to its confluence with the Weber River at Coalville (figure 1).

Provo River and Tributaries

The Provo River and associated tributaries are in the southwestern Uinta Mountains in the southern part of the study area (figure 1). The Provo River flows west-northwest through the southern part of the study area, then due west through a narrow canyon in the West Hills. Surface-water diversions, irrigation return flow, and an indistinct ground-water divide connect the Weber River and Provo River drainages in Kamas Valley.

Ground Water

Ground water is relatively abundant in Kamas Valley, and recharge and discharge appear to be in equilibrium at a regional scale (Baker, 1970). Water levels in unconsolidated deposits are typically within 10 feet (3 m) of the land surface in the topographically lower parts of Kamas Valley, and within 100 feet (30 m) of the land surface on the benches. Significant zones of perched or confined water in these sediments are apparently absent (Baker, 1970). The potentiometric surface typically slopes away from mountainous areas and toward the major streams (Baker, 1970).

The ground-water divide between the Provo and Weber drainages in the unconsolidated deposits of Kamas Valley is indistinct. Baker (1970) placed the divide just northeast of and parallel to a northwest-trending bluff above the Provo River, but recent unpublished studies by the Utah Division of Water Resources and data collected by the U.S. Geological Survey suggest a diffuse, northwest-trending divide that passes through the town of Francis. The Weber-Provo ground-water divide in bedrock is poorly understood due to the lack of wells screened in bedrock in this area.

Springs are used for water supply in the mountains adjacent to Kamas Valley, near Peoa, and in side canyons of the Weber River valley north of Rockport Reservoir (figure 1). Springs emanate from many different geologic units, but are most common in Paleozoic rocks and Quaternary sediments.

All water wells for municipal supply in Kamas Valley are in bedrock, whereas most wells for private residences in the valleys are screened in the unconsolidated deposits. New development is largely in the foothills adjacent to the valleys, in the eastern part of the valley north of Kamas, and on the topographic bench north of Oakley.

Principal aquifers in the Kamas-Coalville region include unconsolidated deposits, the Tertiary Keetley Volcanics, Cretaceous sedimentary rocks, the Pennsylvanian Weber Sandstone, and the Mississippian Humbug Formation and Madison Limestone. The Jurassic Twin Creek Limestone and Nugget Sandstone, and the Triassic Thaynes Limestone, which serve as aquifers for many public water systems in the Snyderville basin area, about 14 miles (22 km) west of the study area, crop out along the northern margin of Kamas Valley.

GEOLOGY OF UNCONSOLIDATED DEPOSITS

Description and Stratigraphy

Quaternary deposits in the study area are found in Kamas Valley, the valleys of the Weber and Provo Rivers, and in numerous tributary drainages (figure 7; plate 1); additionally, landslides are abundant in and north of the western Uinta Mountains. In Kamas Valley, alluvium deposited by the Weber and Provo Rivers grades into and interfingers with alluvial fans emanating from the western Uinta Mountains. The Weber and Provo River valleys contain alluvium in channels and flood plains of the modern streams, remnants of up to four higher levels of alluvial-terrace deposits, and small alluvial and alluvial-fan deposits at the mouths of tributary drainages. The western Uinta Mountains contain abundant glacial till and outwash, which formed during at least three glacial episodes (Sullivan and others, 1988).

Quaternary deposits in the study area can be classified into four age groups (Sullivan and others, 1988): Pre-Bull Lake, Bull Lake, Pinedale, and Holocene. Bull Lake- and Pinedale-age deposits formed throughout the Rocky Mountains in response to major glacial cycles. Glacial deposits older than Pinedale age are difficult to date, and are categorized as either pre-Bull Lake (older than about 150 ka) or Bull Lake (130-150 ka) age by Sullivan and others (1988). Pinedale-age deposits include those formed during the maximum glacial advance (about 15 to 18 ka) and during the subsequent retreat (about 14 to 15 ka) (Sullivan and others, 1988). After the Bull Lake episode, regional degradation of basins, characterized by downcutting of older deposits by streams, prevailed so that younger fluvial and glacial deposits are typically topographically lower than older deposits (Sullivan and others, 1988). This relationship is reversed at the mouths of some canyons, where younger alluvial fans overlie older ones.

Outwash deposits south of Kamas were deposited by the Provo River, which during early Pleistocene time flowed north through Kamas Valley to join the Weber River. Around 130 to 150 ka, the Provo River was diverted to its present course, cutting westward through the southern West Hills (Anderson, 1915; Sullivan and others, 1988).

There are five main types of unconsolidated deposits in the study area.

1. Alluvium, which is deposited in the channels and flood plains of streams, consists of interlayered, well-sorted beds of gravel, sand, silt, and clay. Lateral continuity of any particular sediment type is limited, and different sediment types are complexly interlayered.
2. Alluvial-fan deposits, formed primarily by debris flows and alluvial deposition at the mouths of canyons, are massive to layered, poorly to moderately sorted gravel, sand, and silt, and contain angular to subrounded clasts in a muddy to sandy matrix. Their composition depends strongly on the composition of bedrock and colluvium in their drainage areas.
3. Outwash is sediment derived from glaciers, including rock flour to boulder-size clasts, transported in glacial streams. Outwash is composed of gravel, sand, and silt in a clayey matrix, and may be internally massive and poorly sorted to layered and moderately well sorted.
4. Glacial till is deposited as moraines by glaciers, is internally massive, and is composed of boulder- to pebble-size clasts in a poorly sorted, clayey matrix.
5. Landslide deposits are internally massive and contain clasts of widely varying size. Their composition depends on the composition of their source, which may vary from unconsolidated deposits to bedrock, including any volumetric combination of the two.

Distribution and Subsurface Geometry of Unconsolidated Deposits in Kamas Valley

Surface Relations

The primary source for the following description of unconsolidated deposits in Kamas Valley is Sullivan and others (1988), who provide greater detail than Bryant's (1990) map in the following ways. Bryant's (1990) older alluvial-fan deposits (map unit Qof) includes both Bull Lake and pre-

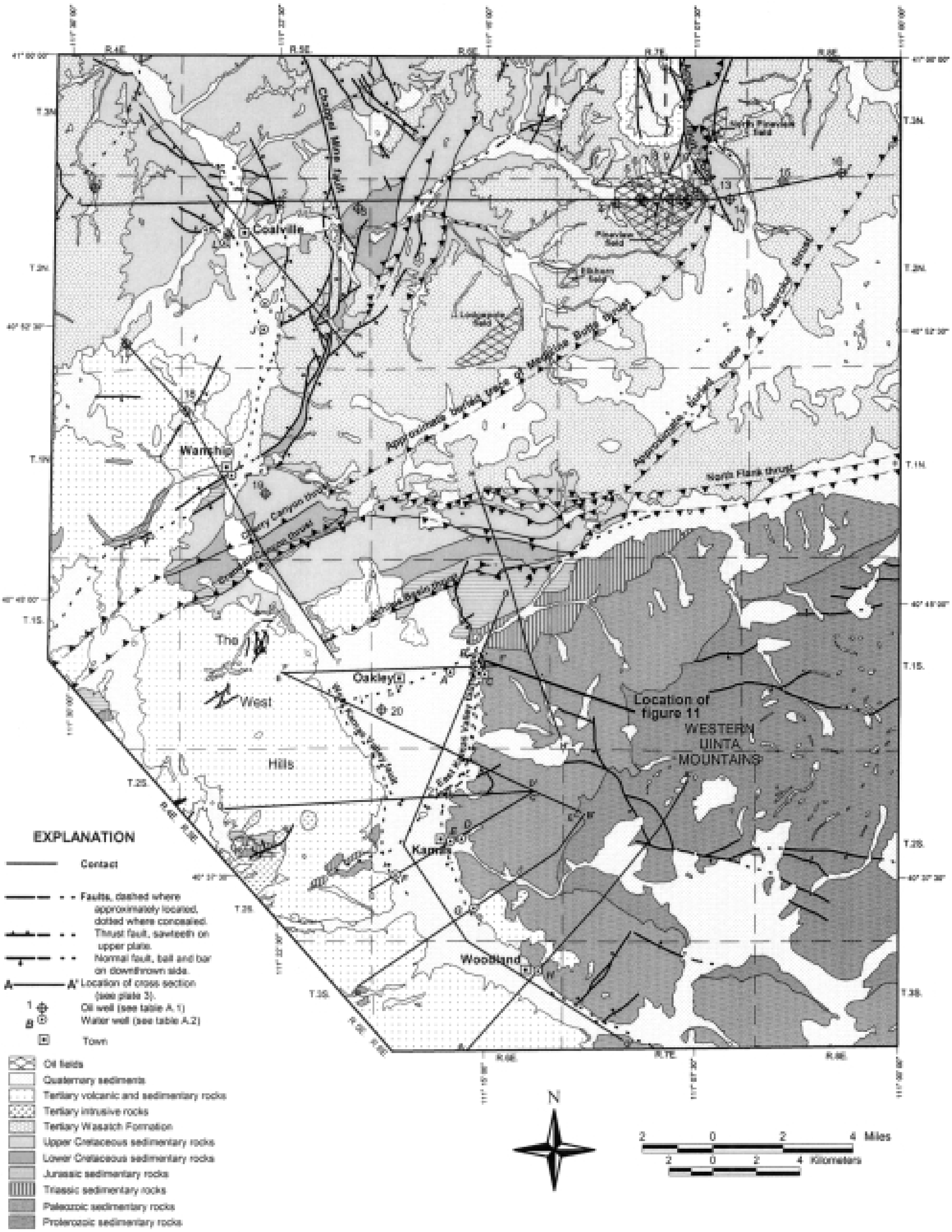

***Figure 7.** Simplified geologic map of Kamas-Coalville region. Compiled and generalized from plate 1, which is mainly from Bryant (1990).*

Bull Lake deposits, which Sullivan and others (1988) differentiate. The age relations between alluvial-terrace deposits (Qtg_1 and Qtg_2), Pinedale-age outwash (Qop), and younger alluvial-fan deposits (Qf, which contains both Pinedale and Holocene deposits) in Kamas Valley are obscure in Bryant's (1990) work but are delineated by Sullivan and others (1988). Thus, the discussion below includes details not apparent on plate 1 but which elucidate the present distribution and depositional history of Quaternary units in Kamas Valley.

Plate 1 incorporates Bryant's (1990) Quaternary contacts and map units where they are consistent with Sullivan and others' (1988) work. However, Bryant's (1990) Quaternary units have been modified in the following ways: (1) deposits in the northeast part of Kamas Valley adjacent to the western Uinta Mountains are shown by Bryant (1990) as colluvium, but are designated on plate 1 as older alluvial-fan deposits following Sullivan and others (1988), who interpret them as pre-Bull Lake age; (2) landslide deposits in the western Uinta Mountains between Kamas and the Weber River are modified from Bryant (1990) based on interpretations by Mike Lowe of the Utah Geological Survey (verbal communication, 1999) and unpublished mapping completed as part of this study; and (3) the surficial deposit north of where the Weber River enters Kamas Valley, shown as Tertiary conglomerate (unit Toc) by Bryant (1990), is interpreted here as a landslide deposit (Ql), based on Woodfill (1972) and field observations completed as part of this study.

Pre-Bull Lake-age alluvial fans (Qof) and alluvial-terrace deposits (Qtg_2) occupy the topographic bench north of the Weber River in Kamas Valley, and are incised by Bull Lake-age alluvial-terrace deposits (Qtg_1). Pinedale-age outwash (Qop) south of the Weber River incises alluvial-fan deposits of pre-Bull Lake age (Qof) which emanate from the western Uinta Mountains. The latter deposits are overlain by Pinedale- and Holocene-age alluvial-fan deposits (Qf) emanating from Hoyt Canyon and Beaver Creek. The younger alluvial fans are presently inactive, based on their high degree of vegetation and incision by modern streams. Alluvium deposited by the Weber River and Beaver Creek is confined to the western margin of Kamas Valley, likely due to building of the alluvial fans westward from the western Uinta Mountains. South of Kamas, Bull Lake-age alluvial-terrace deposits (Qtg_1) are incised by modern alluvium (Qal) and local Pinedale-age outwash (Qop); alluvial fans are absent. Glacial till and outwash are abundant in the upper canyons of the Weber and Provo Rivers in the Uinta Mountains.

Subsurface Relations

Gravity study: Data on the thickness and subsurface geometry of unconsolidated deposits below Kamas Valley are sparse. Water-well drillers' logs can in some cases be used to determine depth to bedrock and the presence of clay layers. Examination of water-well drillers' logs for Kamas Valley and the upper and middle Weber River valleys, available from the Utah Division of Water Rights, reveals discontinuous clay layers, but these layers are difficult to correlate aerially or laterally.

Peterson (in Baker, 1970) attempted to estimate the thickness of Quaternary deposits below Kamas Valley by performing a gravity survey of the valley. Peterson found that the gravity technique could not distinguish between Quaternary deposits and the underlying Keetley Volcanics, which consist predominantly of poorly consolidated volcanic breccia. Peterson's map showed the inferred combined thickness of Quaternary sediments and Keetley Volcanics, featuring a north-northeast-trending, oval-shaped basin with a maximum thickness of 1,600 feet (488 m) approximately 0.75 miles (1.2 km) south of the Weber River and 0.75 miles (1.2 km) west of the eastern valley margin. The thickness of low-density deposits decreases radially away from this maximum and is relatively constant, ranging from about 200 to 400 feet (61-122 m) south of the midway point between Marion and Kamas. This thickness distribution does not reflect the morphology of the valley and is not readily explained in the context of the geologic evolution of the region.

A new gravity survey of Kamas Valley was performed as part of this study by Dr. Basil Tikoff of the University of Wisconsin (figures 8 and 9; appendix B). The goals of this work were to increase the density of survey points in the valley and to perform traverses that cross the valley margins. The northern traverse spans most of the valley, crossing the eastern valley margin near the town of Marion, and the southern traverse trends east-west from Kamas into the West Hills west of the valley (figures 8 and 9). It was anticipated that the new results could be combined with Peterson's data (in Baker, 1970) to perform three-dimensional modeling of the basin subsurface geometry. However, only the new data are considered in this report due to partial disagreement between the two data sets (appendix B). The following paragraphs summarize the new data, modeling results, and geologic interpretations, and appendix B describes the gravity survey in greater detail. On the whole, the new gravity data are not as definitive as hoped, and the resultant schematic model geometry of low-density material below Kamas Valley may require revision if new gravity or well data become available.

The new Bouguer anomaly values generally decrease to the northwest and show a northwest-trending low over the western part of the valley (figure 8; table B.1). The eastern valley margin shows a steep, eastward-increasing gradient in Bouguer anomaly values, in contrast to the relatively gentle gradient measured across the western valley margin west of Kamas.

The new gravity data (figure 8; table B.1) likely reflect the combined effects of the low-density basin fill below Kamas Valley and a north- to northwest-sloping regional gravity gradient. Data from the northern part of Kamas Valley indicate a steeper eastern basin margin and greater thickness of low-density deposits than depicted by Peterson (in Baker, 1970). Results from the southern part of the valley are similar to those of Peterson (in Baker, 1970), suggesting that the thickness of low-density deposits there is relatively low and uniform.

Because the new gravity data could not be combined with those of Peterson (in Baker, 1970), the north- to northwest-sloping regional gravity gradient could not be subtracted from the data. Modeling of the gravity data along two east-west traverses crossing the valley margins largely eliminates the effects of the regional gradient and provides estimates of the shape and thickness of low-density material beneath Kamas Valley (figure 9).

Gravity modeling of the northern traverse shows an

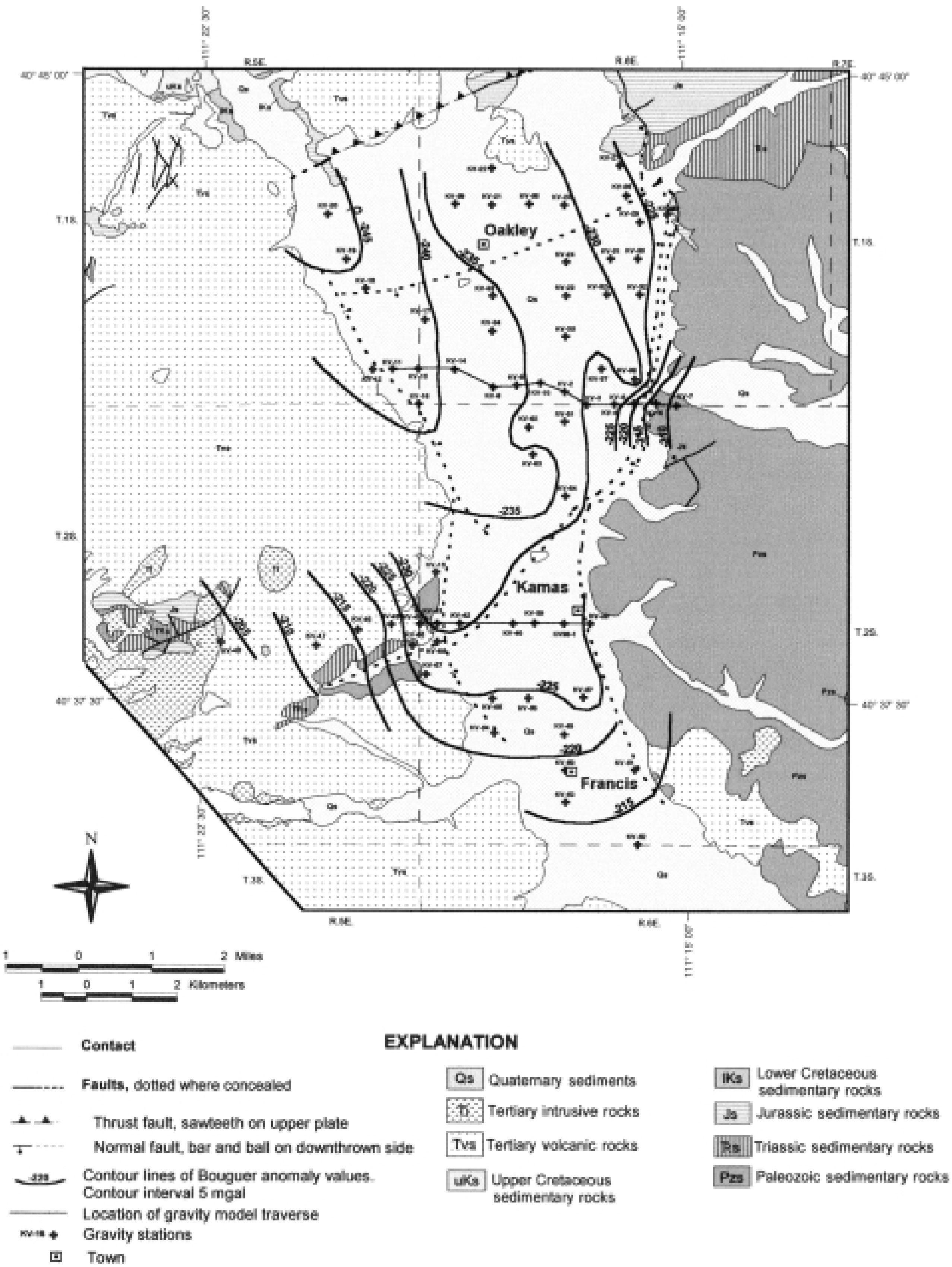

Figure 8. *Bouguer gravity map for Kamas Valley, and locations of gravity model traverses. See text and appendix B for data and interpretation.*

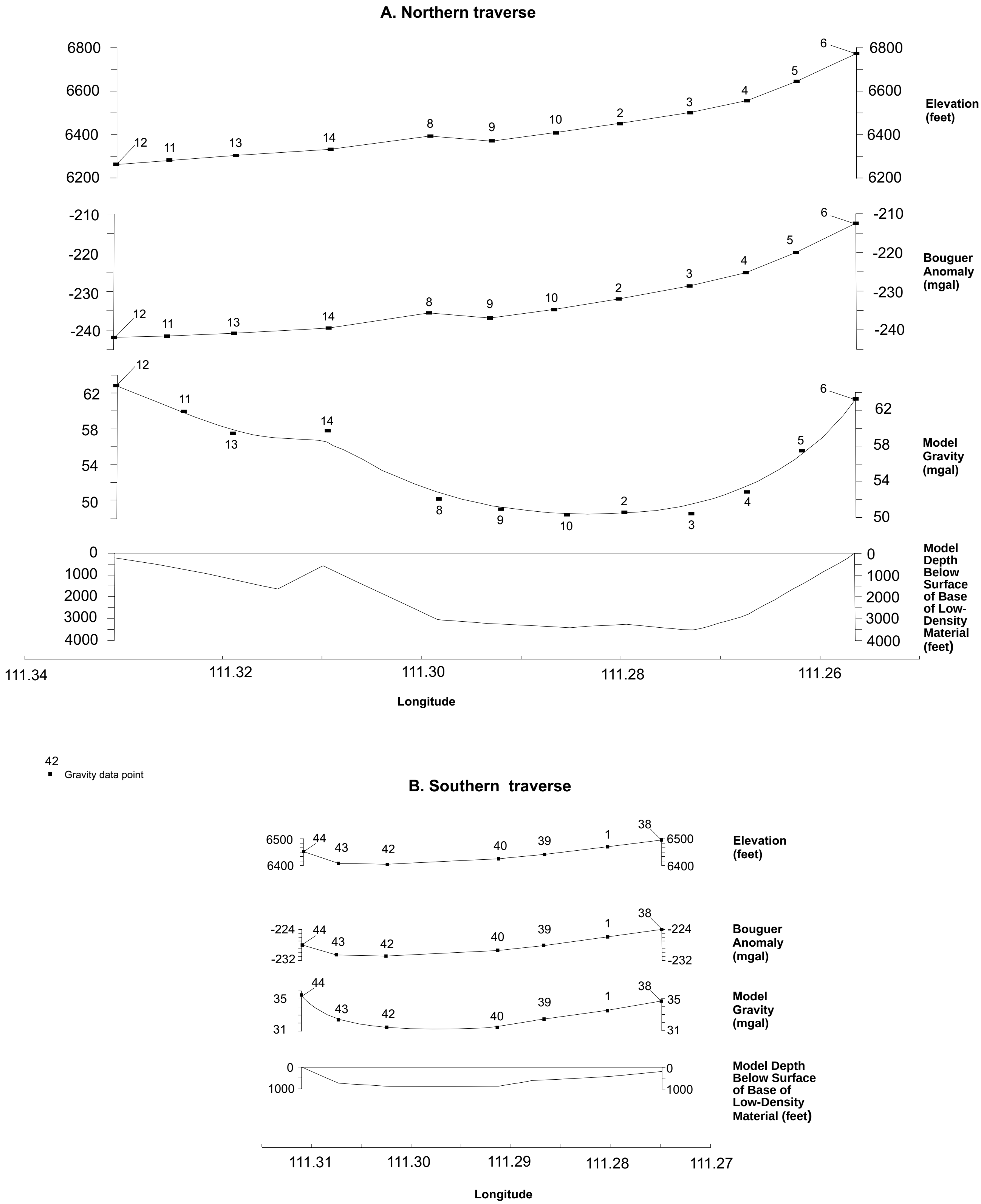

Figure 9. *Gravity data and inversion modeling results for the two model traverses discussed in the text and in appendix B. See figure 8 for locations of traverses.*

asymmetric, east-thickening wedge of low-density material. The model in figure 9A assumes that the entire gravity gradient results from variation in thickness of unconsolidated sediments, and indicates a maximum thickness of these deposits of about 3,500 feet (1,067 m). This shape strongly suggests a genetic relation between the basin and the East Kamas Valley fault zone. This thickness is unreasonably large for the unconsolidated deposits below Kamas Valley, based on comparison with other normal-fault-bounded basins in northern Utah (see appendix B). The gravity model is tentatively interpreted to represent the shape of low-density deposits, including both Quaternary deposits and Keetley Volcanics, below the valley, but to underestimate their combined thickness. In other words, Quaternary deposits are likely thinner, and the base of the combined Quaternary-Keetley package is likely deeper, than the model indicates. The gravity model for the southern traverse (figure 9B) suggests that the low-density material is substantially thinner than along the northern traverse.

Basin thickness and subsurface facies distribution: Plate 4 is a schematic isopach map showing the inferred thickness of unconsolidated deposits below Kamas Valley. This map is derived from logs of water and oil-test wells (appendix A), and the results of the new gravity survey and models (appendix B). The thickness of unconsolidated deposits below the east-central part of the valley, where the gravity model for the northern traverse indicates that the depositional basin is thickest, is not known. It was, therefore, assumed that unconsolidated deposits are one-third of the model thickness where unconstrained by well logs. This assumption results in a maximum thickness of unconsolidated sediments of approximately 1,100 feet (335 m), which represents a compromise between making the thickness of unconsolidated deposits as close to the model value as possible, yet substantially thinner than Quaternary-Tertiary deposits below Salt Lake Valley, Utah, related to normal displacement on the Wasatch fault. The discussion in appendix B describes these constraints in greater detail.

The isopach map (plate 4) suggests that the Quaternary depositional basin below the northern part of Kamas Valley is asymmetric, thickening eastward toward the East Kamas Valley fault zone and reaching its maximum thickness just west of the fault zone. Thickness contours in the eastern part of the valley trend northeast, parallel to the East Kamas Valley fault zone. The thickness of Quaternary sediments decreases gradually to the northwest and abruptly to the south across the fault trace.

Two schematic cross sections (figure 10) illustrating possible subsurface relations of Quaternary sediments below Kamas Valley are based on the isopach map (plate 4), the surficial relations and evolution of Quaternary deposits of Kamas Valley (Sullivan and others, 1988), and principles of

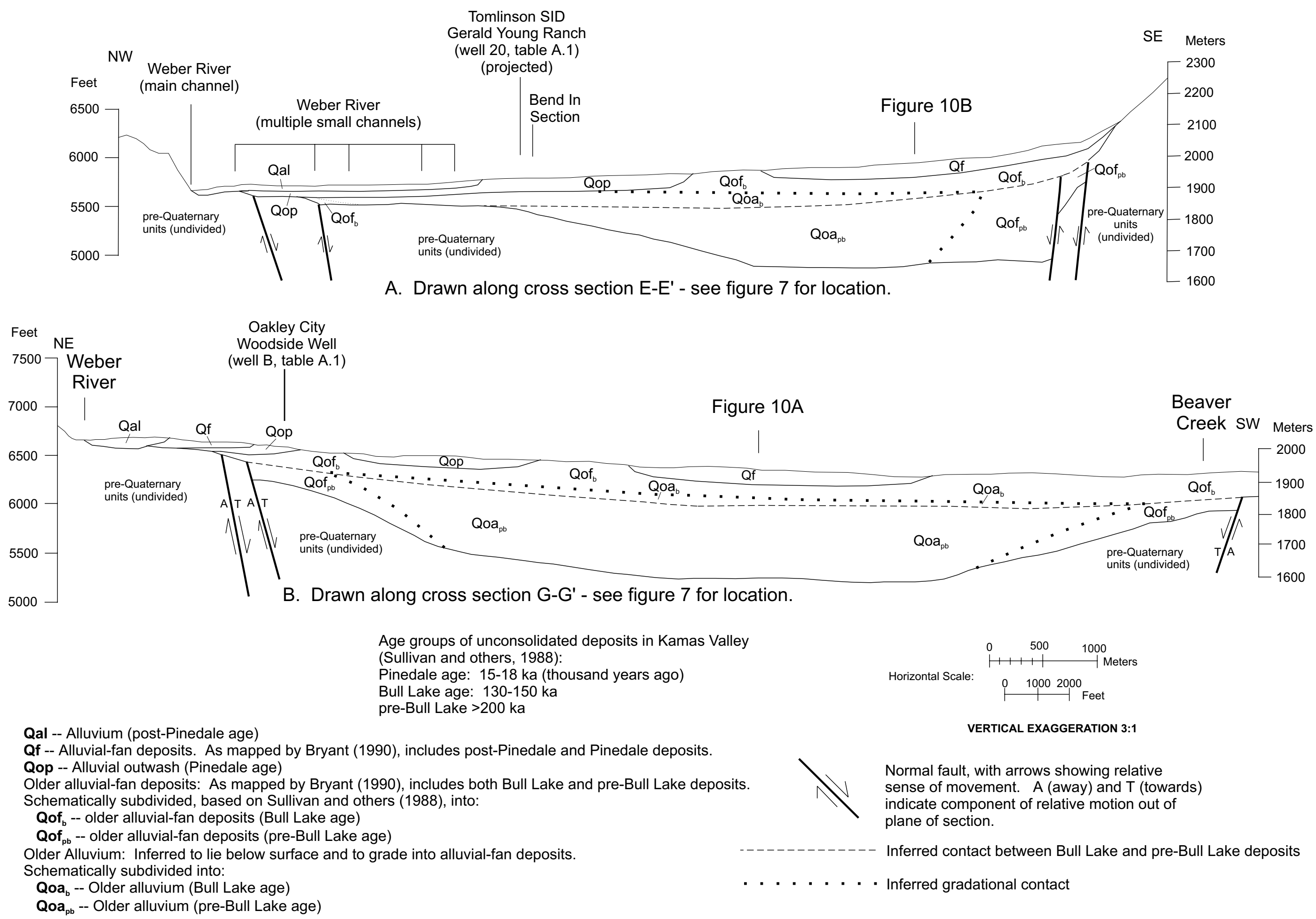

Figure 10. Schematic cross sections illustrating possible subsurface geometry and lateral variations of Quaternary units below Kamas Valley. The Quaternary to pre-Quaternary surface is derived from gravity and water-well data (appendices A and B). Subsurface relations of individual Quaternary units are schematically drawn to be consistant with Sullivan and others (1988), but are not based on specific data.

sedimentation in normal-fault-bounded basins (Leeder and Gawthorpe, 1987).

Figure 10A is oriented northwest-southeast, perpendicular to the strike of the East Kamas Valley fault zone. Pre-Bull Lake sediments are the thickest deposits, consisting of alluvial-fan sediment adjacent to the fault zone grading and/or interlayered westward with alluvium deposited by an ancestral Weber River, which at that time included both the modern Weber and Provo River drainages. The location of the ancestral Weber River in Kamas Valley during Pleistocene time is not known, except where an escarpment in the Bull Lake-age alluvial fan, located on the northeast margin of Kamas Valley about 0.5 miles (800 m) south of the present Weber River, was likely cut by the Weber River during late Pinedale time (Sullivan and others, 1988). Subsidence of the hanging wall of the East Kamas Valley fault zone caused alluvial-fan sediments to aggrade vertically but remain close to the fault. Faulting ceased before the Bull Lake glacial episode, allowing alluvial fans to prograde westward from the Uinta Mountains into the central and western parts of Kamas Valley. Pinedale-age and Holocene alluvial and alluvial-fan deposits incise and overlie the older sediments and were not influenced by faulting.

Figure 10B is drawn northeast-southwest, parallel to the basin axis and approximately perpendicular to the dominant transport direction in the alluvial fans, and oblique to the strike of the East Kamas Valley fault zone. This cross section also shows pre-Bull Lake alluvial-fan deposits close to the fault zone interfingering with alluvium, overlain by extensive Bull Lake-age alluvial-fan deposits that prograded into the basin after faulting ceased.

STRUCTURAL GEOLOGY OF BEDROCK

Introduction

This section describes the structural geometry and evolution of the study area in greater detail than the “Geologic Framework” section, emphasizing the geometry of sedimentary layering, major faults and folds, and the fractures in bedrock. This information provides the basis for discussions of the hydrostratigraphy of the study area and the effects of bedrock structure on ground-water occurrence and flow.

Cordilleran Thrust Belt Structures

As noted above, the study area lies in the Idaho-Wyoming-Utah segment of the Cordilleran thrust belt (figure 4), which formed between Cretaceous and Middle Eocene time (about 121 to 50 Ma). Structures of the Cordilleran fold and thrust belt are exposed in the study area north of Kamas Valley (Crittenden, 1976; Bradley and Bruhn, 1988; Bryant and Nichols, 1988) (figures 4 and 7; plate 1), including: thrusts of the Absaroka system exposed along Rockport Reservoir and in the hills north of Kamas Valley; the Medicine Butte thrust; and two thrusts emanating from ramps on the Medicine Butte thrust, exposed along Chalk Creek east of Coalville (figure 7). Fault-related folds are present near Rockport Reservoir and along Chalk Creek (Coalville anticline; Hale, 1976) (plate 1). Geophysical and well data from petroleum exploration reveal that the Absaroka and Medicine Butte thrusts are present below the Tertiary Wasatch Formation in the northeast part of the study area (Lamerson, 1982).

Mesozoic rocks exposed in the study area north of Rockport Reservoir and the Uinta Mountains generally dip 10 to 30 degrees northwest, reflecting folding above a subsurface ramp in the Absaroka thrust system (Lamerson, 1982). However, dips are steep to overturned adjacent to thrusts and in thrust-related folds. Jurassic and Cretaceous rocks are tilted and folded adjacent to Absaroka-system thrusts near Rockport Reservoir, resulting from deformation related to both the Absaroka thrust system and younger thrusting on the North Flank thrust system, which forms the northern boundary of the Uinta Mountains (Crittenden, 1976).

The Cretaceous Kelvin Formation was derived from erosion of mountains to the west, whose uplift was related to movement along the Willard thrust; the Cretaceous Frontier and Henefer Formations and the Echo Conglomerate were deposited during motion on the Crawford thrust system; and the Cretaceous Hams Fork Member of the Evanston Formation and the Tertiary Wasatch Formation accumulated in the hanging wall of the Absaroka thrust system (Royse and others, 1975; Lamerson, 1982; DeCelles, 1994). Rocks older than the Evanston Formation were folded during motion on the Absaroka thrust system (Lamerson, 1982; DeCelles, 1994).

An area northeast of Kamas Valley (plates 1 and 2; cross section H-H′, plate 3) was remapped by the author at 1:24,000 scale, to better delineate folds and faults there and to illustrate the structural style of Mesozoic bedrock north of the valley. The work focused on dividing the Jurassic Twin Creek Limestone into its seven members (Imlay, 1967), and on better delineating a northeast-striking thrust fault, informally referred to here as the Whites Basin fault. The Whites Basin fault is interpreted to be part of the Absaroka thrust system that has been folded to a steep northeast dip during uplift of the Uinta Mountains (figure 7; cross section H-H′, plate 3).

Remapping northeast of Kamas Valley resulted in several changes to Bryant’s (1990) map, in addition to subdividing the Twin Creek Limestone. The Whites Basin fault loses displacement eastward, grading into an overturned anticline (Bryant showed the thrust cutting through this area). Following Bradley (1988), the Mahogany Hills fault, a southeast-dipping thrust fault that is part of the North Flank thrust system, is mapped south and east of the Whites Basin thrust. The Mahogany Hills fault loses displacement westward, grading into an open anticline. Subdividing the Twin Creek Limestone better illustrates the form of folds in the area and reveals several folds not shown on Bryant’s (1990) map. The northern continuation of the East Kamas Valley fault zone cuts the Whites Basin thrust, whereas Bryant (1990) showed the opposite relation.

Rocky Mountain Foreland Structures

The Uinta Mountains were uplifted during latest Cretaceous through middle Tertiary time (about 70 to 38 Ma) by the North Flank and South Flank reverse faults (figure 4; Bruhn and others, 1986; Hansen, 1986). The North Flank fault dips south below the Uinta Mountains and likely merges with the major east-west-trending Proterozoic crustal discontinuity discussed in the "Geologic Framework" section (Bruhn and others, 1986; Bradley and Bruhn, 1988). This thrusting and uplift accentuated the Uinta arch, which became an anticline in the hanging wall of the North Flank fault (Bruhn and others, 1986; Bryant and Nichols, 1988). The North Flank fault cut thrusts and folds of the Absaroka thrust system, and tilted the Absaroka-system thrusts and adjacent sedimentary rocks to steep northwest dips (Crittenden, 1974; Bradley and Bruhn, 1988). Movement on the North Flank fault was synchronous with the Hogsback-Darby-Prospect thrust system of the Cordilleran thrust belt (figure 4), and the two fault systems may have merged deep below the Uinta Mountains (Bruhn and others, 1986).

Tertiary Normal Faults

The dominant tectonic style in much of the western United States changed significantly in Middle to Late Eocene time. At about 55 Ma, normal faulting and volcanism began in much of the Cordilleran thrust belt, though the precise timing of initiation varied throughout the western United States (Constenius, 1996). Volcanism and normal faulting were locally superposed on structures of the Cordilleran thrust belt and Rocky Mountain foreland from about 55 to 17 Ma. Beginning about 17 Ma, volcanism and normal faulting spread to the entire western United States, marking the initiation of the Basin and Range tectonic province. The Basin and Range Province is located mainly between the Sierra Nevada Mountains of California and the Wasatch fault, and is characterized by normal faulting that resulted in long, narrow, fault-bounded mountain ranges paired with adjacent basins. Basin-and-Range-age normal faults are also present east of the Wasatch fault, where they reactivate thrust-fault ramps.

The study area contains three major Tertiary normal-fault systems. Normal faults in the northeast corner of plate 1 are the southern end of the west-dipping Acocks normal-fault zone, which was active from about 49 to 27 Ma (Lamerson, 1982; Constenius, 1996), and which juxtaposes Cretaceous rocks in its footwall against Tertiary rocks in its hanging wall. The Acocks fault zone accommodated about 3,600 feet (1,100 m) of vertical displacement in the study area, and greater amounts of throw to the north (cross section K-K′, plate 3; Lamerson, 1982; Constenius, 1996). Up to 6,890 feet (2,100 m) of volcaniclastic sediment (Norwood Tuff and Bulldog Hollow Member of Fowkes Formation; plates 1 and 2), only a small part of which is preserved in the study area, accumulated on the hanging wall of the Acocks fault zone while it was active, and faulting outlasted deposition.

West of the Acocks normal-fault zone is a west-dipping normal fault with an arcuate trace, herein named the Chappel Mine fault (figure 7; plate 1; cross sections I-I′, J-J′, and K-K′, plate 3; Lamerson, 1982). The Chappel Mine fault merges at depth with the thrust fault that cuts the east limb of the Coalville anticline (cross section K-K′, plate 3; Lamerson, 1982). Vertical displacement on the Chappel Mine fault decreases from about 1,640 feet (500 m) near Chalk Creek (cross sections J-J′ and K-K′, plate 3) to about 984 feet (300 m) near Wanship (cross section I-I′, plate 3).

The third major normal fault system in the study area bounds Kamas Valley, and is discussed in the following section.

Structure of Kamas Valley

Quaternary and Tertiary Units

Peterson (in Baker, 1970) suggested that Kamas Valley is a graben, bounded on its east and west sides by Tertiary normal faults. Sullivan and others (1988) named these faults the East and West Kamas Valley faults, respectively. Both faults are concealed, and their presence is deduced from gravity, well, and geomorphic data (Peterson in Baker, 1970; Sullivan and others, 1988) and from the morphology of the western Uinta Mountains adjacent to the valley (Sullivan and others, 1988). The name East Kamas Valley fault zone is used herein to emphasize that at least two fault strands form the structural boundary between Kamas Valley and the western Uinta Mountains. Sullivan and others (1988) estimated throws of 1,580 feet (482 m) for the East Kamas Valley fault zone and 1,180 feet (360 m) for the West Kamas Valley fault, based on the elevation differences between the base of the Keetley Volcanics in exposures in the footwalls of both faults and in an oil test well in northern Kamas Valley (well 20, table A.1)

The East Kamas Valley fault zone dips west and juxtaposes a hanging wall of unconsolidated sediments and Keetley Volcanics against a footwall composed of Paleozoic rocks locally overlain by Keetley Volcanics (cross sections B-B′ through F-F′, plate 3). The East Kamas Valley fault zone continues into Mesozoic bedrock north of Kamas Valley, and likely splays southward into two strands, one arcuate and concave-northwest and the other concave-east, following the western margin of the Uinta Mountains (figure 7 and plate 1).

The West Kamas Valley fault dips steeply east, and juxtaposes a hanging wall of Quaternary sediments and Keetley Volcanics against a footwall composed of Keetley Volcanics overlying Mesozoic sedimentary rocks (cross sections C-C′ through F-F′, plate 3).

Both the East and West Kamas Valley faults cut the Keetley Volcanics but do not cut Bull Lake-age deposits (Sullivan and others, 1988), constraining much of their displacement to between about 33 Ma, the youngest radiometric age obtained from the Keetley Volcanics (Bromfield and others, 1977), and about 150 ka, the approximate beginning of the Bull Lake glacial event.

Water-well data, geologic mapping, and the gravity survey performed for this study require revision of some of the conclusions about the East and West Kamas Valley faults outlined above. The Oakley City "Woodside well" in the northeast part of Kamas Valley intercepted the Triassic Thaynes and Woodside Formations beneath 295 feet (90 m) of alluvium (well B, table A.2; cross section F-F′, plate 3; Weston Engineering, 1999a), whereas the Pennsylvanian Weber Quartzite is exposed in the western Uinta Mountains just 0.25 miles (0.4 km) to the east. This relationship requires a west-side-down normal fault between the well and the mountain front, as shown by Sullivan and others (1988) and Bryant (1990). Additionally, mapping completed as part of this study in the western Uinta Mountains east of the Oakley well revealed a previously unrecognized north-striking, west-side-down normal fault (figure 11; plate 1; cross section F-F′, plate 3). Outcrops and the log of the Oakley City "Humbug well" (well C, table A.2) tightly constrain the geometry of the footwall. This new information indicates that the East Kamas Valley fault zone in the northeast part of Kamas Valley consists of at least two strands that together

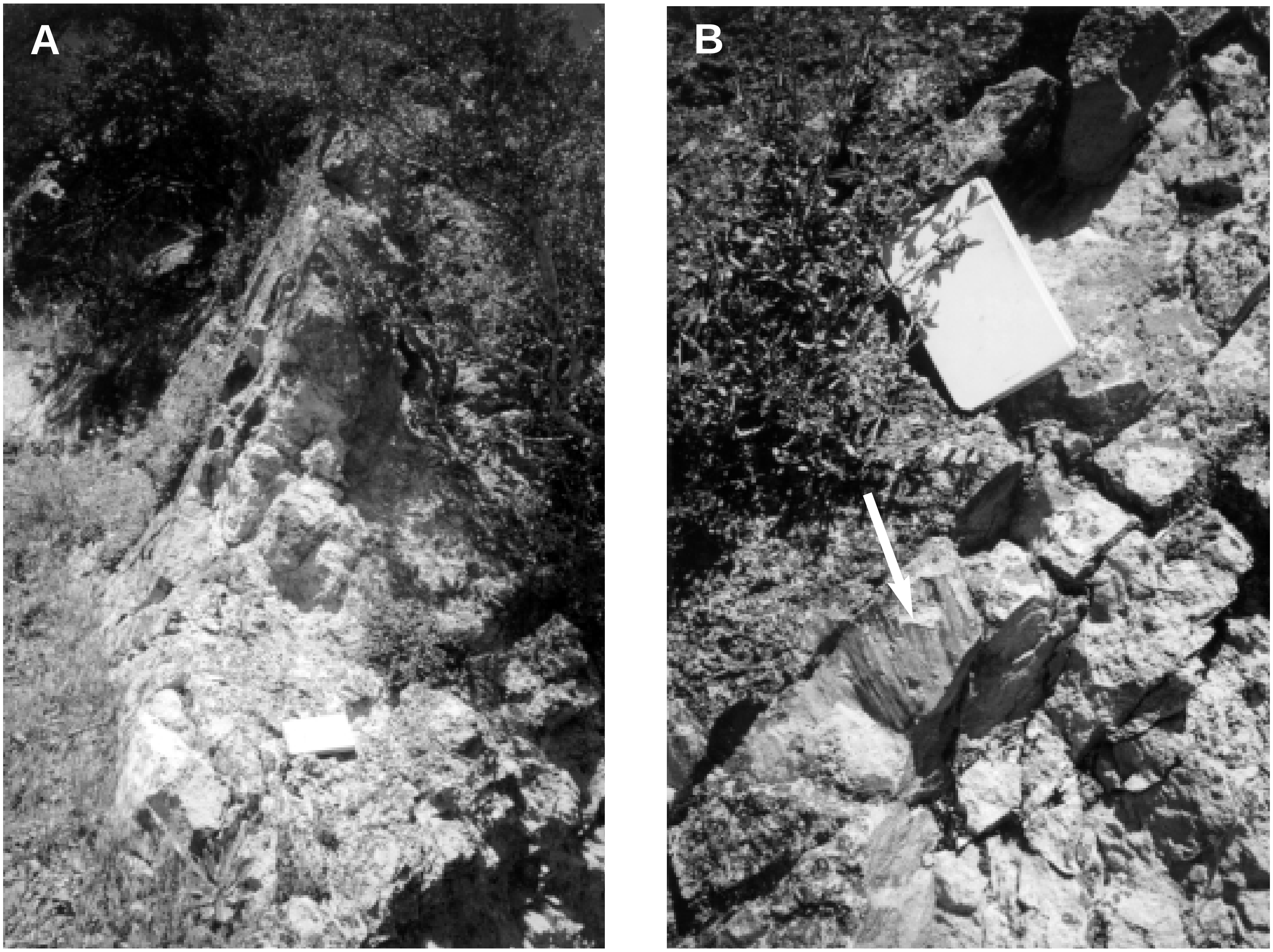

Figure 11. *Exposed strand of East Kamas Valley fault zone, northeast of Kamas Valley. A. View to the north of silicified breccia zone (resistant ridge) derived from Pennsylvanian Weber Sandstone. Recessive rock right (east) of resistant ridge is damage zone in footwall, consisting of densely jointed Weber Sandstone. Area left (west) of ridge is unexposed hanging wall. Notebook is 4.7 x 7.5 inches (12 x 19 cm). B. View to east of silicified fault breccia and slickenside surface (indicated by arrow) with striae (linear streaks on slickenside surface). The slickenside surface strikes north and dips 88 degrees west, and represents the slip plane of an episode of fault movement. The striae plunge about 80 degrees south. Notebook is 4.7 x 7.5 inches (12 x 19 cm).*

accommodated 3,200 feet (975 m) of west-side-down throw (cross section F-F′, plate 3). Throw on the East Kamas Valley fault zone may be greater east of Marion than in the northeast part of the valley (cross section E-E′, plate 3), based on the gravity data discussed above, which indicates that the basin achieves its maximum thickness there.

In the Oakley City “Woodside well” (well B, table A.2), Weston Engineering (1999a) interpreted limestone encountered from 295 to 487 feet depth (90-148 m) as part of the Woodside Formation, based on exposures of limestone in the Park City area. This interpretation would decrease the estimated throw on the East Kamas Valley fault zone by approximately 192 to 900 feet (59-274 m) because the limestone in the well is about 192 feet (59 m) thick and the total thickness of the Woodside Formation is about 700 feet (213 m) (plate 2). The limestone is interpreted here as Thaynes Formation because no limestone was encountered in the Woodside Formation during a traverse of the entire formation in a well-exposed area about 2 miles (3.2 km) northeast of the well.

As discussed above and in appendix B, the new gravity data suggest that low-density material, comprising some combination of unconsolidated to semi-consolidated deposits and Keetley Volcanics, is at least 3,500 feet (1,067 m) thick in the hanging wall of the East Kamas Valley fault zone. The relatively low magnitude of Quaternary displacement on the East Kamas Valley fault zone (Sullivan and others, 1988) implies that Quaternary deposits comprise only a fraction of this thickness. Much of the low-density material must, therefore, be Keetley Volcanics, requiring the maximum thickness of low-density material to be greater than the maximum model value of 3,538 feet (1,067 m). On the basis of test-well drilling near Jordanelle Reservoir, the Keetley Volcanics are approximately 1,600 feet (488 m) thick in the West Hills (T. Jarvis, Montgomery-Watson, Inc., verbal communication, 2000) and are about 1,176 feet (358 m) thick in an oil-test well in the northwest part of Kamas Valley (well 20, table A.1; Sullivan and others, 1988). The gravity model, therefore, indicates thickening of the Keetley Volcanics near the East Kamas Valley fault zone.

Thickening of the Keetley Volcanics in the hanging wall of the East Kamas Valley fault zone may result from the combined effects of a paleovalley along the western margin of the Uinta Mountains, and displacement during deposition. Movement on the East Kamas Valley fault zone during eruption of the Keetley Volcanics would accommodate accumulation of a thick sequence of volcanic deposits adjacent to the fault trace. Paleotopographic lows may have existed in the area prior to eruption of the Keetley Volcanics. For example, scattered inliers of Mesozoic sedimentary rocks in the West Hills interpreted as large mass-movement blocks (Bromfield and Crittenden, 1971) indicate the presence of substantial topographic relief nearby. Uplift of the western Uinta Mountains occurred during Eocene to earliest Oligocene time (Bradley and Bruhn, 1988), and the Keetley Volcanics lap onto the range front in the southern part of Kamas Valley, indicating that the western Uinta Mountains were topographically higher than Kamas Valley prior to eruption of the Keetley Volcanics. The western front of the Uinta Mountains may have been more precipitous during Oligocene time than at present, forming a topographic buttress against which Keetley volcanic deposits accumulated. The presence of paleotopography adds significant uncertainty to Sullivan and others' (1988) estimates of throw on the East and West Kamas Valley faults cited above, because an unknown portion of the elevation difference on the base of the Keetley across the basin-bounding faults may reflect differences in land-surface elevation, rather than fault displacement.

Cross sections D-D′ and E-E′ (plate 3) are based in part on the gravity model and the hypotheses of faulting during deposition of the Keetley Volcanics and paleotopographic lows along the western margin of the western Uinta Mountains, as discussed above. However, the amount of throw on the East Kamas Valley fault zone south of cross section F-F′ (plate 3), the thicknesses of unconsolidated deposits and Keetley Volcanics, and the relative contributions of paleotopography and syn-volcanic fault displacement toward thickening of the Keetley Volcanics are not well constrained.

Pre-Tertiary Units

Cross sections A-A′ through G-G′ (plate 3) and plates 5G, 5H, and 5I illustrate the structure of pre-Tertiary rocks below Kamas Valley. The contours on plate 5 are based on several wells in Kamas Valley (table A.2) that provide limited information about the subsurface structure of pre-Tertiary rocks, and were drawn mainly by connecting control points from the cross sections in a geologically sensible manner. The contours in the footwall of the East Kamas Valley fault zone and in the western Uinta Mountains are significantly better constrained due to their proximity to outcrops and relatively simple structure.

The geometries of the large anticline and syncline below the northern part of Kamas Valley, best illustrated by the contours of the top of the Weber Sandstone (plate 5G), are not well constrained. A water well east of Oakley drilled by the U.S. Bureau of Reclamation (well A, table A.2) encountered Weber Sandstone below 90 feet (27 m) of unconsolidated deposits, but the depth to the base of the Weber is not known. The log of the Oakley City "Woodside well" (well B, table A.2) indicates that the Weber Sandstone is substantially deeper there than at the Bureau of Reclamation well, though there is uncertainty in this estimate because the dip of bedding is not known. These two wells define the anticline shown on plates 5G, 5H, and 5I, which is shown with the minimum possible amplitude allowed by the data. A fault could also account for some or all of the elevation difference on the base of the Weber Sandstone between the two wells.

Fractures

Introduction

The primary porosity and hydraulic conductivity of bedrock is greatly reduced or eliminated by cementation (Fetter, 1994). Ground water in such strata is stored in and flows through fractures and dissolution openings. Therefore, characterizing fractures and dissolution features in consolidated rocks is important to understanding their hydrogeologic properties. This section describes the results of a reconnaissance survey of fracture characteristics of the established and potential aquifers in the study area. Appendix C includes a description of data-collection methods and a data table (table C.1), and the results are summarized on plate 6.

Quantitative data on fracture properties were collected adjacent to Kamas Valley and along Chalk Creek (plate 6), to determine site-specific joint and fault characteristics and to detect regional variations. The vast majority of data are on joints, because most faults are widely spaced and poorly exposed. Joint characteristics recorded in this study include orientation of the joint plane, nature of secondary mineralization if present, relative planarity and roughness of the joint surface, location, and termination geometry. Spatial characteristics such as joint density and spacing between adjacent joints can be derived from the location data. Termination geometry helps to evaluate the degree of connectivity of the joint population.

The joint population for a data-collection site consists of all of the joints measured at that particular outcrop. Joint populations typically contain one or more distinct orientation ranges, referred to here as joint sets. One joint set is commonly most numerous and/or has the greatest average length, but most joint populations contain two or three distinct sets. In this report the most abundant joint set is referred to as the primary set, and other distinct but less abundant joint sets are referred to as secondary sets. Additionally, most units in the study area have bedding planes, which typically host a joint set. Bedding-plane joints are not well represented by the histograms of plate 6, which emphasize steeply dipping joints, but the orientation of bedding and average spacing of bedding-plane joints are reported in table C.1 for each site.

Fracture data were collected from three main geographic areas, in which different groups of rock units are exposed: Paleozoic rocks in the western Uinta Mountains adjacent to Kamas Valley and along Beaver Creek, Jurassic through Cretaceous rocks near Rockport Reservoir and north of the Weber River northeast of Kamas Valley, and Cretaceous rocks near Echo Reservoir and near Chalk Creek east of Coalville (plate 6). Joint populations have distinct characteristics in each area, likely due to differences in lithology and structural setting.

Joints

Western Uinta Mountains: Joint characteristics were measured for six outcrop areas of the Pennsylvanian Weber

Sandstone (sites KCF-1, -3, -4, -10, -12, and -15, plate 6; table C.1) along the flanks of the western Uinta Mountains, and for one outcrop area each of the Pennsylvanian Round Valley Limestone, Mississippian Humbug Formation, and the Madison Limestone and Upper Devonian Rocks unit (sites KCF-11, -5, and -2, respectively, plate 6; table C.1) along Beaver Creek. The Weber Sandstone consists of quartzite, on which the joint measurements were made, and sandstone (not exposed) interlayered at a scale of tens of feet (about 3 to 5 m; Utah Department of Water Resources, unpublished logs of Kamas City and Francis City water wells). Bedding in the Weber Sandstone dips 10 to 30 degrees southwest to west. The Round Valley Limestone, Humbug Formation, and Mississippian-Late Devonian Limestone units consist of medium-grained bioclastic limestone with bed thickness on the order of 1 to 10 feet (0.3-3 m). Bedding in the Humbug Formation (site KCF-5, plate 6) and Madison Limestone and Upper Devonian Rocks (site KCF-2, plate 6) dips 15 to 35 degrees southwest.

The joint-population characteristics of these sites are broadly similar. Most sites have bimodal frequency and average length distributions (plate 6), with primary sets striking west-northwest to northwest and northeast. Either the primary or the secondary set may have the greatest average length. Two secondary joint sets are present at some sites.

Joint density at these sites ranges from 1.1 to 4.7 feet per square foot (3.5-15.5 m/m^2) (table C.1). Members of the primary and secondary joint sets terminate against each other or in undeformed rock, suggesting that they formed at the same time (Lorenz and Finley, 1991). The presence of two near-perpendicular joint sets with comparable average lengths and numerous intersections implies good connectivity of the joint population as a whole (Long and Witherspoon, 1985). Joints in the Weber Sandstone are smooth, planar, and lack mineralization. Joints in limestones of the Round Valley, Humbug, and Mississippian-Late Devonian units are smooth and planar but are typically healed by a layer of microcrystalline calcite about 0.04 inches (1 mm) thick.

West Hills: Fractures in the Indian Hollow area were measured from a black and white aerial photograph, on which they are clearly visible (figure 12; appendix C). Most fractures in the Indian Hollow area strike north-northwest to northwest (sample site KCF-22, table C.1 and plate 6). The distribution of average fracture-trace lengths is relatively uniform, with a north-northwest-striking maximum. Field observations indicate that most fractures are joints with straight traces that lack cement (figure 12A). Due to the scale of observation, joint terminations could not be observed and measured lengths are approximate, so joint densities were not calculated from the joint-length measurements.

Rockport Reservoir and Weber River northeast of Kamas Valley: In this area, joint characteristics were measured in the Cretaceous Kelvin (site KCF-18, plate 6) and Frontier (site KCF-9, plate 6) Formations, the Watton Canyon and Rich-Sliderock Members of the Jurassic Twin Creek Limestone (sites KCF-7 and -14, plate 6), the Jurassic Nugget Sandstone (sites KCF-8 and -13, plate 6), and the Triassic Thaynes Formation (site KCF-6, plate 6). The Kelvin and Frontier Formations consist of interlayered sandstone and mudstone; joints were measured in sandstone beds. The Watton Canyon Member of the Twin Creek Limestone consists of hard, clayey micrite with sharply defined layering about 1 to 5 feet (0.3-1.5 m) thick. Site KCF-7 (plate 6) also includes data from an outcrop of the Rich-Sliderock Member of the Twin Creek Limestone, which is lithologically similar to the Watton Canyon Member. The Thaynes Formation consists of limestone and sandstone interlayered at a scale of 1 to 5 feet (0.3-1.5 m). The Nugget Sandstone consists entirely of cross-bedded eolian sandstone, but lacks distinct compositional layering and bedding-plane joints. These units are deformed by faults of the Absaroka thrust system and by tilting to the northwest during large-scale folding and uplift of the Uinta arch (Crittenden, 1974; Bradley and Bruhn, 1988).

Joint-population characteristics in this area are variable, likely due to differences in composition, layer thickness, and distance from faults and folds. Most sample sites feature bimodal frequency and length distributions, with a north-northwest-striking primary set and a west to west-northwest-striking secondary set. The primary sets typically have the greatest average lengths and are oldest, based on joint-termination relations. Joints of the secondary sets are bounded by joints of the primary set, providing good connectivity parallel to the north-northwest-striking primary sets. Understanding the controls of lithology and structural position on joint-population characteristics in this complex area would require extensive work beyond the scope of this project.

Joint density varies from 2.0 to 3.8 feet per square foot (6.5-12.5 m/m^2) near Rockport Reservoir, and from 1.4 to 2.1 feet per square foot (4.8-7.1 m/m^2) along the Weber River northeast of Kamas Valley (table C.1). The greater joint density near Rockport Reservoir reflects the presence of several thrust faults and greater tilting related to uplift of the Uinta arch. Most joints in the Cretaceous formations are smooth, planar, and filled with calcite. Joints in the Twin Creek Limestone are moderately rough at a scale of about 1 foot (0.3 m), and some are lined by a veneer of microcrystalline calcite. Joints in the Nugget Sandstone and Thaynes Formation are planar, smooth, and lack mineralization. Joint zones are present in the Thaynes Formation.

Echo Reservoir and Chalk Creek: These sample sites are in sandstone layers of the Cretaceous Frontier and Kelvin Formations. Layer thickness is about 1 to 10 feet (0.3-3.0 m). Bedding at these sites dips 10 to 30 degrees northwest; they are located on the west limb of the Coalville anticline.

The joint-population characteristics of these sample sites are quite consistent. The primary set strikes northwest, has the greatest average length, and formed the earliest based on joint-termination relations. An exception is site KCF-21, at which the primary set strikes northeast. One or two secondary sets typically occur, one perpendicular to the primary set and the other (if present) bisecting the first two sets. Joint density ranges from 0.6 to 4.5 feet per square foot (2.0-14.9 m/m^2) (table C.1). This joint-density range is lower than in the western Uinta Mountains and Rockport areas, likely reflecting the less-deformed structural setting. Joint zones are common in the Oyster Ridge Sandstone Member of the Frontier Formation, not only at site KCF-16 but everywhere this unit crops out in the study area. A joint density of 4.5 feet per square foot (14.9 m/m^2) (table C.1) was measured in a joint zone at site KCF-16. The secondary joint sets produce good connectivity parallel to the primary set. Joints are planar, smooth, and filled with microcrystalline to crystalline calcite deposits as thick as 0.2 inches (5 mm).

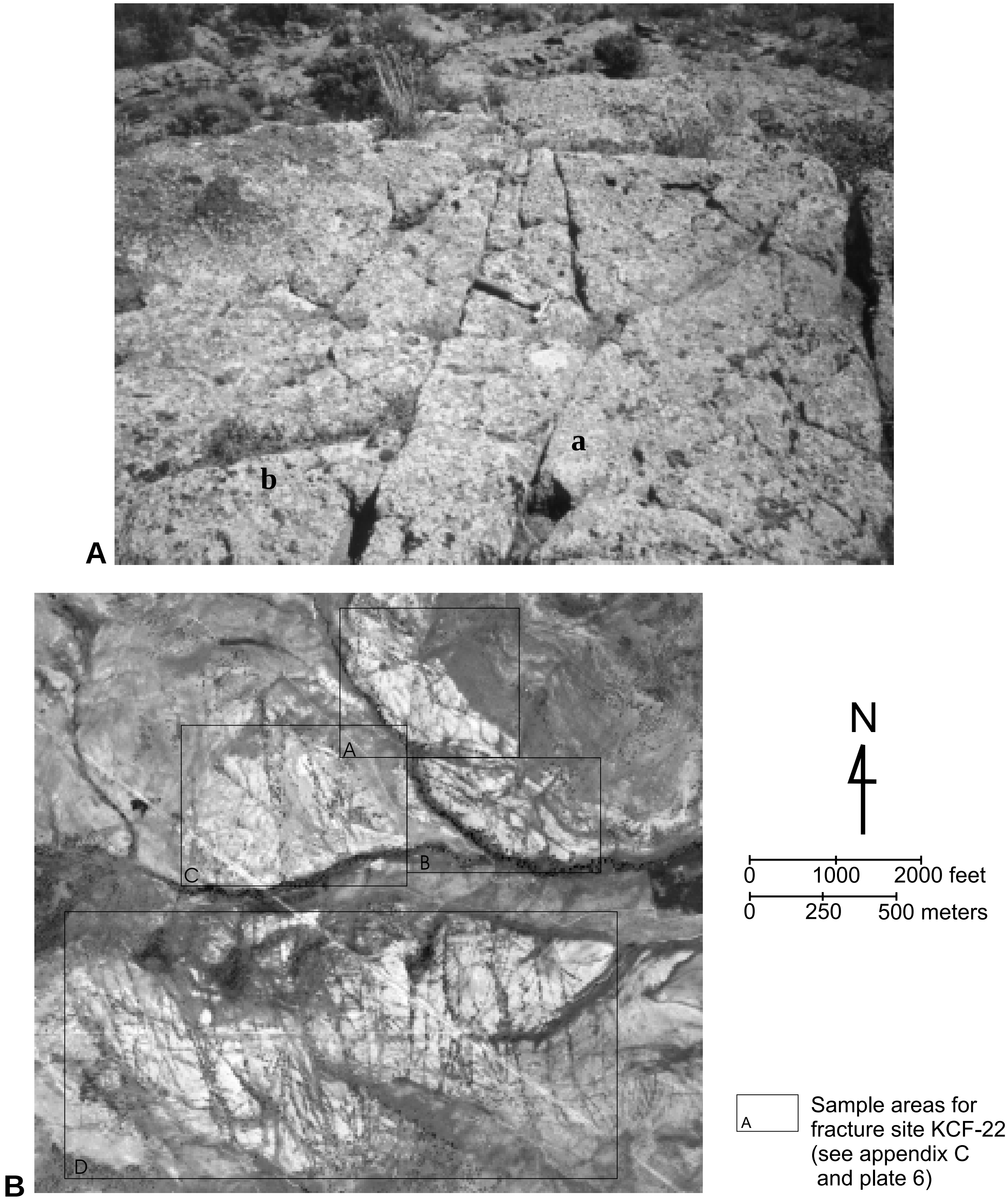

Figure 12. *Joints in Keetley Volcanics. A. View to the northeast of lava flow on ridge north of Indian Hollow. Primary joint sets strike northeast (labeled a) and east-northeast (labeled b). Hammer is 11 inches (28 cm) long. B. Aerial photograph of ridge south of Indian Hollow, showing large-scale joints or joint zones.*

Faults

Although several faults are present in the study area, exposures of fault zones are rare. Two localities described below provide limited information on the internal structure of faults in the study area.

A strand of the East Kamas Valley fault zone is exposed in the Uinta Mountains adjacent to the northeast corner of Kamas Valley (figures 7 and 11). This fault strikes north, dips steeply west, juxtaposes the Permian Park City Formation in the hanging wall against the Weber Sandstone in the footwall, and accommodated about 1,000 feet (305 m) of throw (cross section F-F′, plate 3)

The well-exposed internal structure of this fault consists of a fault core and an adjacent damage zone (figure 11; Caine and others, 1996). The fault core consists of a 2- to 3-foot-thick (0.6-0.9 m) tabular breccia zone, composed of angular clasts of quartzite of the Weber Sandstone in a very hard silica cement (figure 11). The western margin of the core contains striated slickensides that record normal dip-slip. The damage zone is characterized by a dense array of joints cut by subsidiary faults. The joints include two steeply dipping sets and one gently dipping bedding-plane set, all closely spaced (plate 6 and table C.1). Joint density in this damage zone is 3.6 to 16.8 feet per square foot (12-56 m/m^2) (table C.1). Individual joints are planar, smooth, and lack mineralization. The subsidiary faults are approximately perpendicular to the main fault zone, contain a core zone composed of gouge less than 1 inch (2.5 cm) thick, and are spaced 5 to 10 feet (1.5-3 m) apart.

Thrust and normal faults are exposed in the Twin Creek Limestone at sample site KCF-7 (plate 6). The thrust faults strike northeast, dip about 30 degrees southeast, and contain a 3- to 4-inch-thick (8-10 cm) core zone of scaly, clay-rich gouge with sparse calcite veins. The normal faults strike north-northwest, dip about 50 degrees east-northeast, and contain a 1.2- to 2.0-inch-thick (3-5 cm) core zone of scaly, clayey gouge. Fault spacing could not be determined. The faults have prominent damage zones about 6 inches (15 cm) thick with high joint density.

The major fault zones in the study area are not exposed, so their physical properties can only be inferred. It is uncertain how representative the exposure of the East Kamas Valley fault zone described above is of that fault elsewhere or of other faults in the Weber Sandstone. The silica cement resulted from circulation of fluids along the fault plane, but it is unclear whether this was a localized process or whether it occurred along the entire length of the fault, and whether this process occurred along other faults. Fault-zone fabrics in the Twin Creek Limestone described above provide a reasonable model for unexposed faults in that unit, with the thickness and complexity of the gouge zone likely increasing with greater displacement.

Ashland and others (2001) discuss the internal structure of fault zones exposed near Snyderville basin, 14 miles (22 km) west of Kamas Valley. A thrust fault juxtaposing the Triassic Ankareh and Thaynes Formations contains a 6.5-foot-thick (2 m) core zone of scaly, fine-grained gouge derived from both units (table 3 and figures 25 and 26 of Ashland and others, 2001). A densely jointed damage zone is developed in the Thaynes Formation adjacent to the core zone, but the Ankareh Formation lacks a significant damage zone (Ashland and others, 2001). This fault and the thrusts near Rockport Reservoir are part of the Absaroka thrust system (Crittenden, 1974). Faults in the Nugget Sandstone contain a densely jointed damage zone up to 6.5 feet (2 m) thick, and sporadic, thin layers of clay-size gouge (Ashland and others, 2001, table 3).

Based on the examples described above, it is reasonable to assume that the major faults in the study area contain clay-rich gouge zones about 6 inches to 6.5 feet (0.2-2 m) thick, with adjacent densely jointed damage zones in sandstones and limestones. The existence and degree of development of fault gouge and damage zone at any location depend strongly on the rock types juxtaposed by the fault (Caine and others, 1996; Ashland and others, 2001).

IMPLICATIONS FOR GROUND-WATER CONDITIONS

Introduction

This section discusses possible effects of the stratigraphy and structure described above on hydrogeologic properties of geologic units and regional ground-water flow in the study area, focusing on Kamas Valley and the Coalville-Chalk Creek area. This evaluation is necessarily qualitative, invoking general principles and examples from other regions, because data on the hydrogeologic properties of rock and unconsolidated sediments in the study area are sparse. Water wells in the study area provide limited but important hydrogeologic information, and work by the U.S. Geological Survey will also contribute significant data.

Hydrogeology of Unconsolidated Deposits

The U.S. Bureau of Reclamation conducted the only aquifer test in unconsolidated deposits in the study area (Baker, 1970). This test, located near the Wanship dam in alluvial deposits of the Weber River, indicated a transmissivity of about 5,400 square feet per day (502 m^2/d) and a hydraulic conductivity of about 22 feet per day (6.7 m/d) (Baker, 1970).

Due to the lack of data from unconsolidated deposits in the study area, their hydrogeologic properties can only be inferred from their texture and composition. The hydraulic conductivity of sediment increases with mean grain size and with degree of sorting (uniformity of grain size). Clay-rich deposits have high porosity due to the internal structure of clay minerals, but have relatively low hydraulic conductivity. Based on these principles and on Fetter's (1994) compilation of variation in hydraulic conductivity with texture and composition, the sediment types in Kamas Valley and adjacent valleys of the Weber River can be assigned approximate, preliminary hydraulic conductivity ranges (table 1). Pleistocene sediments are assigned lower hydraulic conductivity estimates than equivalent Holocene sediment types because they typically have higher clay content and finer grained matrix material, due to their derivation in part from glacial deposits. Aquifer testing coupled with detailed well logs would better characterize the hydrogeologic properties of unconsolidated sediments in the study area.

Most of the sediment types in table 1 contain discrete beds of varying texture and composition, interlayered both vertically and horizontally at scales of one to tens of feet (0.3-3 m). Hydraulic conductivity parallel to layering is typically at least ten times greater than hydraulic conductivity perpendicular to layering (Fetter, 1994). The values in table 1 represent hydraulic conductivity parallel to layering and do not account for lateral variations in composition.

The schematic cross sections in figure 10 suggest possible spatial variations in the layer-parallel hydraulic conductivity of unconsolidated deposits below Kamas Valley. Holocene deposits likely have greater hydraulic conductivity than their Pleistocene counterparts, due to lower clay content. Based on its greater degree of layering and sorting, alluvium likely has a wider range and greater internal variability of hydraulic conductivity than alluvial-fan deposits. Hy-

Table 1. Hydraulic conductivity estimates for unconsolidated sediments in Kamas Valley and adjacent Weber River valleys (after Fetter, 1994).

Sediment Type	Texture	Hydraulic Conductivity Range in feet per day (cm/s) (Fetter, 1994)
Pleistocene till	Massive, poorly sorted, boulder- to pebble-size clasts; clay-rich matrix	10^{-6} - 10^{-3} (10^{-9} - 10^{-6})
Pleistocene and Holocene alluvial fans	Massive to weakly layered, poorly to moderately sorted, boulder- to pebble-size clasts; Pleistocene fans have clay-rich matrix	10^{-2} -1 (10^{-5} - 10^{-3})
Pleistocene outwash and alluvium	Layered, moderately to well sorted; clay-rich matrix	1 - 100 (10^{-3} - 10^{-1})
Holocene alluvium	Layered, well-sorted, sandy to silty matrix	1 - 1,000 (10^{-3} - 1)
Holocene and Pleistocene landslides	Massive, poorly sorted, boulder- to pebble-size clasts; volumetric ratio of rock to sediment may vary widely	Hydrologic properties are difficult to predict

draulic conductivity may decrease with depth, due to the higher clay content of older sediments and the effects of compaction. Hydraulic conductivity at all depths may increase from east to west as the relative proportion of alluvial to alluvial-fan deposits increases. This possible westward increase in hydraulic conductivity may not be uniform with depth, however, because Bull Lake-age alluvial fans apparently prograded farther west than older and younger alluvial fans.

Over 300 wells are screened in the unconsolidated deposits of Kamas Valley; most are located along the eastern and northern margins of the valley and are used for domestic, irrigation, and stock watering purposes (Utah Division of Water Resources data; table A.3 contains a subset of wells in Kamas Valley). Several springs emanate from the unconsolidated deposits; Tater Hollow and Jacks Spring (figure 1) are used for public supply.

Hydrogeology of Fractured Rock

Introduction

The following paragraphs discuss the concepts of aquifer compartmentalization and the effects of fractures on groundwater flow, to provide background for discussion of the relations among stratigraphy, structure, and regional groundwater flow. The terms stratigraphic ground-water compartment (SGWC), heterogeneous SGWC, and structural ground-water compartment are used as described in the introduction to this report and in the glossary.

Effects of Fractures on Ground-Water Flow

Joints: Delineation of stratigraphic ground-water compartments requires an evaluation of the relative hydraulic conductivity of geologic formations and members. Density and connectivity of fractures largely determine the hydraulic conductivity and storage of water in consolidated rock units. In rocks that have no primary porosity and permeability, joints and faults provide both storage and transport pathways for ground water. In fractured rocks that retain some primary porosity and permeability, storage occurs chiefly in the matrix pore spaces and transport occurs primarily along fractures or dissolution features. The "Structural Geology of Consolidated Rock" section above describes the properties of joints and faults that most strongly affect hydraulic conductivity, and the "Proposed Hydrostratigraphy" section below evaluates the relative hydraulic conductivity of geologic units based in part on these properties.

The aperture of individual joints and the connectivity of a joint population are the most important characteristics affecting the hydraulic conductivity of jointed rock. Joint aperture on outcrops is strongly influenced by weathering processes, so cannot be used to predict aperture at depths below the weathering zone, which is approximately 10 to 50 feet (3-15 m) deep. Mineral deposits lining joint faces may reduce or eliminate aperture.

Connectivity refers to the degree of interconnection of a joint population (Long and Witherspoon, 1985). The direction of greatest hydraulic conductivity in a jointed rock mass is parallel to the direction of greatest joint connectivity (Long and Witherspoon, 1985; LaPointe and Hudson, 1985). However, connectivity is a complex function of joint density, size (length and width), and orientation distribution; determining the directions of greatest connectivity and hydraulic conductivity in a rock mass requires extensive data collection and time-intensive computer modeling beyond the scope of this study. Consequently, the discussion below notes observable joint characteristics such as joint density and the presence or absence of mineralization and qualitatively evaluates the relative connectivity of joint populations, but does not estimate values or directional properties of hydraulic conductivity.

Faults: The hydrogeologic properties of faults depend on the nature and degree of development of fault-zone material in the fault core, and on the characteristics of the adjacent damage zone (Caine and others, 1996). Fault cores containing fine-grained, clay-rich gouge have very low hydraulic conductivity transverse to the fault plane (Caine and others, 1996). Fault cores are well developed where faults cut fine-grained and/or clay-rich units, and are poorly developed in quartz-rich sandstone and clay-poor limestone (Caine and others, 1996; Ashland and others, 2001). Damage zones with high joint density and unmineralized joint faces have high hydraulic conductivity parallel to the fault plane (Caine and others, 1996). Damage zones are well developed in tightly cemented sandstone and limestone units and are poorly developed in weakly cemented and/or fine-grained, clay-rich units. The nature and degree of development of fault-zone structure and materials also depend on the temperature, pressure, and presence of fluids during faulting (Twiss and Moores, 1994) and are, therefore, difficult to predict for unexposed faults.

Proposed Hydrostratigraphy

The Snyderville basin, located about 14 miles (22 km) west of Kamas Valley, provides a hydrostratigraphic model, including well-test and production data, for the present study (figures 13 and 14) (Weston Engineering, 1996 and 1999a; Ashland and others, 2001). This model is qualitative, however, because lithologic properties affecting ground-water flow and storage, such as porosity and fracture-derived permeability, may vary between Snyderville basin and the Kamas-Coalville area, as does the hydrologic setting. The most important SGWCs are described briefly here and in greater detail in appendix D.

Kamas Valley and adjacent mountains: The Keetley SGWC, composed of the Tertiary Keetley Volcanics, crops out in the West Hills, the hills north of Kamas Valley, and parts of the Uinta Mountains adjacent to the valley, and it underlies much of the valley (figures 13 and 14; plates 1 and 2). The Keetley Volcanics consist of complexly interlayered volcanic breccia, tuff, and flows (plate 2; Woodfill, 1972; Leveinen, 1994). The volcanic breccia likely derives its hydraulic conductivity from both joints and its weakly to moderately cemented, poorly sorted matrix. Hydraulic conductivity in flows is likely provided by joints and by discontinuities along flow boundaries. The tuff may have the lowest hydraulic conductivity due to its fine-grained, ash-rich matrix. The Keetley SGWC overlies folded and faulted Mesozoic and Paleozoic sedimentary rocks in the West Hills. On the basis of test wells drilled near Jordanelle Reservoir, the basal tuff facies may provide a confining or leaky confining layer where present (T. Jarvis, verbal communication, 2000). Numerous private wells in the West Hills draw water from the Keetley SGWC.

Mesozoic sedimentary rocks are important aquifers in the Snyderville basin - Park City area (Ashland and others, 2001) but host very few wells in the study area, in part because their outcrop areas are limited and they occur in sparsely populated areas. Sandstones or well-cemented clayey limestones form SGWCs, and intervening mudstones are low-permeability units (figure 13). The sandstones may retain some primary hydraulic conductivity in addition to that provided by joints.

The Kelvin-Preuss heterogeneous SGWC is exposed near Rockport Reservoir, where it is folded and cut by thrusts of the Absaroka system (figure 14; cross section I-I′, plate 3). Joints in sandstones in this area are typically filled with calcite, reducing fracture-related hydraulic conductivity.

The Jurassic Twin Creek Limestone contains three SGWCs - the Rich-Sliderock, Watton Canyon, and Giraffe Creek - and three low-permeability units (figure 13; Ashland and others, 2001). The Twin Creek SGWCs are exposed north of Kamas Valley, where they are folded and cut by thrusts (cross sections G-G′ through I-I′, plate 3). The Nugget SGWC is exposed just north of the Weber River northeast of Kamas Valley, and dips northwest. Plates 5A through 5D illustrate the subsurface structure of the Watton Canyon and Nugget SGWCs.

The Thaynes SGWC is composed of interbedded sandstone and limestone of the Triassic Thaynes Formation, and is bounded above and below, respectively, by the Mahogany Member of the Triassic Ankareh Formation and the Triassic Woodside Formation, both low-permeability units (figure 13). In the Snyderville basin area, a shale layer in the middle of the Thaynes Formation divides it into two aquifers with little or no hydrologic communication (Weston Engineering, 1996). A single exposure in Weber River canyon indicates that this shale unit is about 5 feet (1.5 m) thick in the study area. This report delineates upper and lower Thaynes SGWCs, based on comparison with the Snyderville basin area.

Joints in the Thaynes SGWC are relatively long, closely spaced, lack secondary mineralization, have good connectivity, and are locally clustered into joint zones. The structure of the Thaynes SGWC on the northwest flank of the Uinta Mountains is illustrated by cross section H-H′ (plate 3) and on plates 5E and 5F.

The Weber SGWC consists of interbedded sandstone and quartzite of the Pennsylvanian Weber Sandstone and overlying limestones of the lower part of the Permian Park City Formation (figure 13; Ashland and others, 2001). The Weber SGWC is exposed along a horseshoe-shaped arc on the margin of the western Uinta Mountains, and bedding everywhere dips away from the mountains (cross sections A-A′ through H-H′, plate 3; plates 5G and 5H). Low-permeability units consisting of phosphatic mudstone in the Park City Formation and interbedded mudstone and siltstone in the upper part of the Pennsylvanian Morgan Formation bound the Weber SGWC above and below, respectively. Joints in quartzites of the Weber SGWC provide secondary hydraulic conductivity; they are relatively long, moderately dense, have good connectivity, smooth surfaces, and lack mineralization. The sandstone layers are poorly exposed, but presumably have similar joint characteristics.

The Weber SGWC provides culinary water through wells to the towns of Kamas, Francis, and Woodland (wells E, G, and H, figure 1 and table A.2) as well as many private users, and through springs to Oakley and (formerly) Kamas (see appendix D for details). Recharge is provided by infiltration of snowmelt and rainfall in the western Uinta Mountains.

The Humbug-Uinta SGWC is composed of limestone and sandstone of the Mississippian Humbug Formation, limestone of the Madison Limestone and Upper Devonian Rocks unit, quartzite of the Tintic Quartzite, and interbedded quartzite and shale of the Proterozoic Uinta Mountain Group

EON	PERIOD	GEOLOGIC UNIT	MAP SYMBOL (plate 1)	THICKNESS IN FEET (m)	LITHOLOGY (see fig. 6 for symbols)	HYDROSTRATIGRAPHY
CENOZOIC	Quaternary	Alluvial, glacial, landslide, & colluvial deposits	Q	0-500 (0-152)		Unconsolidated deposits
CENOZOIC	Tertiary	Keetley Volcanics and related intrusive rocks	Tkf, Tkb, Tkt, Tlp, Tki	0-1,640 (0-500)		Keetley SGWC
CENOZOIC	Tertiary	older conglomerate	Toc	0-984 (0-300)		Keetley SGWC
CENOZOIC	Tertiary	Bulldog Hollow Mbr. of Fowkes Fm.	Tfb	0-500 (0-152)		Keetley SGWC
CENOZOIC	Tertiary	Wasatch Formation	Tw, Twc	3,930 (1,200)		
MESOZOIC	Cretaceous	Hams Fork Member of Evanston Formation	Keh	<2,620 (<800)		Wasatch-Evanston heterogeneous SGWC
MESOZOIC	Cretaceous	Adaville & Hilliard Formations	Kah	4,495? (1,370?)		Adaville-Hilliard heterogeneous SGWC
MESOZOIC	Cretaceous	Echo Canyon Conglomerate	Ke	2,620 (800)		Echo-upper Frontier heterogeneous SGWC
MESOZOIC	Cretaceous	Henefer Formation	Khe	2,620 (800)		Echo-upper Frontier heterogeneous SGWC
MESOZOIC	Cretaceous	Frontier Formation: upper member	Kfu	2,620-3,600 (800-1,100)		Echo-upper Frontier heterogeneous SGWC
MESOZOIC	Cretaceous	Frontier Formation: Oyster Ridge Sandstone	Kfo	200-330 (60-100)		Oyster Ridge SGWC
MESOZOIC	Cretaceous	Frontier Formation: lower member	Kfl	4,495 (1,370)		lower Frontier heterogeneous SGWC
MESOZOIC	Cretaceous	Aspen Shale & Sage Junction Fm.	Ka, Ksj	<525 (<160)		
MESOZOIC	Cretaceous	Kelvin Fm: upper member; Cokeville & Thomas Fork Fms.	Kk, Kc, Ktf	1,640-4,265 (500-1,300)		Kelvin-Preuss heterogeneous SGWC
MESOZOIC	Cretaceous	Kelvin Fm: Parleys Member	Kkp	164 (50)		Kelvin-Preuss heterogeneous SGWC
MESOZOIC	Jurassic	Morrison Formation	Jm, Jms	260 (80)		Kelvin-Preuss heterogeneous SGWC
MESOZOIC	Jurassic	Stump Formation	Js, Jms	200 (60)		Kelvin-Preuss heterogeneous SGWC
MESOZOIC	Jurassic	Preuss Sandstone	Jp	984 (300)		Kelvin-Preuss heterogeneous SGWC
MESOZOIC	Jurassic	Twin Creek Limestone: Giraffe Creek Member	Jtgc	82 (25)		Giraffe Creek SGWC
MESOZOIC	Jurassic	Twin Creek Limestone: Leeds Creek Member	Jtl	776 (236)		
MESOZOIC	Jurassic	Twin Creek Limestone: Watton Canyon Mbr	Jtw	220 (67)		Watton Canyon SGWC
MESOZOIC	Jurassic	Twin Creek Limestone: Boundary Ridge Mbr	Jtb	107 (33)		
MESOZOIC	Jurassic	Twin Creek Limestone: Rich & Sliderock Mbrs	Jtrs	172 (52)		Rich-Sliderock SGWC
MESOZOIC	Jurassic	Twin Creek Limestone: Gypsum Spring Mbr	Jtg	22 (7)		
MESOZOIC	Jurassic	Nugget Sandstone	Jn	919-1,250 (280-381)		Nugget SGWC
MESOZOIC	Triassic	Ankareh Formation: upper member	TRau	361 (110)		
MESOZOIC	Triassic	Ankareh Formation: Gartra Member	TRag	66-98 (20-30)		Gartra SGWC
MESOZOIC	Triassic	Ankareh Formation: Mahogany Member	TRam	738 (225)		
MESOZOIC	Triassic	Thaynes Limestone	TRt	650-1,175 (148-358)		upper, lower Thaynes SGWCs
MESOZOIC	Triassic	Woodside Formation	TRw	700 (213)		
PALEOZOIC	Permian	Park City Formation	Ppc	775-950 (236-290)		upper Park City SGWC
PALEOZOIC	Penn	Weber Sandstone	IPw	1,730-2,600 (527-792)		Weber SGWC
PALEOZOIC	Penn	Morgan Formation	IPm	200-500 (61-52)		Morgan-Round Valley heterogeneous SGWC
PALEOZOIC	Penn	Round Valley Limestone	IPr	170-700 (52-213)		Morgan-Round Valley heterogeneous SGWC
PALEOZOIC	Miss	Doughnut Formation	Mdo	175-650 (53-198)		
PALEOZOIC	Miss	Humbug Formation	Mh	420-1,500 (128-457)		Humbug-Uinta SGWC
PALEOZOIC	Miss / Dev	Madison Limestone & Upper Devonian rocks	MDmu	325-1,250 (99-381)		Humbug-Uinta SGWC
PALEOZOIC	Cam	Tintic Quartzite	Ct	0-328 (0-100)		Humbug-Uinta SGWC
PROTEROZOIC	Middle Proterozoic	Uinta Mtn Group: Red Pine Shale	Yur	2,953 (900)		Humbug-Uinta SGWC
PROTEROZOIC	Middle Proterozoic	Uinta Mtn Group: Hades Pass unit	Yuh	5,906 (1,800)		Humbug-Uinta SGWC
PROTEROZOIC	Middle Proterozoic	Uinta Mtn Group: Mount Watson unit	Yuw	3,281 (1,000)		Humbug-Uinta SGWC

Figure 13. Proposed hydrostratigraphy for Kamas-Coalville region. SGWC stands for stratigraphic ground-water compartment; cross-hatched pattern indicates low-permeability unit. Weber through Nugget SGWCs are from Ashland and others (2001). See appendix D for description of each SGWC and figure 14 for map. Volumetrically insignificant map units Tlam and Tlae are not shown.

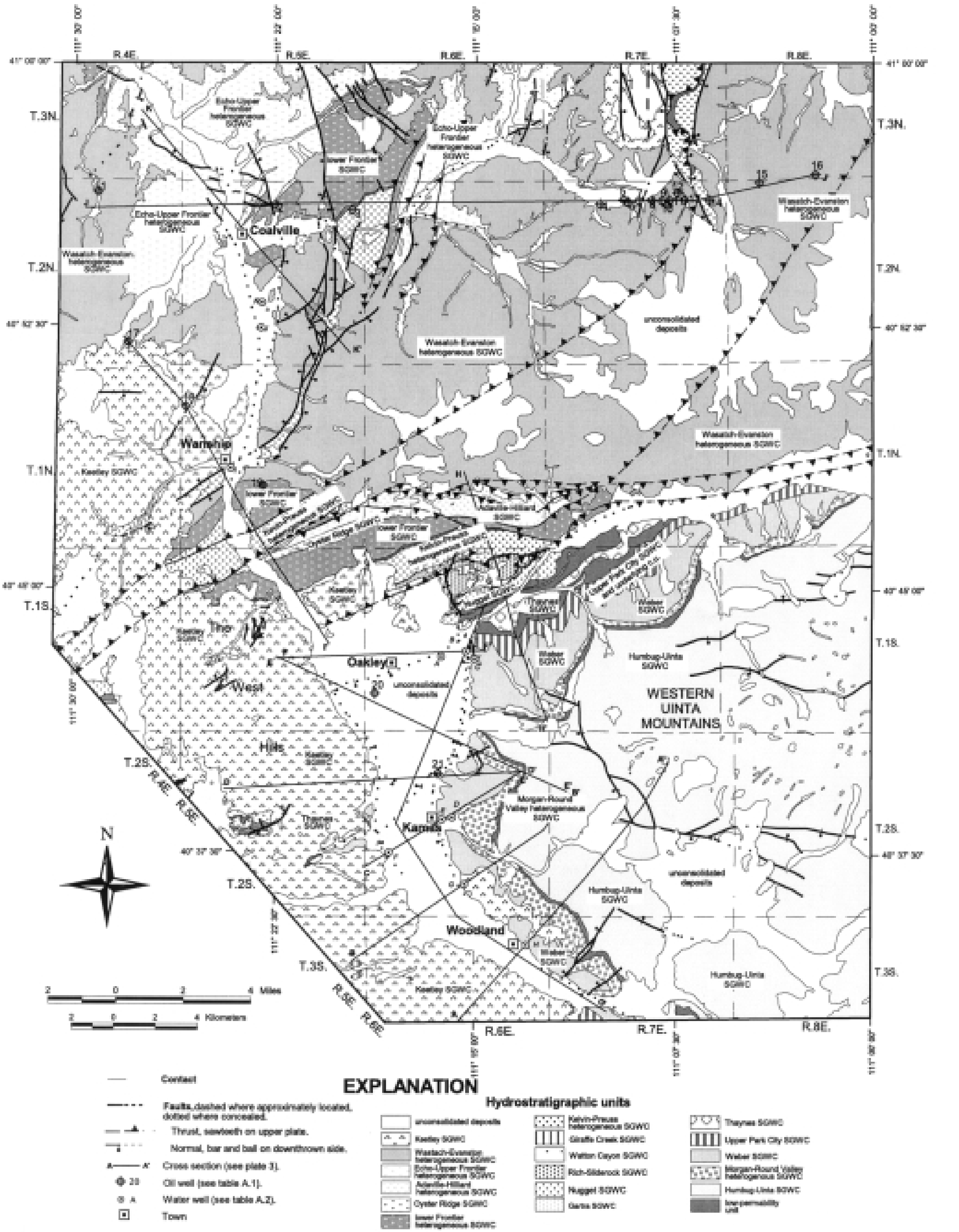

Figure 14. *Hydrostratigraphic map of the Kamas-Coalville region.*

(figure 13). The Humbug-Uinta SGWC is exposed in the western Uinta Mountains, and its structure is illustrated by cross sections A-A′ through H-H′ (plate 3) and plate 5I. Mudstones of the Mississippian Doughnut Formation form a low-permeability unit above the Humbug-Uinta SGWC, but its lower boundary is uncertain. A Mississippian-age weathering zone, characterized by cemented dissolution breccia and local fine-grained deposits, underlies the Humbug Formation. This zone is potentially a SGWC boundary, but its thickness and hydrogeologic properties are not known. The Red Pine Shale of the Uinta Mountain Group yields water to wells along Beaver Creek (appendix D), so is not considered a low-permeability unit.

Joints and dissolution features provide secondary hydraulic conductivity in limestones of the Humbug-Uinta SGWC. The dissolution features consist of tubes, less than about 3 feet (1 m) diameter where observed, along the intersection of bedding planes and steeply dipping joints (figure 15).

The Oakley City Humbug well (well C, table A.2) intersects the upper part of the Humbug Formation between 1,750 and 1,840 feet (533-561 m) depth (Weston Engineering, 1998). The well is artesian with a shut-in pressure of 26 pounds per square inch, is screened from 1,420 to 1,830 feet (433-558 m) in the lower part of the Doughnut Formation and the upper part of the Humbug Formation, and pump-tested at 650 gal/min (2,464 L/min) (Weston Engineering, 1998). Age dates of water from the Oakley Humbug well indicate that it is between 44 and 18,000 years old (Weston Engineering, 1999a), suggesting a long-term recharge path between the well and its recharge area. Recharge likely occurs where the Humbug Formation is exposed about 4.5 miles (7.2 km) southeast of the well in a topographically higher part of the western Uinta Mountains, with flow moving toward Kamas Valley. Water-level changes during drilling suggest that the upper part of the Morgan Formation and the Doughnut Formation are confining units (Weston Engineering Co., 1999a).

Left-Hand Canyon Spring, used by Kamas City (figure 1), is in the canyon bottom, underlain by the upper part of the Madison Limestone (map unit MDmu, plate 1). The spring box is in thin alluvium deposited by Left Fork Beaver Creek so the bedrock geology of the spring is not directly observable. However, exposures of the Madison Limestone about 300 feet (91 m) upstream of the spring are highly jointed and contain dissolution features along bedding-joint intersections (figure 15). It is reasonable to assume that Left-Hand Canyon Spring issues from a similar feature just below the alluvium.

Echo Reservoir to Chalk Creek: The SGWCs in this subarea are composed of Cretaceous units characterized by laterally discontinuous, interfingering layers of interbedded sandstone, mudstone, and conglomerate (figure 13; plate 2). Bedding typically dips 10 to 30 degrees northwest, except near the Coalville anticline, the Clark Canyon syncline, the Chappel Mine fault, and in the northeast part of the study area where the Medicine Butte thrust and Acocks normal fault crop out. The latter areas are structurally complex, characterized by numerous closely spaced faults and local overturned bedding (cross sections J-J′ and K-K′, plate 3).

The Wasatch-Evanston and lower Frontier heterogeneous SGWCs consist of several Paleocene to Cretaceous formations (figure 13), grouped together because their hydrogeologic properties are poorly known and they presently do not constitute significant aquifers in the study area. The lower contacts of the Wasatch Formation and the Hams Fork Member of the Evanston Formation are angular unconformities, and these units have variable thicknesses (Lamer-

__Figure 15.__ View to north of dissolution features in the Madison Limestone of map unit MDmu about 300 feet (91 m) north of Left-Hand Canyon Spring, about 3 miles (4.8 km) southeast of Kamas (see figure 1 for location). Small tunnels are present along intersection of bedding plane (dipping to the left [west]) and joints (vertical and north-striking). Hammer is 11 inches (28 cm) long.

son, 1982). Vertically stacked clusters of sandstone beds, present in parts of all of the formations in this SGWC, are the best prospective aquifers. Wells screened in the Wasatch Formation supply water to the cities of Coalville and Hoytsville (wells J and K, table A.2).

The Oyster Ridge SGWC consists of the Oyster Ridge Sandstone Member of the Frontier Formation, and is bounded by mudstones of the upper and lower members of the Frontier Formation (figure 13). The Oyster Ridge Sandstone is well-sorted marine sandstone with primary porosity and joint characteristics favorable for high hydraulic conductivity. Clustered sandstone beds in the lower Frontier heterogeneous SGWC also likely have significant secondary hydraulic conductivity due to joints, but are more tightly cemented.

Structural Compartmentalization

The major thrust- and normal-fault zones in the study area delineate eight large-scale structural compartments, each with varying internal complexity (figure 16; table 2). Table 2 briefly describes each structural compartment, and the following paragraphs discuss possible implications of compartmentalization for regional ground-water hydrology.

As discussed above, the physical characteristics of thrust faults in the study area are poorly known but, based on the examples described above, they likely contain significant core zones composed of fine-grained gouge, making them barriers or retardants to transverse flow. Thrust faults may also retard ground-water flow across their planes where they juxtapose SGWCs against low-permeability units. The internal structure of normal faults in the study area is even less well known than that of the thrust faults, and they may impart compartmentalization primarily due to severing of SGWCs.

Because the Western Uinta Mountains structural compartment is structurally simple, regional ground-water flow is likely down the dip direction and parallel to the topographic slope (cross sections A-A′ through H-H′, plate 3), though this flow pattern may be significantly altered where fractures trend obliquely to the dip. Much of the ground water in the Western Uinta Mountains compartment probably enters streams that flow into Kamas Valley; the quantity of underflow from the Western Uinta Mountains to the Kamas Valley-West Hills structural compartment is poorly known, but is considered to be very small (Baker, 1970; L. Brooks, U.S. Geological Survey, verbal communication, 2000).

The internal structure of the exposed strand of the East Kamas Valley fault zone in the northeast corner of Kamas Valley (figure 7) suggests that it has low permeability there, but it is unknown how representative this segment is of the entire fault zone. The East Kamas Valley fault zone likely retards ground-water flow north of Kamas due to severing of SGWCs (cross sections D-D′ through F-F′, plate 3). South of Kamas, the East Kamas Valley fault zone does not completely sever the Weber SGWC (cross sections A-A′ through C-C′, plate 3), so its effect on ground-water flow depends on whether a silicified breccia similar to that exposed in the northeast part of the valley (figure 11) is present, which is not known.

The lithologic heterogeneity of the Keetley SGWC and the structural complexity of older SGWCs underlying the Keetley SGWC and Quaternary deposits in the West Hills-Kamas Valley compartment probably result in ground-water flow patterns that are complicated and difficult to predict. The effect of the West Kamas Valley fault on ground-water flow is not known.

The structural compartments north of Kamas Valley were shaped by thrusting and folding in the Cordilleran thrust belt and along the North Flank thrust zone, and their interiors and boundaries are structurally complex. The Absaroka and North Flank thrust zones form a broad, internally complex northern boundary to the Uinta Mountains and Rockport structural compartments (figure 16), characterized by numerous northeast- to east-striking reverse faults (cross sections H-H′ and I-I′, plate 3). SGWCs in this boundary zone are truncated by faults, locally folded, and cut by small-scale faults not shown on plates 1 and 3. The internal structure of the Rockport compartment is relatively simpler, with moderately northwest- to north-dipping bedding.

Structural compartments in the hanging walls of the Absaroka and Medicine Butte thrust zones are characterized by thrust faults and associated tight to open folds in rocks below the Wasatch-Evanston heterogeneous SGWC, and by gentle dips in the Wasatch-Evanston heterogeneous SGWC (cross sections J-J′ and K-K′, plate 3). The structurally complex boundaries of these compartments, which consist of thrust faults and associated folds and, in some cases, normal faults, are best referred to as boundary zones. Bedding and SGWC boundaries in these compartments are generally parallel to the thrust faults, suggesting that ground-water flow is likely greater parallel to than across compartment boundaries.

The Absaroka Footwall, Coalville Anticline, and Echo Reservoir compartments have complex boundary zones but relatively simpler internal structure, characterized by northwest-dipping bedding and few internal faults (cross sections I-I′ through K-K′, plate 3; cross sections A-A′ and C-C′ of Bryant, 1990). Ground-water flow in these compartments is likely dominated by the combined effects of topography and SGWC geometry.

All or parts of several structural compartments underlie younger SGWCs that are relatively undeformed. Most of the hanging wall of the Medicine Butte thrust, and the hanging wall and footwall of the Absaroka thrust system underlie the Wasatch-Evanston SGWC, which is only locally affected by these thrusts (cross sections J-J′ and K-K′, plate 3). The western part of the Echo Reservoir, Rockport, and Kamas Valley-West Hills structural compartments underlie younger deposits, so their internal structure and boundaries are poorly known there.

Potential Well Targets

This section presents general guidelines for identifying potential water-well sites in the study area, and describes how the cross sections (plate 3), the isopach map (plate 4), and the structure-contour maps (plate 5) can be used for preliminary evaluation of potential sites. These suggestions refer only to geologic aspects of well-site selection; more detailed geologic evaluation of potential sites is necessary to accurately predict the subsurface location of targets and to account for local complications not shown in this report. Many other non-geologic factors also influence the selection of test-well sites.

Specific SGWCs should be targeted for test wells because they have the greatest chance of providing high

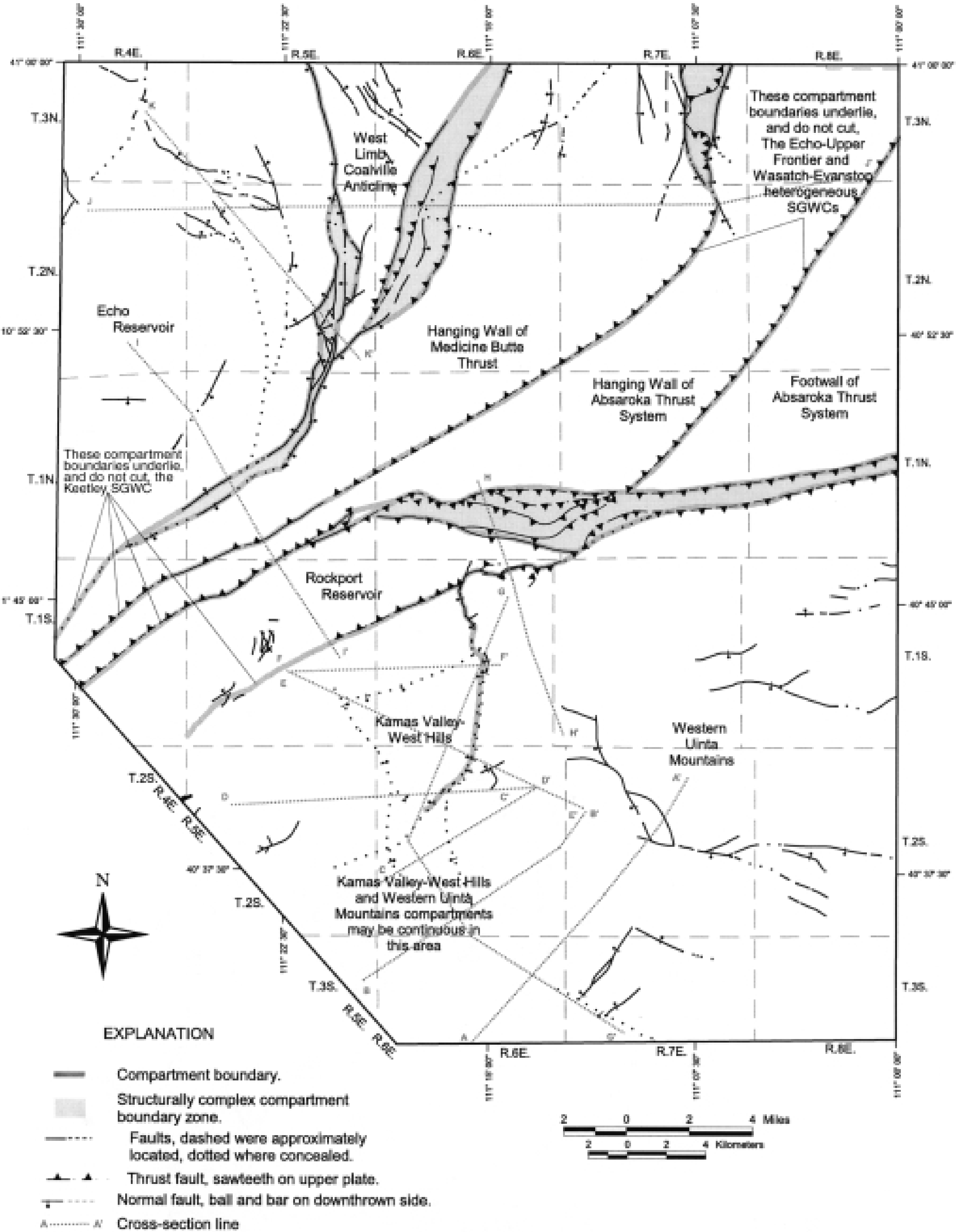

Figure 16. *Structural compartments in Kamas-Coalville region. See text and table 2 for description and discussion.*

Table 2. Summary descriptions of structural compartments.

Compartment	**Boundaries**	**Cross Sections Illustrating Structure (plate 3)**	**Internal Structure**
Western Uinta Mountains	North Flank thrust; East Kamas Valley fault zone	A-A′ through H-H′	Dominated by west-plunging Uinta arch. Twin Creek, Nugget, Thaynes, and upper part of Weber SGWCs truncated by faults. Paleozoic-age SGWCs wrap continuously around nose of arch and are truncated above by erosion.
Kamas Valley-West Hills	East Kamas Valley fault zone; Absaroka thrust zone	A-A′ through G-G′	Quaternary sediments and Keetley SGWC have relatively simple structure. Geometry of underlying SGWCs poorly known but likely complex. Continuous with Uinta Mountains compartment south of Kamas.
Rockport Reservoir	Northernmost and southernmost thrusts of Absaroka thrust zone	H-H′ and I-I′	Bedding dips 45 to 80 degrees northwest, locally modified by folds related to small-scale thrusts. Small-scale faults are adjacent to some thrusts.
Footwall of Absaroka Thrust System	Absaroka thrust zone	K-K′	Relatively simple structure; gentle west dips.
Hanging Wall of Absaroka Thrust System	Absaroka and Medicine Butte thrusts; Acocks normal fault	I-I′, J-J′, and K-K′	Complex structure; closely spaced thrusts and related tight folds.
Hanging Wall of Medicine Butte Thrust	Medicine Butte thrust; thrust cutting east limb of Coalville anticline	J-J′ and K-K′	Complex structure; closely spaced thrusts and related tight folds. Northwest boundary zone is indistinct and very complex.
West Limb Coalville Anticline	Thrust cutting east limb of Coalville anticline; Chappel Mine normal fault	J-J′ and K-K′	Boundary fault zones have complex structure. Internal structure relatively simple, with homoclinal northwest dips.
Echo Reservoir	Chappel Mine normal fault; west boundary of study area	I-I′, J-J′, and K-K′	Relatively simple internal structure, with homoclinal northwest dips. Eastern fault boundary is complex.

yield, based on lithologic characteristics as discussed above. Plates 3, 4, and 5 may be used for preliminary assessment of potential well sites. The geometry of SGWCs and hydrogeologic relations are likely complex and difficult to predict near structural-compartment boundary zones (figure 16).

It is important to understand the degree of uncertainty associated with the cross sections and isopach and structure-contour maps (plates 3, 4, and 5). Although they depict geologic formations at specific depths and locations, these diagrams represent hypotheses for subsurface relations and, therefore, are working documents that are subject to change based on new data. Subsurface data in the study area is limited, so these diagrams are derived from careful projection of surface data, existing wells, application of basic geologic reasoning and principles of cross-section construction (Woodward and others, 1985), and the new gravity survey. Undetected structures covered by younger deposits may result in different subsurface relations than those shown on plates 3, 4, and 5. The geologic structure below Kamas Valley should be considered speculative, whereas the structure depicted in the footwall of the East Kamas Valley fault zone is much better constrained. Cross sections I-I′ through K-K′ incorporate oil-well data (table A.1), and are most accurate near these wells. The thicknesses and depths below the surface of SGWCs can be measured directly from the cross sections. Methods for estimating these parameters in other parts of Kamas Valley are described on plates 4 and 5.

The cross sections (plate 3) and structure-contour maps (plate 5) show that several Paleozoic SGWCs along the eastern margin of Kamas Valley apparently project uninterrupted (by faults, folds, or topography) to higher parts of the western Uinta Mountains. Such sites are considered the most favorable for potential wells because the depth and structure of the SGWCs are relatively well known, and because of their proximity to potential recharge areas in the Uinta Mountains.

Mesozoic SGWCs (Thaynes, Nugget, and Watton Canyon) are likely accessible below the topographic bench in the north part of Kamas Valley, but this area should be approached with caution because it is structurally complex, bedding dips are steep and may change abruptly, and undetected structures may exist below the Quaternary deposits. These units may receive recharge from saturated unconsolidated deposits adjacent to the Weber River, but their limited exposure at relatively low elevation may limit their recharge from precipitation and snowmelt.

Where Cretaceous SGWCs are exposed, specific sandstone beds or, preferably, clusters of beds, should be the principal well targets. Predicting the subsurface geometry of these beds is considerably more reliable in areas of simple structure and homoclinal dips than in and adjacent to major structures such as the Coalville anticline.

CONCLUSIONS

The Kamas-Coalville area is situated above two major crustal boundaries that influenced its structural evolution: (1) an east-west-trending paleo-basin boundary across which Middle Proterozoic siliciclastic rocks thicken dramatically to the south, and (2) the Cordilleran hinge line, across which Late Proterozoic through Mesozoic rocks thicken dramatically to the west. Three additional tectonic events shaped the structure of the region: (1) east- to southeast-directed thrusting and related folding of the Idaho-Wyoming-Utah segment of the Cordilleran thrust belt during Cretaceous to Paleocene time, (2) north- and south-directed reverse faulting and related folding of the Uinta Mountains during latest Cretaceous through Late Eocene or Early Oligocene time, and (3) normal faulting from Oligocene through mid-Quaternary time, accompanied by volcanism in Oligocene time.

Kamas Valley owes its present geometry and subsurface relations to a protracted geologic history. The region west of the western Uinta Mountains was likely a topographic basin by Late Oligocene time, defined by the westward plunge of the Uinta arch. Normal faulting along the western margin of the western Uinta Mountains began as early as Late Oligocene time, continued sporadically through mid-Quaternary time, and ended prior to the 130-150 ka Bull Lake glacial event.

New gravity data from Kamas Valley show that the depositional basin underlying the valley is asymmetric, thickening eastward toward the East Kamas Valley fault zone. Quaternary unconsolidated deposits may be 1,100 feet (335 m) thick below the eastern part of Kamas Valley, but this value has not been directly confirmed. The composite thickness of Quaternary sediments plus Keetley Volcanics in the hanging wall of the East Kamas Valley fault zone is at least 3,500 feet (1,067 m). This great thickness, combined with the steep, planar eastern boundary of the low-density deposits coincident with the East Kamas Valley fault zone, implies that faulting occurred during eruption of the Keetley Volcanics, and during deposition of pre-Bull Lake alluvial fans derived from the western Uinta Mountains. Paleotopography between the western Uinta Mountains and the adjacent basin may also have facilitated accumulation of the thick section of Keetley Volcanics.

The hydraulic conductivity of unconsolidated sediments in Kamas Valley may decrease with depth and decrease eastward toward the East Kamas Valley fault zone. Sediments deposited during Quaternary glacial events likely have greater clay content, and therefore lower hydraulic conductivity, than overlying Holocene sediments. Alluvial-fan sediments derived from the western Uinta Mountains dominate the eastern part of the valley, and interfinger with alluvium in the central to western part of the valley. The alluvial fans were likely restricted to the easternmost part of the valley during pre-Bull Lake time, due to subsidence of the eastern basin floor in the hanging wall of the East Kamas Valley fault zone. Bull Lake-age and younger alluvial fans prograded farther west into the valley. Compared to alluvium, alluvial-fan sediments are poorly sorted and less stratified, resulting in lower, but more homogeneously distributed, hydraulic conductivity. It is important to recognize that these conclusions are based solely on surface relations and geologic principles, because there is presently no empirical data for the hydraulic conductivity and subsurface distribution of sedimentary facies of the Quaternary deposits.

The hydrogeology of bedrock units can be qualitatively predicted by employing the principles of hydrostratigraphy and the hydrostratigraphic framework established for the Snyderville basin area by Weston Engineering (1999a, 1999b) and Ashland and others (2001). The stratigraphic column can be divided into stratigraphic ground-water compartments (SGWCs) with relatively high hydraulic conductivity and intervening low-permeability units. The principal controls on whether a stratigraphic unit is a SGWC or a low-permeability unit include composition, average grain size, grain-size distribution, sedimentary structures, and fracture characteristics, each of which may vary considerably between formations. SGWCs and confining units may be composed of a single formation or member, or groups of formations or members.

The Watton Canyon, Nugget, Thaynes, Weber, and Humbug-Uinta SGWCs have the best potential for groundwater development in Kamas Valley. These SGWCs are exposed in the western Uinta Mountains and in the hills north of Kamas Valley, and occur in the subsurface below Kamas Valley. Near Rockport and Echo Reservoirs and along Chalk Creek, sandstone beds in Cretaceous sedimentary formations are good potential aquifers where they are clustered into sequences 50 to >100 feet (15->30 m) thick. The Oyster Ridge Sandstone Member of the Upper Cretaceous Frontier Formation is especially promising, based on observations of its lithologic and joint characteristics. These SGWCs should be specifically targeted, and their subsurface structure should be carefully evaluated, as part of the planning process for new water wells.

Structures, principally faults and folds, may also influence regional and local ground-water movement. Faults in Mesozoic sedimentary rocks contain gouge-rich core zones, resulting in very low hydraulic conductivity transverse to the fault planes. Faults in Paleozoic units localize joints near their planes, resulting in high hydraulic conductivity parallel to the fault planes. Regionally continuous, large-displacement fault zones may form fundamental hydrologic boundaries, dividing the area into several structurally defined ground-water compartments characterized by relatively homogeneous (but possibly complex) internal structure and very complex boundary zones. Ground-water flow in the boundary zones may be complex and difficult to predict, and the amount of flow between adjacent compartments is not known.

ACKNOWLEDGMENTS

This study was funded by the Utah Division of Water Rights, the Weber Basin Water Conservancy District, the Davis and Weber Counties Canal Company, and the Weber

River Water Users Association. Alison Corey and Becky Gonzales performed GIS work for plate 1, and Basia Matyjasik and Alison Corey drafted the cross sections, illustrations, and plates 2 through 5. Chris Eisinger and Becky Gonzales were able field assistants for geologic field work and surveying of gravity stations. Viki Bankey of the U.S. Geological Survey generously provided elevation, latitude, and topographic corrections to the gravity data. I thank Bill Laughlin, Todd Jarvis, Jim Coogan, and Jon King for discussions of the geology and hydrogeology of the study area, and Mayor Doug Evans for an informal tour of Oakley City's springs and wells. I also thank the numerous private land owners who granted permission for me to perform field work on their land. Reviews by Jerry Olds and Chuck Williamson of the Utah Division of Water Rights, Lynnette Brooks and Bert Stolp of the Water Resources Division of the U.S. Geological Survey, Todd Jarvis of Montgomery Watson, Inc., Bill Laughlin of Kleinfelder, Inc., (both Jarvis and Loughlin were at Weston Engineering, Inc., when they reviewed the manuscript) and Mike Lowe, Mike Hylland, Jon King, and Kimm Harty of the UGS led to substantial improvements of the manuscript.

REFERENCES

Allmendinger, R.W., 1992, Fold and thrust tectonics of the western United States exclusive of the accreted terranes, *in* Burchfiel, B.C., Lipman, P.W., and Zoback, M.L., editors, The Cordilleran Orogen - Coterminous U.S.: Boulder, Colorado, Geological Society of America, The Geology of North America, v. G-3, p. 583-607.

Al-Raisi, M.H., Slatt, R.M., and Decker, M.K., 1996, Structural and stratigraphic compartmentalization of the Terry Sandstone and effects on reservoir fluid distributions - Latham Bar trend, Denver Basin, Colorado: The Mountain Geologist, v. 33, p. 11-30.

Anderson, G.E., 1915, Stream piracy of the Provo and Weber Rivers, Utah: American Journal of Science, v. 40, p. 314-316.

Armstrong, R.L., 1968, Sevier orogenic belt in Nevada and Utah: Geological Society of America Bulletin, v. 79, p. 429-458.

Ashcroft, G.L., Jensen, D.T., and Brown, J.L., 1992, Utah climate: Logan, Utah, Utah Climate Center, 127 p.

Ashland, F.X., Bishop, C.E., Lowe, Mike, and Mayes, B.H., 2001, The geology of the Snyderville basin, western Summit County, and its relation to ground-water conditions: Utah Geological Survey Water Resource Bulletin 28, 59 p., 15 pl.

Baker, C. H., Jr., 1970, Water resources of the Heber-Kamas-Park City area, north-central Utah: Utah Department of Natural Resources Technical Publication No. 27, 79 p.

Bergosh, J.L., Good, J.R., Hillman, J.T., and Kolodzie, Stan, 1982, Geological characterization of the Nugget Sandstone, Anschutz Ranch East, in Overthrust Belt of Utah, *in* Nielson, D.L., editor, The Overthrust Belt of Utah: Salt Lake City, Utah, Utah Geological Association Publication 10, p. 253-265.

Best, M.G., Henage, L.F., and Adams, J.A.S., 1968, Mica peridotite, wyomingite, and associated potassic igneous rocks in northeastern Utah: American Mineralogist, v. 53, p. 1,041-1,048.

Bradley, M.D., 1988, Structural evolution of the Uinta Mountains, Utah, and their interaction with the Utah-Wyoming salient of the Sevier overthrust belt: Salt Lake City, University of Utah, Ph.D. thesis, 178 p.

Bradley, M.D., and Bruhn, R.L., 1988, Structural interactions between the Uinta arch and the overthrust belt, north-central Utah; Implications of strain trajectories and displacement modeling, *in* Schmidt, C.J., and Perry, W.J., Jr., editors, Interaction of the Rocky Mountain foreland and the Cordilleran thrust belt: Geological Society of America Memoir 171, p. 431-445.

Bromfield, C.S., and Crittenden, M.D., Jr., 1971, Geologic map of the Park City East quadrangle, Summit and Wasatch Counties, Utah: U.S. Geological Survey Map GQ-852, scale 1:24,000.

Bromfield, C.S., Ericksen, A.J., Jr., Haddain, M.A., and Mehnert, H.H., 1977, Potassium-argon ages of intrusion, extrusion, and associated ore deposits, Park City mining district, Utah: Economic Geology, v. 72, p. 837-848.

Bruhn, R.L., Picard, M.D., and Isby, J.S., 1986, Tectonics and sedimentology of Uinta arch, western Uinta Mountains, and Uinta basin, *in* Peterson, J.A., editor, Paleotectonics and sedimentation in the Rocky Mountain region, United States: American Association of Petroleum Geologists Memoir 32, p. 333-352.

Bryant, B.B., 1990, Geologic map of the Salt Lake City 30' x 60' quadrangle, north-central Utah, and Uinta County, Wyoming: U.S. Geological Survey Miscellaneous Investigations Series Map I-1944, scale 1:100,000.

Bryant, B.B., and Nichols, D.J., 1988, Late Mesozoic and early Tertiary reactivation of an ancient crustal boundary along the Uinta trend and its interaction with the Sevier orogenic belt, *in* Schmidt, C.J., and Perry, W.J., Jr., editors, Interaction of the Rocky Mountain foreland and the Cordilleran thrust belt: Geological Society of America Memoir 171, p. 411-430.

Caine, J.S., Evans, J.P., and Forster, C.B., 1996, Fault zone architecture and permeability structure: Geology, v. 24, p. 1025-1028.

Chidsey, T.C., 1995, Petroleum plays in Summit County, Utah, *in* Spangler, L.E., and Allen, C.J., editors, Geology of northern Utah and vicinity: Utah Geological Association Publication 27, p. 233-256.

Constenius, K.N., 1996, Late Paleogene extensional collapse of the Cordilleran foreland fold and thrust belt: Geological Society of America Bulletin, v. 108, p. 20-39.

Coogan, J.C., 1992, Thrust systems and displacement transfer in the Wyoming-Idaho-Utah thrust belt: Laramie, University of Wyoming, Ph.D. thesis, 239 p.

Cook, K.L., Nilsen, T.H., and Lambert, J.F., 1971, Gravity base station network in Utah - 1967: Utah Geological Survey Bulletin 92, 57 p.

Crittenden, M. D., Jr., 1974, Regional extent and age of thrusts near Rockport Reservoir and relation to possible exploration targets in northern Utah: American Association of Petroleum Geologists Bulletin, v. 58, p. 2428-2435.

—1976, Stratigraphic and structural setting of the Cottonwood area, Utah, *in* Hill, J.G., editor, Symposium of the Cordilleran Hingeline: Denver, Colorado, Rocky Mountain Association of Geologists, p. 363-379.

Crittenden, M.D., Jr., and Peterman, Zell, 1975, Provisional Rb-Sr age of the Precambrian Uinta Mountain Group, northeastern Utah: Utah Geology, v. 2, p. 75-77.

Crittenden, M.D., Jr., Stuckless, J.S., and Kistler, R.W., 1973, Radiometric dating of intrusive rocks in the Cottonwood area, Utah: U.S. Geological Survey Journal of Research, v. 1, p. 173-178.

DeCelles, P.G., 1994, Late Cretaceous-Paleocene synorogenic sedimentation and kinematic history of the Sevier thrust belt, northeast Utah and southwest Wyoming: Geological Society of America Bulletin, v. 106, p. 32-56.

Dickinson, W.R., Klute, M.A., Hayes, M.J., Janecke, S.U., Lundin, E.R., McKittrick, M. A., and Olivares, M.D., 1988, Paleogeographic and paleotectonic setting of Laramide sedimentary basins in the central Rocky Mountains: Geological Society of America Bulletin, v. 100, p. 1023-1039.

EWP (Eckhoff, Watson, and Preator Engineering Inc.), 1992, Water system master plan for Kamas City, Salt Lake City, unpublished consultant’s report.

Fetter, C.W., 1994, Applied hydrogeolgy: New York, Macmillan College Publishing Company, 691 p.

Hale, L.A., 1976, Geology of the Coalville anticline, Summit County, Utah, *in* Hill, J.G., editor, Symposium of the Cordilleran Hingeline: Rocky Mountain Association of Geologists, p. 381-386.

Hansen, W.R., 1986, History of faulting in the eastern Uinta Mountains, Colorado and Utah: Rocky Mountain Association of Geologists 1986 Symposium Guidebook, p. 5-17.

Hintze, L. F., 1988, Geologic history of Utah: Brigham Young University Geology Studies Special Publication 7, 202 p.

Imlay, R.W., 1967, Twin Creek Limestone (Jurassic) in the Western Interior of the United States: U.S. Geological Survey Professional Paper 540, 105 p.

Jackson, J.A., 1997, Glossary of geology: Alexandra, Virginia, American Geological Institute, fourth edition, 769 p.

Jacobson, S.R., and Nichols, D.J., 1982, Palynological dating of syntectonic units in the Utah-Wyoming thrust belt - the Evanston Formation, Echo Canyon Conglomerate, and Little Muddy Creek Conglomerate, *in* Powers, R.B., editor, Geologic studies of the Cordilleran thrust belt: Denver, Colorado, Rocky Mountain Association of Geologists Symposium, v. 2, p. 735-750.

Keighley, K.E., Yonkee, W.A., Ashland, F.X., and Evans, J.P., 1997, Bedrock geology of Snyderville basin - Structural geology techniques applied to understanding the hydrogeology of a rapidly developing region, Summit County, Utah: Geological Society of America, p. 325-343.

Kluth, C.F., 1986, Plate tectonics of the ancestral Rocky Mountains, *in* Peterson, J.A., editor, Paleotectonics and sedimentation in the Rocky Mountain region, United States: American Association of Petroleum Geologists Memoir 41, p. 353-369.

Lamerson, P.R., 1982, The Fossil basin and its relationship to the Absaroka thrust system, Wyoming and Utah, *in* Powers, R.B., editor, Geologic studies of the Cordilleran thrust belt: Denver, Colorado, Rocky Mountain Association of Geologists, p. 279-340.

LaPointe, P.R., and Hudson, J.A., 1985, Characterization and interpretation of rock mass jointing patterns: Geological Society of America Special Paper 199, 25 p.

Leeder, M.R., and Gawthorpe, R.L., 1987, Sedimentary models for extensional tilt-block/half-graben basins, *in* Coward, M.P., Dewey, J.F., and Hancock, P.L., editors, Continental extensional tectonics: Geological Society of London Special Publication 28, p. 139-152.

Leveinen, J. E., 1994, Petrology of the Keetley Volcanics in Summit and Wasatch Counties, north-central Utah: Duluth, University of Minnesota at Duluth, M.S. thesis, 175 p.

Long, J.C.S., and Witherspoon, P.A., 1985, The relationship of the degree of interconnection to permeability in fracture networks: Journal of Geophysical Research, v. 90, p. 3087-3098.

Lorenz, J.C., and Finley, S.J., 1991, Regional fractures II -- fracturing of Mesaverde reservoirs in the Piceance basin, Colorado: American Association of Petroleum Geologists Bulletin, v. 75, p. 1738-1757.

Lowell, J. D., editor, 1983, Rocky Mountain foreland basins and uplifts: Denver, Colorado, Rocky Mountain Association of Geologists, 392 p.

Mabey, D.R., 1992, Subsurface geology along the Wasatch Front, *in* Gori, P.L., and Hays, W.W., editors, Assessment of regional earthquake hazards and risk along the Wasatch Front, Utah: U.S. Geological Survey Professional Paper 1500-C, 16 p.

Mattick, R.E., 1970, Thickness of unconsolidated to semiconsolidated sediments in Jordan Valley, Utah: U.S. Geological Survey Professional Paper 700-C, p. C119-C124.

Nelson, M.E., 1972, Age and stratigraphic relations of the Fowkes Formation and Norwood tuff, southwestern Wyoming and northeastern Utah: Geological Society of America Abstracts With Programs, v. 4, no. 6, p. 397-398.

Palmer, A.R., and Geissman, John, 1999, 1999 geologic time scale: Boulder, Geological Society of America, Product CTS004.

Peterson, D.L., 1970, A gravity and aeromagnetic survey of Heber and Rhodes Valleys, Utah, *in* Baker, C.H., Jr., 1970, Water resources of the Heber-Kamas-Park City area, north-central Utah: Utah Department of Natural Resources Technical Publication No. 27, 79 p.

Peterson, J.A., editor, 1986, Paleotectonics and sedimentation in the Rocky Mountain region, United States: American Association of Petroleum Geologists Memoir 41, 693 p.

Plouff, Donald, 1977, Preliminary documentation for a FORTRAN program to compute gravity terrain corrections based on topography digitized on a geographic grid: U.S. Geological Survey Open-File Report 77-535, 45 p.

Quitzau, R.P., 1961, A regional gravity survey of the back valleys of the Wasatch Mountains and adjacent areas in Utah, Idaho and Wyoming: Salt Lake City, University of Utah, M.S. thesis, 48 p.

Royse, Frank, Jr., 1993, An overview of the geologic structure of the thrust belt in Wyoming, northern Utah, and eastern Idaho, *in* Snoke, A.W., Steidtmann, J.R., and Roberts, S.M., editors, Geology of Wyoming: Geological Survey of Wyoming Memoir No. 5, p. 272-311.

Royse, Frank, Jr., Warner, M.A., and Reese, D.L., 1975, Thrust belt structural geometry and related stratigraphic problems, Wyoming-Idaho-northern Utah, *in* Bolyard, D.W., editor, Deep drilling frontiers of the central Rocky Mountains: Rocky Mountain Association of Geologists, p. 41-54.

Ryer, T.A., 1976, Cretaceous stratigraphy of the Coalville and Rockport areas, Utah: Utah Geology, v. 3, p. 71-83.

Sanderson, I.D., 1984, The Mount Watson Formation, an interpreted braided-fluvial deposit in the Uinta Mountain Group (upper Precambrian), Utah: The Mountain Geologist, v. 21, p. 157-164.

Schmidt, C.J., and Perry, W.J., editors, 1988, Interaction of the Rocky Mountain foreland and the Cordilleran thrust belt: Geological Society of America Memoir 171, 582 p.

Smithson, S.B., Brewer, J.A., Kaufman, Stanley, Oliver, Jack, and Hurich, Charles, 1979, Structure of the Laramide Wind River uplift, Wyoming, from COCORP deep reflection data and from gravity data: Journal of Geophysical Research, v. 84, p. 5955-5972.

Steidtmann, J.R., 1993, The Cretaceous foreland basin and its sedimentary record, *in* Snoke, A.W., Steidtmann, J.R., and Roberts, S.M., editors, Geology of Wyoming: Geological Survey of Wyoming Memoir No. 5, p. 250-271.

Stewart, J.H., 1980, Geology of Nevada: Nevada Bureau of Mines and Geology, Special Publication 4, 136 p.

Sullivan, J.T., Nelson, A.R., LaForge, R.C., Wood, C.K., and Hansen, R.A., 1988, Regional seismotectonic study for the back valleys of the Wasatch Mountains in northeastern Utah: U.S. Bureau of Reclamation Seismotectonic Study Report 88-5.

Talwani, M., 1973, Computer usage in the computation of gravity anomalies, *in* Bold, B.A., editor, Methods in computational physics - Volume 13: Academic Press, New York.

Telford, W.M., Geldart, L.P., Sheriff, R.E., and Keys, D.A., 1976, Applied geophysics: Cambridge, U.K., Cambridge University Press, 859 p.

Twiss, R.J., and Moores, E.M., 1994, Structural geology: New York, W.H. Freeman and Company, 532 p.

Utah Division of Water Rights, 1982, Water-use data for public water suppliers and self-supported industry in Utah, 1980:

Utah Division of Water Rights, Water Use Report no. 3, 94 p.

—1995, Water-use data for public water suppliers and self-supported industry in Utah, 1992-1993: Utah Division of Water Rights, Water Use Report no. 10, 32 p.

Van Horn, Richard, 1981, Geologic map of pre-Quaternary rocks of the Salt Lake City North quadrangle, Davis and Salt Lake Counties, Utah: U.S. Geological Survey Miscellaneous Investigations Series I-1330, scale 1:24,000.

Wallace, C.A., 1972, A basin analysis of the upper Precambrian Uinta Mountain Group: Santa Barbara, University of California, Ph.D. dissertation, 412 p.

Wallace, J.J., 2000, Geologic logs of water wells in Utah: Data available at: http://nrwrt1.nr.state.ut.us/wellinfo/findwlog.htm.

Weston Engineering, Inc., 1996, Final well report - Summit Park Water Special Service District Well No. 7 located in NW1/4NE1/4, section 16, T.1S, R.3E, Summit County, Utah: Park City, unpublished consultant's report, 13 p.

—1998, Oakley City Humbug Well No. 1, Summit County, Utah, well drilling and testing report : Park City, unpublished consultant's report, 109 p.

—1999a, Supplemental report - water right number 35-10638, Oakley City Humbug well no. 1: Park City, unpublished consultant's report, 32 p.

—1999b, Well siting study for Park City: Park City, unpublished consultant's report, x p.

Woodfill, R.D., 1972, A geologic and petrographic investigation of the northern part of the Keetley volcanic field, Summit and Wasatch Counties, Utah: West Lafayette, Indiana, Purdue University, Ph.D. thesis, 168 p.

Woodward, N.B., Boyer, S.E., and Suppe, John, 1985, An outline of balanced cross sections: Knoxville, University of Tennessee Department of Geological Sciences Studies in Geology, v. 11, 170 p.

GLOSSARY

Most definitions are after Jackson (1997).

Alluvial terrace - a stream terrace composed of unconsolidated alluvium, produced by renewed downcutting of the flood plain or valley floor.

Anticline - a fold, the core of which contains stratigraphically older rocks, and is convex upward.

Aperture - the width of a fracture opening measured perpendicular to the two rock surfaces on either side of the fracture (may be infilled).

Aquifer - a body of rock that contains sufficient saturated permeable material to conduct ground water and to yield significant quantities of water to wells and springs.

Arkose - a feldspar-rich sandstone, commonly coarse grained and pink or reddish, that is typically composed of angular to sub-angular grains that may be either poorly or moderately well sorted; quartz is usually the dominant mineral, with feldspars constituting at least 25%; matrix commonly includes clay minerals, mica, iron oxide, and fine-grained rock fragments.

Bouguer gravity anomaly - a measurement of the Earth's gravity field after correcting the raw data for the effects of topography and elevation difference between stations.

Confining unit - an impermeable layer that creates confined ground-water conditions, in which ground water is under pressure significantly greater than that of the atmosphere.

Damage zone - fractured rock adjacent to a fault or fault zone.

Dip - the inclination of a planar surface (for example, bedding or a fault), as measured relative to horizontal and in a vertical plane that is perpendicular to the strike of the surface.

Dip slip - fault motion for which the slip direction is roughly parallel to the dip direction of the fault.

Fault - a discrete surface or zone of discrete surfaces separating two rock masses across which one rock mass has slid past the other.

Fault core - the central part of a fault, which accommodated the majority of displacement along the fault and which shows the greatest amount of deformation.

Fold - a curve or bend of a planar structure such as rock strata or bedding planes.

Footwall -the lower block of a non-vertical fault.

Fracture - a general term for any surface within a material across which there is no cohesion, including joints and faults.

Gouge - a thin layer of soft, fault-comminuted rock material in the core of a fault.

Hanging wall - the upper block of a non-vertical fault.

Hydraulic conductivity - a coefficient of proportionality describing the rate at which water can flow through a permeable medium. Hydraulic conductivity is a function of the physical properties of the porous or fractured medium and of the density and viscosity of water.

Hydrostratigraphy - division of a rock mass into hydrostratigraphic units; a hydrostratigraphic unit is a body of rock distinguished and characterized by its porosity and permeability.

Joint - a planar or nearly planar fracture in rock, along which negligible relative movement has occurred.

Joint density - the total length of joints per unit area, as measured on a planar surface.

Joint zone - a discrete zone having significantly higher joint density than the adjacent rock mass.

Litharenite - a sandstone containing more than 25% fine-grained rock fragments, less than 10% feldspar, and less than 75% quartz, quartzite, and chert.

Lithology - the description of rocks on the basis of such characteristics as color, mineralogic composition, and grain size.

Low-permeability unit - a formation, member, or layer that retards or prevents ground-water flow into or out of a SGWC over time scales relevant for flow to wells (days to tens of years).

Micrite - a rock or rock matrix composed of carbonate mud with crystals less than 0.0002 inches (4 micrometers) in diameter.

Mudstone - a fine-grained sedimentary rock in which the proportions of clay and silt are approximately equal.

Normal fault - a fault along which the hanging wall has moved downward relative to the footwall.

Packstone - a sedimentary carbonate rock whose granular material is arranged in a self-supporting framework, yet also contains some matrix of carbonate mud.

Permeability - a coefficient describing the rate at which fluid can flow through a porous or fractured medium.

Plunge - the angle that a linear structure such as a fold axis makes with respect to a horizontal plane, as measured in a vertical plane.

Descriptive Term	Plunge (degrees)
horizontal	0-10
gentle	11-30
moderate	31-60
steep	61-90

Porosity - the percentage of bulk volume of a rock or soil that is occupied by interstices, whether isolated or connected.

Potentiometric surface - a surface representing the total head of ground water and defined by the levels to which water will rise in tightly cased wells.

Primary porosity - the porosity that developed during the final stages of sedimentation or that was present within sedimentary particles at the time of deposition.

Relative gravity anomaly - the difference in Bouguer anomaly value between two distinct points or areas.

Reverse fault - a fault that dips greater than 30 degrees, along which the hanging wall has moved upward relative to the footwall.

Quartzarenite - a sandstone that is composed of more than 95% quartz framework grains.

Quartzite - a metamorphic rock consisting mainly of quartz and formed by recrystallization of sandstone or chert.

Rifting - the process of forming a rift, defined as a long, narrow continental trough bounded by normal faults, marking a zone along which the entire thickness of the lithosphere has ruptured under extension.

Sandstone - a medium-grained clastic sedimentary rock composed of abundant rounded or angular fragments of sand size and more or less firmly united by a cementing material.

Shale - a laminated, indurated rock with >67% clay-sized minerals.

Siltstone - an indurated silt having the texture and composition of shale but lacking its fine lamination or fissility.

Slickenside - a highly polished surface that is the result of frictional sliding.

Stratigraphic ground-water compartment - a consolidated geologic formation, member, or group of formations or members that are bounded by low-permeability units, and which likely have sufficient hydraulic conductivity to serve as aquifers.

Stratigraphy - the science of rock strata, concerned with the original succession and age relations of rock strata and with their form, distribution, lithologic composition, fossil content, and geophysical and geochemical properties.

Stream terrace - one of a series of level surfaces in a stream valley, flanking and more or less parallel to the stream channel, originally occurring at or below, but now above, the level of the stream, and representing the dissected remnants of an abandoned flood plain, stream bed, or valley floor produced during a former stage of erosion or deposition.

Striated - characterized by striae (plural of striation), defined as one of a series of linear grooves or scratches, generally parallel, inscribed on a rock surface, by faulting as used in the context of this report.

Strike - the angle a planar feature makes relative to north, as measured in a horizontal plane.

Descriptive term	Azimuth range (degrees)
North-south	346-014
North-northeast	015-030
Northeast	031-059
East-northeast	060-075
East-west	076-089; 270-284 (270=090)
West-northwest	285-300
Northwest	301-329
North-northwest	330-345

Note that strike lines are horizontal lines. Their attitude can therefore be described as being either north or south, northeast or southwest, etc.

Subarkose - a sandstone that is intermediate in composition between arkose and quartzarenite; contains 75-95% quartz and chert, less than 15% detrital clay minerals, and 5-25% unstable materials in which the feldspar grains exceed the rock fragments in abundance.

Sublitharenite - a sandstone that is intermediate in composition between litharenite and quartzarenite.

Syncline - a fold, the core of which contains stratigraphically younger rocks, and is convex downward.

Thrust fault - a fault that dips 30 degrees or less, along which the hanging wall has moved upward relative to the footwall.

Unconformity - a substantial break or gap in the geologic record where a rock unit is overlain by another that is not next in stratigraphic succession.

APPENDICES

APPENDIX A

Wells shown on plates 1, 3, 4, and 5, and figures 1, 7, and 14

Table A.1. Oil wells1

Map No.	Operator	Well Number and Lease Name	API Number[2]	Location[3] Spot	Sec.	T	R	Elevation (feet)	Formation Tops (feet)[4]
1	Amoco Production	#1 Champlin - 425	43-043-30044	SE SE NW	3	2N	4E	6,171	Tw 000; Kfu 330
2	Colorado Energetics	#13-3 Weber Coal Co	43-043-30024	SW NW SW	3	2N	5E	6,003	Kk 000; Jm 7,698; Js 8,000; Jp 8,020; Jt 9,440; Jn 11,464; ₮c12,675; ₮a 13,165; ₮t 14,088; ₮w 15,135
3	Colorado Energetics	#44-1 UPRR	43-043-30013	SW SW SE	1	2N	5E	6,497	Kfn 910; Kk 2,920; Jp 6,660; Jt 8,736; Jn 10,208[5]
4	Occidental Petroleum	#1 Pineview	43-043-30004	W2 E2 SE	5	2N	7E	6,488	Kfn 910; Kk 2,920; Jp 6,660; Jt 8,736; Jn 10,208
5	American Quasar Petroleum	#4-10S Newton Sheep	43-043-30133	NW NW SE	4	2N	7E	6,530	Kk 450; Js 5,402; Jp 6,304
6	American Quasar Petroleum	#1 Newton Sheep Co	43-043-30006	SW NE SE	4	2N	7E	6,574	Kk 3,700; Jm 6,200; Js 6,600; Jp 7,000; Jt 8,770, Jn 9,820; ₮a 11,360
7	American Quasar Petroleum	#3-2 UPRR	43-043-30015	NW SW	3	2N	7E	6,581	Kk 1,680; Jp 6,424; Js 6,426; Jt 8,320; Jn 9,596; ₮c 10,650; ₮a 11,244; ₮t 11,658; fault 12,546; Kb 12,940; Ka 14,238
8	American Quasar Petroleum	#3-3 Union Pacific	43-043-30019	NW NW SE	3	2N	7E	6,689	Tw 000; Kk 2,000; Js 6,068; Jp 6,458; Jt 8,033; Jn 9,326
9	American Quasar Petroleum	#3-9 UPRR	43-043-30151	C NE SE	3	2N	7E	6,840	Ke 1,702; Kk 3,064; Js 6,809; fault 7,660; Jt 7,932; Jn 9,226[6]
10	American Quasar Petroleum	#2-1A Bingham	43-043-30125	NW SW SW	2	2N	7E	6,880	Kk 3,038; Js 6,788; Jp 7,229; Jt 7,870; Jn 9,314
11	American Quasar Petroleum	#2-1 Bingham	43-043-30026	NE NW SW	2	2N	7E	6,827	Kk 3,040; Js 6,824; Jp 7,510; Jt 7,916; Jn 9,200
12	American Quasar Petroleum	#2-4 Bingham	43-043-30038	SE SE NW	2	2N	7E	6,797	Tw 000; Kk 3,048; Js 5,540; Jp 6,273; Jt 8,274; Jn 9,606

Table A.1 (continued)

Map No.	Operator	Well Number and Lease Name	API Number[2]	Location[3] Spot	Sec.	T	R	Elevation (feet)	Formation Tops (feet)[4]
13	American Quasar Petroleum	#2-5 Bingham	43-043-30073	NW NW SE	2	2N	7E	6,830	Ka 2,980; Kb 3,163; Kk 3,482; Js 5,733; Jp 5,755; Jt 8,842; Jn 10,292; Kn 10,958
14	Amoco Production	#1 Champlin - 239 C	43-043-30105	NE NW SE	1	2N	7E	7,431	Kk 7,620; Js 8,435; Jp 8,850
15	Amoco Production	#1 Champlin - 239 A	43-043-30017	NW NW NW	5	2N	8E	8,002	Kfu 1,989; Kk 3,075; Ju 6,153; Js 6,263; Jp 6,400; fault 8,300; Jurassic undifferentiated; 8,330; Js 8,490; Jp 8,638; Ku 9,103
16	Amoco Production	#1 Champlin - 239 D	43-043-30128	SE SE SE	33	3N	8E	8,066	Kg 6,206; Js 6,318; Jp 6,483
17	Amoco Production	#1 Champlin - 465 A	43-043-30054	SW NE NW	35	2N	4E	6,200	Ku 1,263; Kfo 2,531
18	Amoco Production	#1 Champlin - 464 A	43-043-30055	NE SW NW	7	1N	5E	6,693	Kfu 488; Kfo 3,028
19	Amoco Production	#1 Rockport Reservoir	43-043-30094	SE SW SE	21	1N	5E	6,715	Kfu 000; Ka 2,000; Kb 2,300; Kk 2,500; Js 8,350; Jp 8,606; Jt 10,302; Jn 12,175
20	Tomlinson Sid	#1 Gerald Young Ranch	43-043-30049	NW SE SW	30	1S	6E	6,346	Tkb 200; Mesozoic undifferentiated 1,480[7]
21	Combined O&G	# 1 D & T Simpson	43-043-30137	SW SE NW	9	2S	6E	6,550	Tkb 250; IPw 2,083[8]

Notes:
1. Data from Utah Division of Oil, Gas and Mining files, except where noted.
2. Database number.
3. Relative to Salt Lake 1855 Base Line and Meridian. Sec = section, T = Township, R = Range.
4. Formation abbreviations are on plates 1 and 2, except: Kb - Bear River Formation (equivalent of Frontier Formation but not shown on plates 1 and 2); Kg - Gannet Group (equivalent to Kelvin Formation but not shown on plates 1 and 2); Ku - Cretaceous undifferentiated; Ju - Jurassic undifferentiated.
5. Log from Lamerson (1982), plate 12.
6. Log from Lamerson (1982), figure 10.
7. Log from Sullivan and others (1988) and UGS data files.
8. Log from Sullivan and others (1988) and EWP (1992).

Table A.2. Water wells discussed in report[1]

Map Letter	Owner	POD	Location[2] Sec	T	R	Depth to Bedrock (feet)	Formation Tops (feet)[3]	Source[4]
A	U.S. Bureau of Reclamation[5]	see note 5	21	1S	6E	90	IPw 90	1
B	Oakley City	S2410 E1610 NW	22	1S	6E	295	TRt 295; TRw 487	2
C	Oakley City	N1700 W2200 SE	22	1S	6E	0	IPw 0; IPu 520; IPr 877; Mdo 1,290; Mn 1,750	2
D	Beaver & Shingle Creek Irrigation Co.	N1000 E1700 S4	16	2S	6E	60	IPw 60	3
E	Kamas City	N650 W30 S4	16	2S	6E	82	IPw 82	3
F	Unknown[6]	N250 E1020 S4	19	2S	6E	200	Tkb 200; IPw 900	4
G	Town of Francis	N134 E1168 SW	27	2S	6E	14	IPw 14	3
H	Woodland Mutual Water Co.	N312 W1246 SW	1	3S	6E	19	IPw 19	3
I	Wanship Mutual Water Co.	S1893 E3130 NW	20	1N	5E	51	Tkb 51; Kk 98	3
J	Hoytsville Pipe Water Co.	N1111 E450 S4	28	2N	5E	130	Tw 130	3
K	Coalville City Corp.	S5018 W1469 NE	21	2N	5E	33	Tw 33	3
L	Coalville City Corp.	S300 E1980 NW	17	2N	5E	15	Kfu 15	3

Notes:

1. Water right data are available on the Utah Division of Water Rights World Wide Web page: http://nrwrt1.nr.state.ut.us.
2. Location is given in "Point of Diversion" (POD) notation. Example: well B is located 2,410 feet south and 1,610 feet east of the northwest corner of section 22 in Township 1 South, Range 6 East, relative to the Salt Lake 1855 Base Line and Meridian. Sec = section, T = Township, R = Range.
3. Formation abbreviations are on plates 1 and 2.
4. Sources of data: 1 - Utah Division of Water Resources files; 2 - Weston Engineering Co. (1999a); 3 - Utah Division of Water Rights well log; 4 - EWP (1992).
5. Data from Utah Division of Water Resources files. Location given as "about $1^1/_2$ miles east of Oakley, Utah, and north of Weber River in $SW^1/_4$, section 21."
6. Data from table 5-1 of EWP. This was originally an oil-test well that was converted to water production.

Table A.3. Water wells used to construct isopach contours on plate 4.

ID[1]	Location[2] POD					Sec	T	R	Depth to Bedrock (feet)[3]
1	S	240	W	1050	E4	10	1S	5E	=20
2	S	200	W	750	N4	14	1S	5E	=63
3	S	500	W	870	N4	14	1S	5E	=90
4	S	750	W	650	NE	15	1S	5E	=160
5	N	930	E	200	W4	14	1S	5E	=72
6	S	1800	E	520	NW	14	1S	5E	=67
7	S	1800	E	2250	NW	14	1S	5E	=65
8	S	400	W	120	N4	23	1S	5E	>100
9	N	925	E	956	S4	14	1S	5E	=48
10	N	2531	E	707	SW	13	1S	5E	=120
11	N	890	W	870	S4	13	1S	5E	>120
12	N	800	W	100	S4	13	1S	5E	=176
13	N	900	E	420	S4	13	1S	5E	=127
14	S	550	W	1900	E4	13	1S	5E	=65
15	N	2384	E	1854	SW	18	1S	6E	=107
16	N	2647	E	2594	SW	18	1S	6E	=91
17	N	1933	E	2424	SW	18	1S	6E	=86
18	N	1280	E	440	S4	18	1S	6E	=137
19	N	1234	E	1837	S4	18	1S	6E	>160
20	N	1500	W	500	SE	18	1S	6E	=60
21	N	600	W	950	S4	17	1S	6E	=51
22	N	150	W	850	S4	17	1S	6E	=80
23	S	70	E	1880	NW	20	1S	6E	=123
24	N	200	W	400	S4	17	1S	6E	=110
25	S	10	E	80	N4	20	1S	6E	=80
26	S	50	E	50	NW	20	1S	6E	=120
27	S	1430	E	348	NW	20	1S	6E	=101
28	S	1400	W	30	NE	19	1S	6E	=100
29	N	2100	E	1150	S4	19	1S	6E	=110
30	S	1550	E	830	N4	19	1S	6E	=127
31	S	1090	W	50	N4	19	1S	6E	=120
32	S	1580	E	115	N4	19	1S	6E	=142
33	S	1270	E	1716	NW	19	1S	6E	=133
34	S	300	W	150	E4	22	1S	5E	>155
35	N	670	W	100	SE	23	1S	5E	>70
36	N	550	W	60	SE	23	1S	5E	>70
37	S	428	E	2539	N4	26	1S	5E	>35
38	S	742	E	130	NW	25	1S	5E	>45
39	S	500	W	200	E4	26	1S	5E	?=81
40	N	120	E	890	W4	25	1S	5E	>75
41	N	1800	W	1200	SE	25	1S	5E	>50
42	N	1150	W	15	SE	25	1S	5E	>120
43	N	250	E	150	SW	29	1S	6E	>119
44	S	930	E	930	W4	29	1S	6E	>124
45	S	2748	E	278	NW	21	1S	6E	>130
46	S	2490	E	300	NW	22	1S	6E	>88
47	S	570	E	360	W4	19	1S	6E	>108
48	N	1200	W	1000	SE	21	1S	6E	>141
49	N	1000	W	200	SE	21	1S	6E	>145
50	N	150	W	150	SE	21	1S	6E	>115
51	S	1200	W	680	NE	28	1S	6E	>102
52	N	175	W	780	SE	21	1S	6E	>162
53	N	150	E	1140	S4	21	1S	6E	>57
54	S	25	E	900	NW	28	1S	6E	>70
55	S	720	W	450	NE	29	1S	6E	>102
56	S	1480	W	70	NE	29	1S	6E	>123
57	N	700	W	550	E4	29	1S	6E	>125
58	N	200	E	1600	W4	28	1S	6E	>115
59	N	100	E	2390	W4	28	1S	6E	>107
60	S	125	E	2310	W4	28	1S	6E	>53
61	S	350	E	950	W4	28	1S	6E	>130
62	N	133	W	280	E4	29	1S	6E	>82
63	S	100	W	570	E4	29	1S	6E	>84
64	S	250	W	557	E4	29	1S	6E	>84
65	S	400	E	50	W4	28	1S	6E	>60
66	N	1320	E	180	SW	28	1S	6E	>100
67	N	900	E	200	SW	28	1S	6E	>85
68	N	465	W	85	SE	29	1S	6E	>45
69	N	200	E	200	SW	28	1S	6E	>52
70	N	50	W	200	SE	29	1S	6E	>110
71	N	1422	W	361	E4	32	1S	6E	>28
72	S	1254	E	130	NW	33	1S	6E	>92
73	S	1200	E	300	NW	33	1S	6E	>100
74	S	1400	E	900	NW	33	1S	6E	>80
75	N	73	E	90	W4	33	1S	6E	>69
76	N	170	E	1042	W4	33	1S	6E	>120
77	S	1300	E	1210	N4	33	1S	6E	>152
78	N	600	E	400	W4	34	1S	6E	>280
79	S	150	W	1400	E4	33	1S	6E	>246
80	S	1300	W	1400	E4	33	1S	6E	>246
81	S	100	E	1400	NW	3	2S	6E	>280
82	S	340	W	3801	NE	3	2S	6E	>220
83	S	110	W	3100	NE	3	2S	6E	=85
84	S	600	W	2900	NE	3	2S	6E	=40
85	S	1200	W	1100	N4	3	2S	6E	>460
86	S	1020	E	1150	NW	3	2S	6E	>423
87	S	2150	W	3900	NE	3	2S	6E	=75
88	S	2940	W	2401	NE	3	2S	6E	=95
89	N	500	E	725	W4	3	2S	6E	=60
90	S	1130	W	500	E4	4	2S	6E	=273
91	N	150	E	1100	SW	33	1S	6E	>120
92	N	438	E	111	SW	33	1S	6E	>75
93	S	39	W	168	NE	5	2S	6E	>106
94	N	800	W	200	E4	5	2S	6E	>115
95	N	262	E	141	W4	4	2S	6E	>130
96	N	470	E	2602	W4	5	2S	6E	>105
97	N	2440	E	200	S4	5	2S	6E	>105
98	S	280	W	2460	E4	5	2S	6E	>102
99	S	15	E	265	W4	6	2S	6E	=50
100	S	1592	E	536	W4	6	2S	6E	>62
101	S	75	E	2563	N4	8	2S	6E	>46
102	S	1470	E	150	NW	9	2S	6E	>324
103	N	2000	W	1200	SE	8	2S	6E	>120
104	S	350	W	1500	W4	8	2S	6E	=160
105	N	2780	W	1080	S4	18	2S	6E	=70
106	N	50	W	200	SE	8	2S	6E	>105
107	S	1995	W	2782	N4	19	2S	6E	>58
108	S	2510	W	2618	N4	19	2S	6E	=25
109	S	625	E	1475	NW	19	2S	6E	=31
110	S	1003	W	983	N4	19	2S	6E	=15
111	S	150	W	1120	N4	20	2S	6E	>65
112	S	135	W	3	N4	20	2S	6E	>42
113	S	130	W	2333	NE	20	2S	6E	>21
114	N	650	W	30	S4	16	2S	6E	=60
115	N	1000	E	1700	S4	16	2S	6E	=82
116	S	2500	E	3550	NW	21	2S	6E	=43
117	S	2975	E	3520	NW	21	2S	6E	=47
118	S	3293	E	3782	NW	21	2S	6E	=57
119	N	1340	E	937	S4	21	2S	6E	=90
120	N	1241	E	1251	S4	21	2S	6E	=30
121	S	3875	E	4000	NW	21	2S	6E	=47
122	S	264	E	2112	W4	22	2S	6E	=96
123	N	965	W	1612	SE	22	2S	6E	=40
124	S	1260	W	810	NE	28	2S	6E	=15
125	N	53	W	1250	SE	21	2S	6E	>72
126	N	150	E	1100	S4	21	2S	6E	>105
127	N	100	E	2100	SW	21	2S	6E	>102
128	S	175	W	880	N4	28	2S	6E	>95
129	N	0	W	2640	SE	20	2S	6E	>124
130	S	1687	E	2134	W4	20	2S	6E	>46
131	S	140	E	372	NW	29	2S	6E	>123
132	N	17	E	181	SW	20	2S	6E	>36

(Table A.3 continued)

ID[1]	Location[2] POD					Sec	T	R	Depth to Bedrock (feet)[3]
133	S	215	E	150	W4	29	2S	6E	=129
134	S	160	E	600	NW	26	2S	6E	=70
135	N	20	E	805	SW	23	2S	6E	=30
136	N	1430	E	1000	SW	23	2S	6E	=25
137	N	1400	E	1400	SW	23	2S	6E	=0
138	N	1070	E	1420	SW	23	2S	6E	=70
139	N	637	E	1390	SW	23	2S	6E	=25
140	N	250	E	1561	SW	23	2S	6E	=41
141	N	140	W	90	S4	23	2S	6E	=20
142	S	465	E	135	N4	26	2S	6E	=70
143	S	680	W	410	N4	26	2S	6E	=48
144	S	943	W	2306	NE	26	2S	6E	=46
145	N	160	E	710	SW	19	2S	7E	=47
146	S	150	E	1210	N4	26	2S	6E	=40
147	S	600	W	650	NE	26	2S	6E	=85
148	S	1630	E	510	NW	25	2S	6E	=70
149	S	2150	E	1010	NW	25	2S	6E	=51
150	N	300	E	1110	W4	25	2S	6E	>90
151	S	2838	E	1717	NW	25	2S	6E	=35
152	S	600	W	2730	E4	25	2S	6E	=51
153	S	600	W	2350	E4	25	2S	6E	=80
154	N	1530	W	65	E4	25	2S	6E	=39
155	N	2037	E	147	W4	30	2S	7E	=42
156	S	300	E	135	NW	30	2S	7E	=31
157	S	290	E	300	NW	30	2S	7E	=45
158	S	220	E	270	NW	30	2S	7E	=32
159	S	140	E	250	NW	30	2S	7E	=38
160			E	200	NW	30	2S	7E	=30
161	S	100	E	400	NW	30	2S	7E	=45
162	N	420	E	370	SW	19	2S	6E	=28
163	N	1201	E	156	SW	28	2S	6E	>33
164	S	95	E	144	NW	33	2S	6E	>59
165	N	105	E	512	SW	28	2S	6E	>50
166	S	126	E	936	NW	33	2S	6E	>60
167	S	1361	E	57	W4	27	2S	6E	>42
168	N	750	W	120	S4	28	2S	6E	>55
169	S	45	W	314	NE	33	2S	6E	>67
170	S	400	W	120	NE	33	2S	6E	>63
171	N	800	W	90	E4	33	2S	6E	>60
172	S	2120	E	73	NW	34	2S	6E	=65
173	N	231	W	107	E4	33	2S	6E	>76
174	N	2550	W	660	SE	33	2S	6E	>140
175	S	141	W	60	E4	33	2S	6E	>64
176	N	100	W	2240	E4	34	2S	6E	=80
177	S	3460	E	151	NW	34	2S	6E	>62
178	S	1229	E	58	W4	34	2S	6E	>69
179	N	1465	W	1420	SE	33	2S	6E	>86
180	S	2960	E	114	NW	33	2S	6E	>107
181	S	235	W	475	N4	4	3S	6E	>100
182	S	93	E	103	NW	34	2S	6E	>100
183	N	580	E	815	SW	34	2S	6E	>87
184	S	2269	E	1607	W4	34	2S	6E	>105
185	S	1437	W	606	NE	4	3S	6E	>100
186	S	1000	E	1450	NW	2	3S	6E	=100
187	S	1100	E	1100	NW	2	3S	6E	?=200
188	N	203	E	105	W4	2	3S	6E	>78
189	N	215	E	81	W4	2	3S	6E	>80
190	S	2140	W	690	N4	3	3S	6E	>100
191	S	2677	W	1130	NE	4	3S	6E	=50
192	N	1562	W	52	NW	10	3S	6E	=31
193	N	75	E	80	SW	3	3S	6E	=107
194	S	1230	E	520	N4	10	3S	6E	=25
195	N	312	E	1246	SW	1	3S	6E	=19
196	S	2470	W	1138	NE	11	3S	6E	=130
197	N	1600	W	1500	SE	11	3S	6E	=20
198	N	60	E	1380	SW	12	3S	6E	=121
199	S	200	E	1755	NW	13	3S	6E	>115
200	S	1050	E	250	N4	13	3S	6E	=50
201	S	1200	W	250	NE	19	3S	7E	=65
202	N	40	W	243	SE	18	3S	7E	=70
203	N	20	W	131	SE	18	3S	7E	=90
204	N	415	W	680	SE	18	3S	7E	=70
205	S	165	E	100	W4	17	3S	7E	>128
206	N	511	E	107	W4	17	3S	7E	>58
207	N	511	E	707	W4	17	3S	7E	>68
208	N	143	E	1020	W4	17	3S	7E	>56
209	N	261	E	1016	W4	17	3S	7E	>55
210	N	28	E	1091	W4	17	3S	7E	>66
211	N	276	E	1313	W4	17	3S	7E	>66
212	N	250	E	1350	W4	17	3S	7E	=35
213	N	100	E	1350	W4	17	3S	7E	=78
214	N	262	E	1571	W4	17	3S	7E	=55
215	N	50	E	2500	W4	17	3S	7E	=75
216	N	2075	W	550	SE	17	3S	7E	=64
217	N	2000	W	200	SE	17	3S	7E	=35
218	N	1555	W	1995	S4	16	3S	7E	>43
219	N	923	E	245	SW	16	3S	7E	>45
220	N	975	E	475	SW	16	3S	7E	=57
221	N	525	E	500	SW	16	3S	7E	=87

[1]Corresponds to number on plate 4.

[2]Location is given in "Point of Diversion" (POD) notation. Sec = Section, T = Township, R = Range. Example: well 1 is located 240 feet south and 1,050 feet west of the midpoint of the eastern boundary of section 10 in Township 1 South, Range 5 East, relative to the Salt Lake 1855 Base Line and Meridian.

[3]Values given are author's interpretations of drillers' logs from Utah Division of Water Rights files. Examples: =35 - well encountered bedrock at 35 feet depth; >100 - well is 100 feet deep, all in unconsolidated deposits, so bedrock is deeper than 100 feet; ?=200 - best interpretation is that bedrock was encountered at 200 feet, but log is somewhat ambiguous. Drillers' logs and water right data are available on the Utah Division of Water Rights World Wide Web page: http://nrwrt1.nr.state.ut.us.

APPENDIX B

Gravity Survey

by
Basil Tikoff, Department of Geology and Geophysics,
University of Wisconsin-Madison, and Hugh Hurlow, Utah Geological Survey

Methods

A gravity survey of Kamas Valley and its surroundings, an area of 5 miles by 9 miles (8 km by 15 km), was conducted using a Worden gravity meter (0.0930 mgal/div). The survey included 66 gravity stations (figure 8; table B.1), most of which were located on the relatively flat valley floor and benches and avoided major topographic breaks. All station locations were identified on a 1:24,000-scale topographic map. Station elevations were determined from U.S. Geological Survey benchmarks, and by surveying relative to these benchmarks using a laser theodolite. Because surveying has a vertical accuracy of tenths of inches (centimeters) for the distances involved, the major source of elevation error is the accuracy of the benchmark elevations, estimated as better than 0.33 feet (0.1 m). Elevation, latitude, and topographic corrections were made by Viki Bankey of the U.S. Geological Survey, using digital elevation maps and the algorithms of Plouff (1977). The topographic correction assumed a bulk rock density of 0.578 ounces per cubic inch (2.67 g/cm^3). This estimate is accurate for Paleozoic bedrock exposed in the western Uinta Mountains, but is significantly greater than the density of unconsolidated deposits underlying the valley and somewhat greater than the density of the Keetley Volcanics and Mesozoic sedimentary rocks exposed on the west and north sides of the valley. Estimated errors on the Bouguer anomaly values are considered better than 0.2 mgal for most of the valley. The gravity survey was tied into the Utah gravity database, using the reference value from the town of Heber, Utah (979,668.53 gal; Cook and others, 1971). A reference station located in Kamas was re-surveyed every two hours to provide corrections for temporal drift of the instrument.

The gravity technique assumes that the magnitude of gravitational force at any point on the valley floor is in part inversely proportional to the thickness of unconsolidated deposits below that point. Points underlain by thicker unconsolidated deposits are subject to slightly lower gravitational force (detectable only by very sensitive instruments) than those underlain by thinner deposits. The gravity field over the basin, when corrected for several other factors that influence the gravity signal (Bouguer anomaly), ideally shows the qualitative variation in thickness of unconsolidated deposits below the surface. Mathematical models of the gravity data, calibrated to reliable data points, may then be constructed to show the thickness of the unconsolidated deposits.

Two previous gravity surveys were conducted in Kamas Valley. Quitzau (1961) completed a regional-scale survey of several of the back-valleys of the Wasatch Range (Utah-Wyoming-Idaho area), concentrating on the large gravity anomalies associated with Bear Lake on the Utah-Idaho border. The work of Peterson (in Baker, 1970) focused on Heber and Kamas valleys. Quitzau (1961) documented a 6 mgal relative gravity anomaly in Kamas Valley, and Peterson (in Baker, 1970) documented an 8 mgal relative gravity anomaly in the valley.

Results

The Bouguer anomaly map (figure 8) indicates negative values between -249 and -203 mgal. In general, the values are lowest in the northwest, suggesting a sloping regional gravity field. Nonetheless, where the surveys cross the basin, there is clearly a negative relative gravity anomaly associated with the basin.

Where our stations coincide with stations from the previous studies in the northern part of Kamas Valley, we derive approximately 4 mgal lower Bouguer anomaly values. We presently do not know the reason for this discrepancy, but suggest that the increased accuracy of the gravity corrections of our survey may account for this difference.

An important advantage of our survey is that it includes stations outside the basin margin, a feature absent from both previous studies. This approach results in a significantly higher relative gravity anomaly along the northern traverse (figure 8; see below) than the work of Quitzau (1961) and Peterson (in Baker, 1970). The topographic corrections for the stations outside the basin margins are large, and the elevations derived from surveying have relatively high uncertainty. Nonetheless, the results show a larger relative gravity anomaly, and consequently a greater thickness of low-density material, below Kamas Valley than previously known.

Inversion Models

To compensate for the northward regional gradient, we have concentrated on two east-west traverses across the valley (figures 8 and 9), because the relative gravity anomaly values for any local east-west traverse should be independent of a uniformly northward-sloping regional gravity field. The northern traverse starts on very thin alluvial-fan deposits east of the valley and continues westward across the basin (figures 8 and 9), and shows a -28 mgal relative gravity anomaly, centering on the eastern part of the valley. The gradient in Bouguer anomaly values from east to west into the valley is very steep, suggesting that this side of the valley is fault bounded, consistent with the observed scarp-like geomorphology and other geologic evidence cited by Sullivan and others (1988). The southern traverse starts on bedrock west of the valley and continues eastward across the basin through the town of Kamas (figures 8 and 9). There is a -7 mgal anomaly in the western part of the valley relative to the valley margins.

Inversion modeling of the gravity data along the two east-west traverses used the program GMODEL, version 2 (Lacoste and Romberg, University of Wisconsin). The models assume that geologic units are shaped like infinitely long horizontal polygons (Talwani, 1973). The models also assume: (1) a density difference between bedrock and low-density material constituting the valley fill of 0.5 g/cm^3, and (2) a constant density for bedrock beneath the unconsolidated deposits. The depth to bedrock at the endpoints of the traverses are critical inputs to the model, and were constrained using geologic and/or well data. The shape and depth of the model basins result from the relative magnitudes and gradients of the Bouguer anomalies along the traverses.

The inversion model of the northern traverse (figure 9A) suggests that there is about 3,538 feet (1,078 m) of low-density material below the eastern valley margin. Along this traverse, Kamas Valley is underlain by an asymmetric, east-thickening basin, a geometry typical of fault-bounded basins. The geometry of the low-density material suggests that it accumulated in the hanging wall of the East Kamas Valley fault zone during displacement. The along-strike orientation of these features cannot be resolved from the new data, because the regional, north-sloping gravity field cannot be removed. However, the gravity signal from the basin combined with the geomorphology of the scarp on the east side of the valley (Sullivan and others, 1988) suggest that the East Kamas Valley fault zone strikes north-northeast along this part of the western range front.

The inversion model of the southern traverse (figure 9B) suggests a relatively shallow, flat-bottomed basin, with a maximum thickness of low-density material of 879 feet (268 m). From east to west, stations 38, 1, 39, 40, 42, 43, and 44 were used for this traverse. Station 44 is directly on Keetley Volcanics, and a depth of 200 feet (61 m) to bedrock was assumed for station 38 based on logs of water wells in Kamas City.

Geologic Interpretation

The relative gravity anomaly and steep gradient along the northern traverse (figure 8) indicate substantial thickening of low-density material from west to east toward the East Kamas Valley fault zone. This geometry strongly implies accumulation of much of the low-density material during movement on the East Kamas Valley fault zone. Some of the material may also have been deposited against pre-existing topography, namely the paleo-western range front of the Uinta Mountains. Less clear, however, is the nature and thickness of the low-density material.

It is unlikely that all, or even most, of the approximately 3,500-foot-deep (1,067 m) model basin fill is Quaternary unconsolidated sediment, based on the following comparison. Salt Lake Valley, Utah (see figure 4 for location), is underlain by approximately 5,000 feet (1,525 m) of Quaternary-Tertiary unconsolidated to semiconsolidated deposits (Mattick, 1970; Mabey, 1992) in the hanging wall of the Wasatch fault, which accommodated approximately 12,000 feet (3,660 m) of west side-down throw (plate 1, cross section H-H′ of Royse, 1993). Although there is no precise way to scale the relation between normal-fault displacement and basin depth, it seems unreasonable that the depositional basin in the hanging wall of the East Kamas Valley fault zone, which accommodated a maximum of about 7,000 feet (2,135 m) of vertical displacement (cross section E-E′, plate 3), should be comparable in thickness to Salt Lake Valley.

This comparison suggests that the low-density material in the gravity model consists of Quaternary unconsolidated deposits overlying other low-density deposits, most likely the Keetley Volcanics because they are the youngest known deposits of considerable extent and thickness near Kamas Valley, and they are present beneath the valley as indicated by logs of water and oil-test wells along the eastern valley margins (tables A.1 and A.2). The Keetley Volcanics are composed chiefly of weakly consolidated volcanic breccia and tuff, which are likely denser than unconsolidated sediment but less dense than the Paleozoic to Proterozoic sedimentary rocks in the western Uinta Mountains (Telford and others, 1976, table 2.2, p. 25, and table 2.3, p. 26). Substituting Keetley Volcanics for unconsolidated sediment requires deepening of the model basin because this increases the average density of the low-density material, but the same total mass difference, which produces the observed relative gravity anomaly and gradient, must be accounted for. Too little is known about the density of the Keetley Volcanics and the nature of the deposits below Kamas Valley to perform additional modeling varying the density structure of the hanging wall.

Although it is difficult to assign quantitative limits, it is reasonable to assume that the thickness of the Keetley Volcanics below Kamas Valley should not greatly exceed known values. A maximum thickness of about 3,000 feet (914 m) is regarded as reasonable, compared to thicknesses of approximately 1,600 feet (488 m) encountered in wells on the west slope of the West Hills (T. Jarvis, written communication, 2000). Gravel deposits below the Keetley Volcanics (unit Toc of Bryant, 1990; plate 1), if present below Kamas Valley, would likely have a lower density than the volcanic rocks and would allow a lesser thickness of Keetley Volcanics in the gravity model.

These complications and the lack of constraints on subsurface geology below Kamas Valley preclude interpretation of the inversion-model cross sections as true geologic sections. The model cross sections do, however, provide important constraints on the subsurface thickness and distribution of low-density material in the hanging wall of the East Kamas Valley fault zone below Kamas Valley (plates 3 and 4).

In summary, the gravity survey and inversion modeling show that basin-fill material below Kamas Valley is significantly thicker than Peterson (in Baker, 1970) indicated, that the thickest accumulations are located farther east, and that the basin is an asymmetric graben.

Table B.1. Gravity data for Kamas Valley.

Station[1] (feet)	**Longitude**	**Latitude**	**Elevation**	**Gravity (mgal)**	**Bouguer Anomaly[2]**
1	111.2805	40.64	6,484	979,610.9	-225.91
2	111.2803	40.6865	6,452	979,610.73	-231.96
3	111.2732	40.684	6,502	979,610.48	-228.6
4	111.2675	40.684	6,557	979,610.16	-225.22
5	111.2625	40.6842	6,646	979,609.65	-219.95
6	111.2565	40.6843	6,774	979,608.87	-212.4
7	111.2512	40.684	6,931	979,607.6	-203.66
8	111.2993	40.6873	6,394	979,611.28	-235.57
9	111.2932	40.6878	6,372	979,611.13	-236.88
10	111.2867	40.688	6,409	979,610.91	-234.7
11	111.3255	40.6908	6,285	979,612.02	-241.5
12	111.3308	40.6908	6,266	979,612.23	-241.83
13	111.3188	40.691	6,306	979,611.69	-240.75
14	111.3093	40.6908	6,333	979,611.4	-239.49
15	111.2722	40.6915	6,384	979,611.65	-233.82
16	111.3187	40.684	6,296	979,611.89	-240.28
17	111.317	40.7008	6,330	979,611.54	-240.48
18	111.3327	40.707	6,278	979,612.39	-243.05
19	111.3378	40.7127	6,235	979,612.93	-245.44
20	111.3427	40.7217	6,175	979,613.38	-249.2
21	111.2997	40.7237	6,498	979,611.12	-232.71
22	111.2997	40.731	6,553	979,610.74	-230.26
23	111.2803	40.7055	6,464	979,609.91	-233.62
24	111.2802	40.7122	6,485	979,610.9	-232.05
25	111.2807	40.7238	6,525	979,610.88	-230.67
26	111.2643	40.7258	6,583	979,610.26	-227.33
27	111.2662	40.732	6,617	979,610.2	-225.76
28	111.2537	40.722	6,622	979,609.81	-222.66
29	111.2608	40.7205	6,570	979,610	-227.23
30	111.2613	40.713	6,536	979,609.99	-228.1
31	111.2685	40.713	6,529	979,610.19	-229.45
32	111.2608	40.706	6,505	979,610.09	-228.36
32A	111.2693	40.706	6,487	979,610.31	-230.91
33	111.2995	40.7055	6,403	979,611.26	-236.69
34	111.2997	40.6987	6,382	979,611.15	-237.43
35	111.2803	40.6977	6,431	979,610.73	-233.94
36	111.2623	40.689	6,382	979,609.68	-232.88
37	111.2707	40.6913	6,524	979,610.32	-227.93
38	111.2738	40.64	6,514	979,610.78	-223.98
39	111.2883	40.64	6,450	979,611.08	-228.11
40	111.294	40.64	6,430	979,611.15	-229.41
42	111.3077	40.64	6,406	979,611.28	-230.81
43	111.3137	40.64	6,410	979,611.24	-230.54
44	111.318	40.64	6,463	979,610.82	-227.94
45	111.3257	40.64	6,585	979,609.95	-221.78
46	111.3512	40.6257	6,715	979,609.21	-213.39
47	111.347	40.634	6,763	979,608.99	-211.62
48	111.3478	40.653	6,948	979,608.01	-202.79
49	111.2802	40.6178	6,544	979,610.14	-221.31
50	111.2798	40.6105	6,560	979,609.97	-219.9
51	111.2617	40.6108	6,612	979,609.86	-216.72
52	111.2608	40.5958	6,654	979,609.13	-213.97
53	111.2798	40.6033	6,578	979,609.76	-218.56
54	111.299	40.6183	6,482	979,610.45	-225.08
55	111.2992	40.625	6,494	979,310.56	-224.88
56	111.2897	40.6252	6,495	979,610.45	-224.65
57	111.2752	40.6252	6,473	979,610.51	-225.76
58	111.2902	40.7238	6,518	979,610.98	-231.38
59	111.3092	40.7238	6,467	979,611.41	-234.4
61	111.2803	40.6803	6,444	979,610.87	-231.74
62	111.2665	40.6972	6,373	979,611.25	-233.75
63	111.2888	40.6738	6,363	979,611.49	-235.61
64	111.28	40.6657	6,378	979,611.49	-233.42
65	111.3137	40.6362	6,435	979,610.92	-229.1
66	111.32	40.6353	6,457	979,610.86	-227.71
67	111.3163	40.6298	6,456	979,610.58	-227.46

Notes:

[1]Data collected by B. Tikoff, 4/24-4/26/98 using Worden gravimeter with scale constant = 0.0930 mgal/div. Heber base gravity = 979,668.53 gal; 1967 measurement.

[2]See appendix B for descriptions of methods of data collection and reduction.

APPENDIX C

Fracture Data - Methods, Interpretation, and Data Table

This study includes a reconnaissance survey of joint characteristics of the stratigraphic ground-water compartments (SGWCs) in the study area that are current or prospective aquifers (table C.1; plate 6). The objectives of this work were to: (1) describe, both quantitatively and qualitatively, the joint characteristics most pertinent to ground-water flow; (2) evaluate the relative intensity and style of jointing in different formations; and (3) delineate possible spatial variations in joint characteristics both within formations and relative to major structures.

Joint characteristics were measured at twenty-two sampling sites in the study area using a grid-sampling technique, except at two sites: KCF-15, at which a line sampling technique was employed, and KCF-22, which was analyzed from an aerial photograph (figure 12). One to five (typically three or four) grids were measured at each sample site, on a single outcrop or on several outcrops in a maximum area of approximately $^1/_4$ square mile (0.65 km^2). Sampling grids were square, with edges 3.3 to 6.5 feet (1-2 m) long, though the shapes and sizes of some grids were adjusted to match the outcrop shapes. The following characteristics were recorded for each joint within the grid: orientation, length, location, termination relationships, joint surface roughness, and mineralization. Grids were located on smooth, well-exposed, gently dipping bedding planes and, where available, vertical joint surfaces. The latter grids provide information on joint heights and on bedding-plane joints.

Fractures at sample site KCF-22 were measured from a 1:20,000-scale, black and-white aerial photograph of the Indian Hollow area (figure 12B). The photograph was scanned, then lines were drawn over clearly visible fracture traces and their orientations were recorded. Four sample rectangles, totaling about 1.11 square miles (2.85 km^2), were analyzed. Field observations confirmed that most fractures dip about 70 degrees or greater, resulting in straight traces on the aerial photograph that correspond to their true strikes. The area was not extensively field checked, so it is not known if some of the fracture traces are faults.

Results of the joint survey are presented in table C.1 and on plate 6. The rose diagrams on plate 6 combine all bedding-plane grids for each sample site. Data depicted in the rose diagrams (plate 6) are in boldface type in table C.1. Grids measured on vertical joint surfaces are excluded from the rose diagrams because such surfaces were not measured at every sample site. The rose diagram for each sample site represents average joint orientations and density over about $^1/_4$ square mile (0.65 km^2), judging from the typical spatial distribution of grid sites and observation of joint properties in nearby exposures. Joint characteristics are typically consistent among the different grids at each sample site, except at sites KCF-6 and KCF-16, which contain joint zones.

Sample site KCF-15 is in the damage zone in the footwall of an exposed strand of the East Kamas Valley fault zone (figure 11). This site was measured to illustrate the difference in joint density between damage zones and regions far from faults. The high joint density and limited exposure made grid sampling impractical, so linear sampling traverses were employed. Thus, the results from this site are only generally comparable to those from the other sample sites.

The reported joint density for each grid is the total joint length divided by the grid area. This value is useful for comparison of different grids and sample sites, but does not represent a true three-dimensional density. Joint properties useful for hydrologic modeling, such as three-dimensional density and connectivity, could be modeled using data from sample sites that include grids on three mutually perpendicular surfaces, but such work is beyond the scope of this project.

Table C.1. Fracture data.

Site[a]	Unit	Sample Grids[b]	Strike and Dip of Bedding[c]	Bed Thickness in feet (m)	N[d]	Area	Joint Sets[e] ft^2 (m^2)	Joint Density[f] ft/ft^2 (m/m^2)	Notes
KCF-1	Weber Sandstone	A: 40, 130 on bedding plane	144 4	1-5 (0.3-1.5)	25	14.0 (1.3)	30-60; 285-315	2.5 (8.4)	Clean, smooth joint surfaces. Good connectivity.
		B: 10, 100 on bedding plane			30	10.8 (1.0)	30-60; 285-330	2.3 (7.8)	
		C: 30, 120 on bedding plane			9	10.8 (1.0)	30-60; 285-315	1.0 (3.4)	
		A, B, & C combined			**64**	**35.6 (3.3)**	**30-60; 285-315**	**2.0 (6.7)**	
KCF-2	Madison Limestone and Upper Devonian Rocks	A: on joint face 0, 90	135 20	0.5-3 (0.2-1)	63	10.8 (1.0)	300-330; 60-74	4.5 (15)	Lowest part of unit. Many joints are calcite-cemented.
		B: 25, 115 on bedding plane			19	10.8 (1.0)	75-105	1.9 (6.2)	
		C: on joint face 15, 90			32	6.5 (0.6)	75-105; 15-30	4.7 (15.5)	
		D: on joint face 110, 90			27	10.8 (1.0)	0-30; 315-330	2.5 (8.2)	
		A & B combined			**122**	**38.8 (3.6)**	**315-330; 240-285; 15 30**	**3.5 (11.8)**	
KCF-3	Weber Sandstone	A; 30, 120 on bedding plane	307 40	1-5 (0.3-1.5)	20	10.8 (1.0)	0-30; 45-60; 285-300	1.9 (6.2)	Clean, smooth joint surfaces. Good connectivity.
		B: on joint face 305, 90			13	8.6 (0.8)	0-45; 75-105	1.7 (5.8)	
		C: 30, 120 on bedding plane			35	10.8 (1.0)	30-45; 285-315	4.6 (15.2)	
		D: on joint face 0, 90			29	10.8 (1.0)	30-45	4.4 (14.7)	
		A & C combined			**55**	**40.9 (3.8)**	**15-45; 285-315**	**3.5 (11.8)**	

(Table C.1 continued)

Site[a]	Unit	Sample Grids[b]	Strike and Dip of Bedding[c]	Bed Thickness in feet (m)	N[d]	Area ft² (m²)	Joint Sets[e]	Joint Density[f] ft/ft² (m/m²)	Notes
KCF-4	Weber Sandstone	A: 75, 165 on bedding plane B: 70, 160 on bedding plane C: on joint face 350, 90 **A & B combined**	165 15	1-5 (0.3-1.5	22 59 32 **81**	10.8 (1.0) 10.8 (1.0) 10.8 (1.0) **21.6 (2.0)**	15-45; 60-90 60-75; 330-345 60-75; 330-345 **60-75; 330-345; 30-45**	2.0 (6.7) 4.7 (15.7) 4.1 (13.6) **3.4 (11.2)**	Clean, smooth joint surfaces. Good connec-tivity. A few minor faults.
KCF-5	Humbug Formation	A: 75, 165 on bedding plane B: 65, 145 on bedding plane C: 60, 150 on bedding plane D: 75, 165 on bedding plane **A, B, C, & D combined**	154 20	0.5-5 (0.2-1.5)	1 7 2 20 **30**	10.8 (1.0) 10.8 (1.0) 2.2 (0.2) 10.8 (1.0) **34.4 (3.2)**	45 315-0; 45-75 56, 65 330-15; 60-75 **330-15; 45-75**	0.1 (0.2) 1.0 (3.4) 1.4 (4.8) 2.3 (7.5) **1.1 (3.5)**	Only uncemented joints reported; many calcite-cemented veins are present.
KCF-6	Thaynes Formation	A: 35, 125 on bedding plane B: 85, 175 on bedding plane C: 15, 285 on bedding plane **A, B, & C combined**	230 35	1-5 (0.3-1.5)	20 14 35 **69**	10.8 (1.0) 10.8 (1.0) 10.8 (1.0) **32.3 (3.0)**	345-360; 60-75 345-360; 60-75 315-360; 20-60 **345-360; 60-75**	1.9 (6.4) 1.4 (4.6) 3.1 (10.2) **2.1 (7.1)**	Smooth joint surfaces with minor calcite cement. Good connectivity. Sample grid C contains a joint zone.
KCF-7	Twin Creek Limestone	A: 69, 159 on bedding plane B: 75, 165 on bedding plane C: 67, 157 on bedding plane **A, B, & C combined**	249 65 255 69 247 72	0.5-3 (0.2-1)	33 37 46 **115**	10.8 (1.0) 10.8 (1.0) 10.8 (1.0) **32.3 (3.0)**	345-15 345-360; 255-285 345-15; 315-330 **345-360**	2.9 (9.8) 4.4 (14.8) 3.9 (12.9) **3.8 (12.5)**	A & B in Watton Canyon Member, C in Rich Member. Uncemented joints reported; many calcite-cemented veins are present.
KCF-8	Nugget Sandstone	A: 67, 157 on bedding plane B: 41, 131 on bedding plane C: 43, 133 on bedding plane D: 55, 145 on bedding plane **A, B, C, & D combined**	247 74 221 64 223 65 235 55	Cross-bedding 0.25-2 (0.1-0.6)	18 21 37 16 **92**	10.8 (1.0) 10.8 (1.0) 10.8 (1.0) 10.8 (1.0) **43.1 (4.0)**	330-345; 270-300 60-105 315-0 0-15 **330-15; 255-300**	1.9 (6.4) 2.3 (7.5) 2.9 (9.5) 1.7 (5.5) **2.2 (7.2)**	Joints are smooth, uncemented, and relatively long. Good connectivity.
KCF-9	Kelvin Formation	A: 88, 178 on bedding plane B: 0, 90 on bedding plane C: 88, 178 on bedding plane **A, B, & C combined**	268 45	1-5 (0.3-1.5)	14 25 20 **59**	10.8 (1.0) 10.8 (1.0) 10.8 (1.0) **32.3 (3.0)**	345-15 345-15; 285-315 330-15 **345-15**	2.4 (8.1) 2.9 (9.8) 2.1 (7.0) **2.5 (8.3)**	Most joints calcite-cemented.
KCF-10	Weber Sandstone	A: 30, 120 on bedding plane B: 30, 120 on bedding plane C: 30, 120 on bedding plane D: on joint plane 42, 54 **A, B, & C combined**	311 6	1-5 (0.3-1.5)	10 12 7 11 **40**	6.5 (0.6) 10.8 (1.0) 4.3 (0.4) 10.8 (1.0) **32.3 (3.0)**	330-360; 255-270 330-360; 30-75 0-30 30-60; 345-360 **330-15; 30-45**	1.2 (4.1) 1.2 (4.0) 1.4 (4.8) 1.9 (6.3) **1.5 (4.9)**	Clean, smooth joint surfaces. Good connectivity.
KCF-11	Round Valley Limestone	A: 30, 120 on bedding plane B: 64, 154 on bedding plane C: 80, 350 on bedding plane **A, B, & C combined**	190 40 154 83 80 40	1-3 (0.3-1)	23 37 40 **100**	10.8 (1.0) 10.8 (1.0) 15.1 (1.4) **36.7 (3.4)**	75-90; 300-315; 330 345 45-75 15-60 **15-75**	2.4 (8.1) 2.8 (9.3) 2.7 (8.9) **2.7 (8.9)**	Most joints calcite cemented. Note variation in bedding orientation.
KCF-12	Weber Sandstone	A: 20, 110 on bedding plane B: 64, 154 on bedding plane C-1: 20, 110 bedding plane C-2 joint face 290 90 C-3 joint face 18 75 D: 40, 130 on bedding plane **A, B, C-1, & D combined**	138 24	1-5 (0.3 1.5)	14 8 15 12 15 16 **53**	10.8 (1.0) 10.8 (1.0) 10.8 (1.0) 10.8 (1.0) 10.8 (1.0) 10.8 (1.0) **43.1 (4.0)**	15-45 60-75; 300-315 15-45; 315-330 75-90; 315-330 285-315 30-45 **15-45**	2.7 (9.1) 1.3 (4.3) 1.8 (5.9) 1.1 (3.6) 1.5 (5.1) 1.4 (4.7) **1.8 (6.0)**	Clean, smooth joint surfaces. Good connectivity.
KCF-13	Nugget Sandstone	A: 80, 170 horizontal surface B: 85, 175 horizontal surface C: on joint surface 84 55 **A & B combined**	232 30	Cross-bedding 0.25-2 (0.1-0.6)	9 8 19 **17**	10.8 (1.0) 10.8 (1.0) 10.8 (1.0) **21.5 (2.0)**	255-285; 345-360 45-90; 345-360 0-60; 330-345 **255-285; 345-360**	1.4 (4.6) 1.5 (5.0) 2.6 (8.5) **1.4 (4.8)**	Joints are smooth, uncemented, and relatively long. Good connectivity.

(Table C.1 continued)

Site[a]	Unit	Sample Grids[b]	Strike and Dip of Bedding[c]	Bed Thickness in feet (m)	N[d]	Area ft^2 (m^2)	Joint Sets[e]	Joint Density[f] ft/ft^2 (m/m^2)	Notes
KCF-14	Twin Creek Limestone	70, 160 on bedding plane	248 30	0.5-3 (0.2-1)	**7**	**3.2 (0.3)**	**345-360; 60-75**	**0.8 (2.8)**	Watton Canyon Member. Uncemented joints reported; many calcite-cemented veins are present.
KCF-15[g]	Weber Sandstone	A:127 0 on joint plane 127 84 B: 37 15 on joint plane 116 64 C: 32 25 on joint plane 215 82 D: 27 0 on joint plane 27 57 E: 37 15 on joint plane 27 57 **A through E combined**	280 25	1-5 (0.3-1.5)	10 16 11 13 10 **60**	1.0 (0.3) 1.3 (0.4) 2.0 (0.6) 3.0 (0.9) 1.6 (0.5) **8.9 (2.7)**	330-15; 45-90 0-30 15-30 300-315 315-345 **0-30; 290-330**	10.5 (34.0) 12.7 (41.6) 6.0 (19.6) 4.5 (14.8) 5.6 (18.5) **6.9 (22.6)**	Adjacent to strand of East Kamas Valley fault (figure 11) ***See note f below for explanation of values.***
KCF-16	Frontier Formation - Oyster Ridge Sandstone Member	A: 75, 165 on bedding plane B: 13, 103 on bedding plane C: 40, 310 on bedding plane **A, B, & C combined**	198 23	5-15 (1.5-4.6)	13 15 38 **66**	43.2 (4.0) 6.5 (0.6) 6.5 (0.6) **56.0 (5.2)**	285-300; 0-30 60-120; 0-15 315-345; 45-60; 75-120 **255-300; 315-345**	0.8 (2.7) 2.4 (7.9) 4.5 (14.9) **1.4 (4.8)**	Grid C contains a joint zone.
KCF-17	Frontier Formation - upper member	A: 20, 110 on bedding plane B: 50, 140 on bedding plane C: 50, 140 on bedding plane D: 25,115 on bedding plane **A through D combined**	216 28	1-5 (0.3-1.5)	15 5 4 12 **27**	10.8 (1.0) 10.8 (1.0) 10.8 (1.0) 10.8 (1.0) **43.1 (4.0)**	15-30; 285-315; 345 360 285-315 285-315 285-300; 330-345 **285-300; 330-360; 15-30**	1.6 (5.3) 0.7 (2.3) 0.5 (1.6) 1.5 (5.1) **1.1 (3.6)**	Grids A and D are on thin-bedded sandstone; grids B and C are on thick-bedded sandstone.
KCF-18	Kelvin Formation	A: 80, 170 on bedding plane B: 75, 165 on bedding plane C: 85, 175 on bedding plane **A, B, & C combined**	260 43	1-3 (0.3-1)	39 15 5 **59**	43.1 (4.0) 10.8 (1.0) 10.8 (1.0) **64.6 (6.0)**	345-360; 285-300 345-15; 285-300 **345-15; 285-300**	2.6 (8.5) 1.7 (5.7) 1.0 (3.4) **2.0 (6.5)**	Northeast Rockport Reservoir. Most joints are calcite cemented.
KCF-19	Kelvin Formation	30, 120 on bedding plane	197 8	1-3 (0.3-1)	**4**	**10.8 (1.0)**	**300-315; 0-15; 45-60**	**0.6 (2.0)**	Most joints are calcite-cemented.
KCF-20	Kelvin Formation	A: 50, 140 on bedding plane B: 45, 135 on bedding plane **A, & B combined**	200 15	1-3 (0.3-1)	11 13 **24**	6.5 (0.6) 10.8 (1.0) **17.2 (1.6)**	315-330; 285-300; 345-360 315-345; 0-15; 30-45 **315-330; 330-15; 30-45**	2.7 (9.1) 1.4 (4.7) **1.9 (6.3)**	Most joints are calcite-cemented.
KCF-21	Kelvin Formation	A: 30, 120 on bedding plane B: 80, 170 on bedding plane C: 50, 140 on bedding plane **A, B, & C combined**	164 17	1-3 (0.3-1)	15 13 11 **39**	43.1 (4.0) 10.8 (1.0) 10.8 (1.0) **64.8 (6.0)**	15-30; 45-60 15-30; 60-75; 300-315 60-75; 0-15 **15-30; 45-75**	1.0 (3.4) 1.5 (5.0) 1.3 (4.4) **1.2 (3.8)**	Most joints are calcite-cemented.
KCF-22[h]	Keetley Volcanics	Sampling rectangles A: 2,070 ft x 1,725 ft B: 2,238 ft x 1,328 ft C: 2,608 ft x 1,855 ft D: 6,383 ft x 3,077 ft **A, B, C, & D Combined: 1,113 mi^2 (2.85 km^2)**	not known	not known	 150 73 135 484 **842**	mi^2 (km^2) 0.13 (0.33) 0.11 (0.27) 0.17 (0.45) 0.70 (1.8) **1.11 (2.85)**	 270-15 285-330 315-360; 270-300 330-15; 300-315 **330-360; 300-315**	not calculated	Most joints are uncemented

Notes:

a. See plate 6 for locations and rose diagrams. Data in boldface are shown in rose diagram on plate 6.

b. Joints were measured within a square sampling grid, except for site KCF-15 (see note g). The orientations of sampling grids are reported as the directions, in azimuth notation, of two perpendicular edges of the grid. In azimuth notation, the compass is divided into 360 degrees: 0°and 360° are both North, 90° is East, 180° is South, and 270° is West. The orientations of planar features, including bedding, joints, and surfaces on which the grids were measured, are reported as the strike and dip of the surface, in right-hand-rule notation. The strike of a planar feature is the direction of the line of intersection between a horizontal plane and the feature. In right-hand rule notation, the strike is reported as the compass reading when looking in the strike direction such that bedding dips down to the right. The dip of a planar feature is the acute angle between the feature and a horizontal plane, measured in a vertical plane with values from 0 to 90 degrees increasing downward.

c. Strike and dip of bedding is given in right-hand-rule azimuth notation; see note b for explanation.

d. N is the number of joints measured.

e. Joint sets are subjectively determined from rose diagrams, and are defined as distinct ranges of orientations with significantly higher numbers compared to other orientations.

f. Joint density is in two-dimensional units of total joint length per sample area.

g. Site KCF-15 was sampled by linear traverses on steeply dipping joint faces. Data in “Sample Grids” column are the trend and plunge of the sampling traverse, followed by the strike and dip of the joint surface, in right-hand-rule notation. Data in the “Area” column are the lengths of the sampling traverses, in feet (meters). Data in the “Joint Density” column are number of joints per unit length, in feet (meters).

h. Data derived from analysis of aerial photograph. See text, appendix C, and figure 12.

APPENDIX D

Descriptions of Stratigraphic Ground-Water Compartments

This appendix describes the stratigraphic ground-water compartments (SGWCs) in the study area (figures 13 and 14) in greater detail than in the main body of the text. These descriptions include the constituent formations, thickness, stratigraphic boundaries, areal extent, lithology, structure, fracture characteristics, and current ground-water production for each SGWC. Test yields for water wells are from drillers' logs in the Utah Division of Water Rights database and roughly indicate the production potential of the SGWCs, but are not useful for inferring hydraulic conductivity of producing units. Production potential varies with location, and the production of one well does not quantitatively predict the production of a well in a different location within the same SGWC.

Keetley SGWC

The Keetley Volcanics and underlying Tertiary conglomerate make up an internally heterogeneous stratigraphic ground-water compartment exposed in the West Hills, the hills north of Kamas Valley, and along the lower range front of the western Uinta Mountains in southern Kamas Valley (figure 14). The Keetley SGWC also underlies Kamas Valley (cross sections A-A′ through G-G′, plate 3). The Keetley SGWC is overlain by the unconsolidated Quaternary fill of Kamas Valley and by local Quaternary deposits in the West Hills, and overlies late Paleozoic to Mesozoic rocks below Kamas Valley and in the West Hills.

The thickness of the Keetley SGWC is variable and unknown in much of the study area, due to lack of well data; Bryant (1990) lists a maximum thickness of 1,640 feet (500 m) for the Keetley Volcanics, and notes that the underlying conglomerate has highly variable thickness. Oil-test and water wells in the hanging wall of the East Kamas Valley fault zone penetrated 700 to 1,833 feet (213-560 m) of Keetley Volcanics (well F, table A.2 and well 21, table A.1, respectively). Well logs on the eastern valley margin east of Marion, in the footwall of the East Kamas Valley fault zone, penetrated from 80 to 200 feet (24-61 m) of Keetley Volcanics (Wallace, 2000).

The Keetley Volcanics consist of poorly sorted, massive to well-layered tuff and volcanic breccia interlayered with hard andesitic to dacitic flows, locally intruded by small plutons and dikes (plates 1 and 2; Woodfill, 1972; Bryant, 1990). Facies have variable thickness and limited lateral extent (Woodfill, 1972), and the informal members on plates 1 and 2 are themselves internally heterogeneous. The tuffs likely have the lowest hydraulic conductivity due to their fine-grained, ash-rich matrix. The flows have by far the longest and most dense joint populations (figure 12).

At least 32 private wells draw water from the Keetley SGWC in the study area, especially in Indian Hollow west of Kamas, where test capacities typically range from 2 to 30 gallons per minute (114 L/min) (Utah Division of Water Rights data). EWP (1992) reported capacities of 150 and 250 gallons per minute (569-948 L/min) for two private wells screened in the Keetley Volcanics at the west margin of Kamas Valley. These wells are near the intersection between the City Creek fault in the West Hills and the west Kamas Valley fault, so they may derive their high production in part from high fracture density associated with these faults. However, both faults are concealed and the geologic setting of these wells is not precisely known. Indian Hollow Spring (figure 1), which supplies water to several private users, emanates from volcanic breccia along a stream bed just above a 10-foot-wide (3 m) dike. The dike likely has lower hydraulic conductivity than the breccia, so forms a barrier to ground water flowing from above, forcing it to the surface at the elevation of the stream bed.

Wasatch-Evanston Heterogeneous SGWC

This SGWC is composed of the Tertiary Wasatch Formation and the Upper Cretaceous Hams Fork Member of the Evanston Formation (figures 13 and 14). The Hams Fork Member of the Evanston Formation is absent near Echo Reservoir due to either non-deposition or erosion, and the Wasatch Formation within the study area crops out north of the Uinta Mountains (Lamerson, 1982; Bryant, 1990; DeCelles, 1994). The Wasatch-Evanston heterogeneous SGWC is about 6,550 feet (2,000 m) thick along Chalk Creek, and thins to the southwest. The upper boundary of the Wasatch-Evanston SGWC either crops out or is overlain by Tertiary and/or Quaternary deposits, and its lower boundary is the angular unconformity separating the Hams Fork Member of the Evanston Formation from underlying formations.

Both the Wasatch Formation and the Hams Fork Member of the Evanston Formation consist of interbedded mudstone, sandstone, and conglomerate, and the proportion of conglomerate increases toward the base of both formations. Sandstone and conglomerate beds have limited lateral extent, approximately 100 to 5,000 feet (30-1,524 m). Sandstone beds are generally well sorted, may retain some primary porosity and permeability, have the greatest joint density, and are likely the best prospective aquifers of the three main constituent facies. Conglomerate beds are poorly sorted, well cemented, and typically have low joint density, and mudstone layers have very low to zero joint density; both rock types are likely low-permeability units.

The Wasatch Formation is deformed at three locations in the study area: the northeast corner of the study area where it dips 20 to 30 degrees east due to motion on an unexposed splay of the Medicine Butte thrust; near the thrust that cuts the Coalville anticline; and along the Chappel Mine fault (Lamerson, 1982; cross sections J-J′ and K-K′, plate 3). The Hams Fork Member of the Evanston Formation was deposited during and after the final stages of slip on the Absaroka thrust system (Lamerson, 1982), so is locally deformed near these faults (Lamerson, 1982; cross section K-K′, plate 3). The Hams Fork Member of the

Evanston Formation near Rockport Reservoir was tilted to the northwest during folding associated with uplift of the western Uinta Mountains, but the deposition of Wasatch Formation postdated this deformation (Crittenden, 1974; Bryant and Nichols, 1988). Joints in these units were not studied systematically, but are typically widely spaced and filled with calcite, especially in the Wasatch Formation.

Wells owned by Coalville City (well K, table A.2), Hoytsville Pipe Water Co. (well J, table A.2), and numerous private residential and industrial wells produce water from the Wasatch-Evanston heterogeneous SGWC, principally the Wasatch Formation.

Adaville-Hilliard Heterogeneous SGWC

The Adaville and Hilliard Formations are stratigraphically equivalent to the Upper Cretaceous Frontier Formation, and are found principally in southwest Wyoming (Lamerson, 1982; Royse, 1993). Bryant (1990) mapped these formations in a small belt north of the Uinta Mountains, bounded by thrust faults of the Absaroka and North Flank fault systems (plate 1), and they may also be present in the subsurface in the footwall of the Absaroka thrust system (Lamerson, 1982). Their structure northwest of the Uinta Mountains is complex due to deformation by two thrust systems with different directions of motion (cross section H-H′, plate 3); therefore, the stratigraphic thickness of the Adaville-Hilliard heterogeneous SGWC is poorly known but is estimated to be about 4,495 feet (1,370 m) (Bryant, 1990). The stratigraphic boundaries of the Adaville-Hilliard heterogeneous SGWC are not exposed due to faulting.

The Adaville and Hilliard Formations consist of mudstone with interbedded sandstone and conglomerate (Bryant, 1990; plate 2). Northwest of the Uinta Mountains, a cluster of sandstone and conglomerate beds about 100 feet (30 m) thick forms a prominent ridge in the study area where they are vertical to overturned, and are cut by northeast-striking faults not shown on plate 1. No wells are known in this SGWC, and its complex structure makes it an unlikely prospective aquifer.

Echo-Upper Frontier Heterogeneous SGWC

The Upper Cretaceous Echo Canyon Conglomerate, Henefer Formation, and the upper member of the Frontier Formation comprise the Echo-upper Frontier heterogeneous SGWC, which is present north of the Uinta Mountains and Kamas Valley (figures 13 and 14). The Echo-upper Frontier heterogeneous SGWC is approximately 7,860 to 8,840 feet (2,400-2,700 m) thick, but facies and thickness variations exist in each unit due to deposition during deformation in the Cordilleran thrust belt (Lamerson, 1982; DeCelles, 1994). The Echo-upper Frontier heterogeneous SGWC is bounded above by the Wasatch-Evanston heterogeneous SGWC along an angular unconformity, and below by a mudstone confining unit in the lower part of the upper member of the Frontier Formation (figure 13).

The Echo-upper Frontier heterogeneous SGWC consists of interbedded mudstone, sandstone, and conglomerate. The thicknesses, relative proportions, and compositions of these facies are variable in each formation. Sandstone beds in the Henefer Formation and the Echo Canyon Conglomerate are interlayered to gradational with conglomerate, whereas those in the upper Frontier Formation are interlayered with mudstone, have more tabular forms, and are clustered into sequences approximately 30 to 150 feet (9-46 m) thick.

The Echo Canyon Conglomerate and Henefer and Frontier Formations predated the Absaroka thrust system and were derived from the west to northwest during uplift in the Wasatch Range associated with movement on the Crawford thrust (Lamerson, 1982; DeCelles, 1994). Their structure, therefore, reflects deformation during and after movement on the Absaroka thrust system, which postdated the Crawford thrust system. Bedding is steeply dipping and complexly faulted near major thrusts and in associated folds, and gently dipping and homoclinal away from these structures (cross sections I-I′ through K-K′, plate 3). Joints in the Echo Canyon Conglomerate and Henefer Formation were not studied systematically but are typically widely spaced, filled with calcite, and most abundant in sandstone. Joints in sandstones of the upper member of the Frontier Formation have good connectivity parallel to the primary set (site KCF-17, plate 6).

A well owned by Coalville City (well L, table A.2) is screened in the upper member of the Frontier Formation. Groundwater production from the Echo-upper Frontier heterogeneous SGWC elsewhere is sparse and is restricted to several private wells, so its hydrogeologic properties are not known. Sandstone layers, especially where they are clustered into sequences at least 50 feet (15 m) thick, are the best prospective aquifers in this SGWC.

Oyster Ridge SGWC

The Oyster Ridge SGWC is composed of the Oyster Ridge Sandstone Member of the Upper Cretaceous Frontier Formation, which is a 200- to 330-foot-thick (61-101 m) sequence of sandstone bounded above and below by mudstone (figure 13). The Oyster Ridge SGWC crops out east of Echo Reservoir, in the Coalville anticline along Chalk Creek, and near Rockport Reservoir (figure 14). The Oyster Ridge SGWC is severed by normal faults near Echo Reservoir and by thrust faults near Rockport Reservoir and in the Coalville anticline (cross sections I-I′, J-J′, and K-K′, plate 3).

The Oyster Ridge Sandstone consists of well-sorted marine quartzarenite that is moderately to weakly cemented. Joint density is moderate to high, with high connectivity due to the presence of several joint sets striking at high angles to each other, and joint zones are common. These characteristics indicate that the Oyster Ridge SGWC may have enhanced hydraulic conductivity and may be a good potential aquifer especially near Echo and Rockport Reservoirs, which would provide recharge. Limited exposure at relatively low altitudes and disruption by faults in this area may, however, limit the yield potential of the Oyster Ridge SGWC.

Lower Frontier Heterogeneous SGWC

The lower 50 to 100 feet (15-30 m) of the lower member of the Upper Cretaceous Frontier Formation consists of a sequence of clustered sandstone beds (Hale, 1976), herein designated the lower Frontier heterogeneous SGWC (figures 13 and 14). This SGWC is exposed on the northwest limb of the Coalville anticline, near the north and south ends of Rockport Reservoir, and north of Kamas Valley (figure 14). The lower Frontier heterogeneous SGWC is severed by faults at both ends of the outcrop belt on the northwest limb of the Coalville anticline (figure 14), but its physical continuity is much greater near Rockport Reservoir (cross section I-I′, plate 3) and northeast of Kamas Valley (cross section H-H′, plate 3). The Aspen Shale forms a 500-foot-thick (152 m) low-permeability layer at the base of the lower Frontier heterogeneous SGWC, and mudstones of the lower member of the Frontier Formation immediately below the Oyster Ridge Sandstone Member form its upper boundary (figure 13).

Sandstones of the lower Frontier heterogeneous SGWC are moderately to well cemented quartzarenite to sublitharenite with individual beds about 1 to 5 feet (0.3-1.5 m) thick. Joint density is moderate to high at the southwest end of Rockport Reservoir (site KCF-9, plate 6), and connectivity parallel to the north-striking primary joint set and to the bedding planes is very good, but many joint surfaces are cemented by calcite. This SGWC is a potential aquifer, though its hydraulic conductivity may be limited by calcite cement lining many joint surfaces. No public supply wells are in the lower Frontier heterogeneous SGWC, but some private wells may be screened in it northwest of Rockport Reservoir.

Kelvin-Preuss Heterogeneous SGWC

Interlayered sandstone, mudstone, and conglomerate of the Lower Cretaceous Kelvin Formation and Jurassic Morrison and Stump Formations and Preuss Sandstone comprise this SGWC (figure 13). In the northeast part of the study area, the Thomas Fork and Cokeville Formations are stratigraphically equivalent to the Kelvin Formation (Bryant, 1990; plate 6). The upper boundary is the Aspen Shale (Sage Junction Formation in the northeast part of the map area) low-permeability unit, and the lower boundary consists of siltstone, mudstone, and salt deposits at the base of the Preuss Sandstone. The Morrison Formation is absent in the hanging wall of the Absaroka thrust system, and the Parleys Member of the Kelvin Formation is absent in its footwall (Crittenden, 1974; Bryant, 1990). The stratigraphic thickness in structurally undisrupted areas is 3,248 to 5,873 feet (990-1,790 m) near Rockport Reservoir and about 5,450 feet (1,661 m) near Chalk Creek. Thicknesses vary near thrusts and in the cores of folds, mainly due to flowage of the Preuss salt layer (Lamerson, 1982).

The Kelvin-Preuss heterogeneous SGWC is exposed in the core of the Coalville anticline near Chalk Creek, in the northeast corner of the study area, near Rockport Reservoir, and northeast of Kamas Valley (figure 14). Bedding in the Kelvin Formation dips uniformly 20 to 30 degrees northwest on the northwest limb of the Coalville anticline and 70 degrees east to vertical on the east limb, where it is truncated by a west-dipping reverse fault (cross section K-K′, plate 3). In the northeast part of the study area, the Kelvin Formation is in the footwall of the Acocks fault zone and the hanging wall of the Medicine Butte thrust, and is tightly folded and highly faulted (cross section K-K′, plate 3). Near Rockport Reservoir, the Kelvin-Preuss SGWC is exposed in both the hanging wall and the footwall of the Absaroka thrust system, where it dips uniformly northwest except adjacent to thrusts and in a fold at the northeast corner of the reservoir (cross section J-J′, plate 3), where dips are highly variable. The Kelvin-Preuss heterogeneous SGWC is structurally intact from top to base only in the hanging wall of the Whites Basin thrust northeast of Kamas Valley, where it forms a broad, open ramp anticline that has been tilted northwest by folding associated with the North Flank thrust (cross section H-H′, plate 3).

Sandstone sequences in the Kelvin Formation are about 10 to 150 feet (3-46 m) thick, and are composed of moderately to well-sorted, fine- to medium-grained litharenite. Joint populations are characterized by two steeply dipping sets and one bedding-plane set and by good connectivity, but calcite cement is ubiquitous (sites KCF-18 through -21, plate 6; table B.1). Sandstone beds in the Stump Formation and Preuss Sandstone are thinner and more tightly cemented than those of the Kelvin Formation.

The town of Wanship owns a well screened partly in the Kelvin Formation (well I, table A.2). Private water wells screened in the Kelvin Formation west of Rockport Reservoir tested at 12 to 55 gallons per minute (45-208 L/min) (Utah Division of Water Rights data). Based on fracture data (appendix C), sandstones of the Kelvin Formation are the best potential aquifer in the Kelvin-Preuss SGWC.

Twin Creek Limestone SGWCs

The Jurassic Twin Creek Limestone consists of seven formally defined members of alternating hard, clayey limestone and soft, clayey limestone to mudstone (Imlay, 1967; figure 6; plate 2). In this study, the hard, clayey limestone members - the Giraffe Creek, Watton Canyon, and Rich-Sliderock (combining the formally defined Rich and Sliderock Members of Imlay, 1967) - are designated as SGWCs and the Leeds Creek, Boundary Ridge, and Gypsum Spring members are regarded as low-permeability units (figure 13), following Ashland and others (2001). These SGWCs are separately designated, rather than lumped as a single heterogeneous SGWC, because the members are regionally continuous in contrast to sandstone beds in the overlying

Cretaceous SGWCs, and they are aquifers in Snyderville basin (Weston Engineering, 1996; Keighly and others, 1997; Ashland and others, 2001).

The Twin Creek SGWCs crop out north of Kamas Valley from the Mahogany Hills to the West Hills. Although the Twin Creek SGWCs are discontinuously exposed west of the Mahogany Hills, they are present beneath Quaternary deposits and the Tertiary Keetley Volcanics. The Twin Creek SGWCs are cut by the Whites Basin thrust (cross sections G-G′ and H-H′, plate 3). Bedding in the hanging wall of the Whites Basin thrust dips 45 to 70 degrees northwest, and is folded into tight, northeast-striking folds and cut by minor faults (cross sections G-G′, H-H′, and I-I′, plate 3). The subsurface structure of the Watton Canyon SGWC is illustrated on plates 5A and 5B.

Joint populations in the Watton Canyon and Rich-Sliderock SGWCs are characterized by two joint sets with relatively long average lengths at high angles to bedding and to each other, and by little or no calcite cement (sites KCF-7 and -14, plate 6; table B.1). These joints cut several sets of veins formed during Cordilleran thrust belt and Rocky Mountain foreland deformation (Bradley and Bruhn, 1988), indicating that they occurred late in the structural history of the region, probably during Tertiary extension.

Ashland and others (2001) and Weston Engineering (1996) discuss evidence from Snyderville basin, 14 miles (22 km) west of Kamas Valley, that the Gypsum Spring Member of the Twin Creek Limestone is a confining unit between the Rich-Sliderock and Nugget SGWCs, and their conclusions are adopted in this report. In Snyderville basin, two water wells about 30 feet (9 m) apart were screened in the Nugget and Rich-Sliderock SGWCs, respectively. The static water level of the Nugget well, which was cased through the Rich-Sliderock SGWC and the Gypsum Spring Member, was higher than that of the well screened at higher elevations in the Rich Sliderock SGWC, indicating that ground water in the Nugget SGWC is confined below the Gypsum Spring Member (Ashland and others, 2001; Weston Engineering, 1996). Furthermore, aquifer tests showed no significant interference between the two wells (Weston Engineering, 1996). Designation of the Boundary Ridge and Leeds Creek Members as confining units and the Giraffe Creek and Watton Canyon Members as SGWCs are based on lithology and the presence of springs in the Watton Canyon.

Two wells and one spring in the study area produce water from Twin Creek SGWCs. A privately owned well about 1 mile (1.6 km) north of Peoa encountered unconsolidated sediments from the surface to 53 feet (16 m), “green clay” and “yellow/gray limestone” from 53 to 216 feet (16-66 m), and “dark gray limestone” from 216 to 320 feet (66-98 m) (Utah Division of Water Rights data). The well was cased over its entire depth, was perforated between 280 and 320 feet (85-98 m), and air-lift tested at 40 gallons per minute (152 L/min) for 1 hour; drawdown was not recorded. The “green clay” and “yellow/gray limestone” is interpreted here as the Leeds Creek Member of the Twin Creek Limestone, which is exposed on the hillside to the east, and the “dark gray limestone” is interpreted as the Watton Canyon Member. The water well log does not provide details of the drilling history, but it is logical to conclude that once bedrock was encountered, drilling continued until sufficient water production was obtained and that the well was perforated over the best-producing interval. The Watton Canyon Member is most likely the producing interval in this well, supporting its designation as a SGWC and supporting, but not proving, designation of the Leeds Creek member as a low-permeability unit.

A privately owned well on the topographic bench northeast of Peoa encountered unconsolidated sediment from 0 to 65 feet (0-20 m), andesite from 65 to 140 feet (20-43 m), and limestone between 140 and 220 feet (43-67 m). The well was perforated between 75 and 215 feet (23-66 m) and tested at 20 gallons per minute (76 L/min) (Utah Division of Water Rights data). The limestone is interpreted here as the Rich-Sliderock member of the Twin Creek Limestone. An unnamed, privately held spring northeast of Oakley emanates from the Watton Canyon SGWC, supporting the interpretation of the underlying Boundary Ridge Member as a low-permeability unit.

These data indicate that the Watton Canyon and Rich-Sliderock SGWCs are potential aquifers in the study area, although they are thinner than in Snyderville basin and are complexly deformed in places. The Giraffe Creek SGWC is likely too thin to be an aquifer.

Nugget SGWC

The Nugget SGWC consists of the Jurassic Nugget Sandstone, which is 919 to 1,250 feet (280-381 m) thick in the study area and is bounded above by the Gypsum Spring Member of the Twin Creek Limestone, and below by mudstone and siltstone of the upper member of the Triassic Ankareh Formation (figure 13), both low-permeability units.

The Nugget SGWC occurs along a narrow, northeast-trending, northwest-dipping band from the West Hills to the northwestern Uinta Mountains (figure 14; plate 1), and is largely concealed by younger units but is structurally continuous for much of this distance. It is in both the hanging wall and footwall of the Whites Basin thrust, and is cut off at its northeastern end by the North Flank thrust (cross sections G-G′, H-H′, and I-I′, plate 3; plates 5C and 5D). The structural continuity of the Nugget SGWC is also disrupted by the northern part of the East Kamas Valley fault zone (figure 14; plate 1).

The Nugget Sandstone consists of fine- to medium-grained, well-sorted eolian sandstone, with a subarkosic composition (Bergosh and others, 1982). Planar to trough cross-bedding is pervasive in the Nugget, and bedding surfaces are laterally discontinuous. Joints occur in two sets at high angles to each other and to the cross-bedding, and are typically long, widely spaced, well connected, and uncemented (sites KCF-8 and KCF-13, plate 6).

The Nugget SGWC is an important aquifer in the Snyderville basin area (Keighley and others, 1997; Ashland and others, 2001). Only two private wells draw water from the Nugget SGWC in the study area: one is near the northeastern end of the outcrop belt, for which the driller reported yields of 8 to 15 gallons per minute (30 57 L/min); the other, located about 1 mile (1.6 km) northwest of Oakley, air-lift tested at 10 gallons per minute (38 L/min) (Utah Division of Water Rights data).

Gartra SGWC

The Gartra SGWC, which consists of the Gartra Member of the Triassic Ankareh Formation (Ashland and others, 2001), crops out southeast of and parallel to the Nugget SGWC (figures 13 and 14) and has a similar structural setting (cross sections H-H′, I-I′, and K-K′, plate 3). The Gartra Member consists of pale gray chert-pebble conglomerate and coarse to medium-grained sandstone, all tightly cemented and densely jointed. Ashland and others (2001) designated the Gartra Member a SGWC based on its lithologic characteristics and position between siltstone and mudstone of the upper and Mahogany members of the Ankareh Formation, but did not discuss its hydrogeology. No wells or springs in the study area are located in the Gartra SGWC.

Thaynes SGWCs

The Triassic Thaynes Formation is divided into upper and lower SGWCs, each approximately 550 feet (168 m) thick, separated by a low-permeability shale unit that is about 5 feet (1.5 m) thick (Weston Engineering, 1999b). The Mahogany Member of the Ankareh Formation bounds the upper Thaynes SGWC above, and the Triassic Woodside Formation bounds the lower Thaynes SGWC below (figure 13). The Thaynes SGWCs crop out along a northeast-trending belt in the northwestern Uinta Mountains and southern Mahogany Hills. The western part of this outcrop belt is transected by the Weber River.

Bedding in the Thaynes SGWCs dips uniformly 30 to 40 degrees northwest, and the outcrop belt of the SGWCs is truncated on the northeast by the North Flank thrust and on the southwest by the East Kamas Valley fault zone (cross sections F-F′ and H H′, plate 3; plates 5E and 5F). The Thaynes consists of interbedded hard, fine-grained calcareous sandstone, medium- to coarse-grained limestone, and greenish-gray shale. Bed thickness ranges from 1 to 10 feet (0.3-3 m). Jointing in the Thaynes is characterized by two long sets at high angles to each other and to bedding planes, and a bedding-plane set, indicating very good connectivity. Joint surfaces lack persistent mineralization. Joint zones are present near the western end of the outcrop belt (site KCF-6, plate 6).

In Snyderville basin, Keighley and others (1997) reported yields of 125 to 1,000 gallons per minute (474-3,790 L/min) for wells screened in the Thaynes, and Ashland and others (2001) noted that significant amounts of water spill from the Thaynes into mine tunnels near Park City. In the study area, several private wells draw water from the Thaynes SGWC along the Weber River in the western part of its outcrop belt.

Upper Park City SGWC

The upper Park City SGWC consists of interbedded cherty limestone and sandstone in approximately the upper 300 feet (91 m) of the Permian Park City Formation (figure 13; Ashland and others, 2001). This SGWC is defined based on lithology; Ashland and others (2001) did not describe its hydrogeologic properties. The upper Park City SGWC crops out along a northeast-trending belt in the northwestern Uinta Mountains, parallel to and southeast of the Thaynes SGWC, and dips 25 to 40 degrees northwest (plate 1; cross section H-H′, plate 3). Joint characteristics of this SGWC were not studied, and no water wells are completed in it.

Weber SGWC

The Weber SGWC consists of the lower 100 feet (30 m) of the Permian Park City Formation and the underlying Pennsylvanian Weber Sandstone (figure 13; Ashland and others, 2001). This SGWC is bounded above and below by low-permeability units consisting of phosphatic shale of the Park City Formation and mudstone and siltstone of the Pennsylvanian Morgan Formation, respectively (figure 13). The thickness of the Weber SGWC varies considerably; it is 2,600 feet (792 m) thick in the northeast and southeast parts of the study area, and 1,730 feet (527 feet) thick in the western Uinta Mountains adjacent to the northeast corner of Kamas Valley.

The Weber SGWC is exposed along the flanks of the Uinta Mountains throughout the study area (figure 14; plate 1); bedding dips 20 to 40 degrees away from the topographically higher parts of the mountains (cross sections A-A′ through H H′, plate 3). The entire SGWC is exposed only along the northern and southern flanks of the Uinta Mountains; the upper third to half has been eroded from the western part. Along-strike structural continuity is broken only by a northeast-striking fault in the southwestern Uinta Mountains (figure 14). The Weber SGWC projects westward below Kamas Valley, and is encountered by several oil-test and water wells. Its structure below Kamas Valley is illustrated on plates 5G and 5H. The Weber SGWC is cut by the East Kamas Valley fault zone just west of the western Uinta Mountains (cross sections B-B′ through F-F′, plate 3).

The Weber Sandstone is composed of interbedded quartzite and sandstone. Joint populations in the Weber Sandstone typically contain two sets at high angles to each other and to an inconsistently developed bedding-plane set (sites KCF-1, -3, -4, 10, -12, and -15, plate 6; table B.1). Although joint density in the Weber SGWC is relatively low to moderate, connectivity is high, and joint surfaces are smooth and lack secondary cement (table C.1), promoting high hydraulic conductivity.

Three municipal and at least 23 private wells draw water from the Weber SGWC. The municipal wells supply the towns of Kamas (700 gallons per minute [2,653 L/min]), Francis (250 gallons per minute [948 L/min]), and Woodland (280 gallons per minute [1,060 L/min]), and the Beaver Creek-Shingle Creek Irrigation Company (300 gallons per minute [1,136 L/min]) (Utah Division of Water Rights data; EWP, 1992). The private wells typically tested at 15 to 30 gallons per minute (57-114 L/min) (Utah Division of Water Rights data).

Two springs emanating from the Weber SGWC are used for public supply. Oakley City obtains water from the Cottonwood Springs (figure 1), in limestones of the lower part of the Park City Formation in the northeastern corner of Kamas Valley (D. Evans, Oakley City Mayor, verbal communication, 1998). The East Kamas Valley fault zone projects just west of these springs, and may partly control their location. Alternatively, the phosphatic shale member of the Park City Formation may underlie the valley just northwest of the springs, forcing ground water to the surface just uphill. Kamas City obtained water until recently from Elder Hollow Spring (figure 1), which emanates from the Weber Sandstone just above its lower contact with the Morgan Formation. Elder Hollow Spring is in a relatively straight, steep canyon, but it is unclear whether a fault underlies this canyon. The upper part of the Morgan Formation consists of fine-grained siltstone and mudstone that is a low-permeability unit (figure 13), so the spring may be entirely stratigraphically controlled.

Morgan-Round Valley Heterogeneous SGWC

The Morgan-Round Valley heterogeneous SGWC consists of the Pennsylvanian Morgan Formation below its upper 50- to 100-foot-thick (15-30 m) confining layer, plus the entire Pennsylvanian Round Valley Limestone (figure 13). Clayey mudstones of the Mississippian Doughnut Formation provide the lower boundary. The Morgan-Round Valley heterogeneous SGWC is about 270 to 1,100 feet (82-335 m) thick, and is exposed along a horseshoe-shaped band parallel to and east of the western margin of the western Uinta Mountains (figure 14). Bedding in the Morgan-Round Valley heterogeneous SGWC dips 20 to 40 degrees away from the topographically higher parts of the Uinta Mountains, and its structure is similar to that of the Weber SGWC.

The lower part of the Morgan Formation and the Round Valley Limestone consist of interbedded cherty limestone, sandstone, and shale, with bed thickness ranging from 1 to 6 feet (0.3-1.8 m). Joint density is moderately high and connectivity is good (site KCF-11, plate 6; table B.1), but calcite typically cements joint surfaces in the limestones. At least one well west of Samak and three wells southeast of Woodland, all privately owned, are in the Morgan-Round Valley heterogeneous SGWC; these wells tested at 15 to 35 gallons per minute (57-133 L/min) (Utah Division of Water Rights data).

Humbug-Uinta SGWC

The Humbug-Uinta SGWC consists of the Mississippian Humbug Formation, the Madison Limestone and Upper Devonian Rocks unit, the Cambrian Tintic Quartzite, and the Proterozoic Uinta Mountain Group (figure 13). The lithology of the constituent formations varies, but no low-permeability unit was identified within the sequence. The upper boundary is the Mississippian Doughnut Formation low-permeability unit, and the lower boundary is undefined.

The stratigraphic thickness of the Paleozoic components of this SGWC varies substantially, from about 745 to 3,078 feet (227-939 m), due to a combination of variable original thickness and subsequent erosion associated with uplift along the Uinta-Cottonwood arch (Bryant and Nichols, 1988). The Tintic Quartzite is present only locally due to varying depositional thickness and erosion during Devonian to Silurian time (Bryant and Nichols, 1988). The Humbug-Uinta SGWC crops out in a horseshoe-shaped belt that wraps around the core of the western Uinta Mountains, which is composed of Proterozoic rocks and forms the topographically highest part of these mountains. Bedding dips 10 to 35 degrees away from the Proterozoic core (cross sections A-A′ through H-H′, plate 3), except near Smith and Morehouse Reservoir in the eastern part of the study area where folding above the North Flank thrust results in dips of 60 to 80 degrees. Plate 5I illustrates the subsurface geometry of the top of the Humbug-Tintic SGWC.

The Humbug Formation consists of interbedded sandstone, bioclastic limestone, and calcite-cemented intraformational breccia. The Madison Limestone and Upper Devonian rocks are medium-grained, locally cherty bioclastic limestone with well-defined bedding planes. The Tintic Quartzite consists of hard, medium- to coarse-grained quartzarenite and quartzite-clast conglomerate. Joints in the Humbug and Madison Limestone and Upper Devonian rocks have moderate to high density, and consist of two sets at high angles to a well- (Madison) to poorly (Humbug) defined bedding-plane set (sites KCF-2 and -5, plate 6; table B.1). Calcite cement is common on joint planes. More important for ground-water flow are dissolution features, principally long, narrow caves along bedding plane-joint intersections, which are common but widely spaced (figure 15).

The Humbug-Uinta SGWC is an important aquifer in the study area, hosting numerous wells and springs. The Oakley City Humbug well (well C, table A.2) is the most successful. At least 27 private wells are screened in the Humbug-Uinta SGWC in developments along Beaver Creek east of Kamas. Most of these wells tested at 15 to 50 gallons per minute (57-190 L/min), and one that penetrated through the Doughnut Formation into the Humbug Formation was artesian (Utah Division of Water Rights data).

At least three springs emanating from the Humbug-Uinta SGWC are used for culinary water supply. Left-Hand Canyon Spring (figure 1) is described in the Proposed Hydrostratigraphy section in the main body of the text. Two unnamed private springs issue from the Humbug Formation in the western Uinta Mountains north of Kamas. Thick soil and vegetation obscure the geologic controls on these springs.

The Uinta Mountain Group consists of the Red Pine Shale, Hades Pass unit, and Mount Watson unit, which together are about 12,140 feet (3,700 m) thick (figure 13). The Red Pine Shale consists of shale and siltstone with rare interbedded quartzite, and the Hades Pass and Mount Watson units consist of interbedded fine to coarse-grained sandstone, shale, and conglomerate. Bedding generally dips toward the surrounding valleys and reflects the trend of the Uinta arch (cross sections A-A′ through H-H′, plate 3). Joints in these units have moderate density and moderate to good connectivity, but were not studied in detail for this report.

At least 16 wells are screened in the Red Pine Shale along Beaver Creek, near its westernmost outcrop area about 4.5 miles (7.2 km) southeast of Kamas (Utah Division of Water Rights data). These wells tested at about 20 to 40 gallons per minute (76-152 L/min). The hydraulic conductivity of this shale unit likely results from joints, which can exist due to its high degree of cementation.